DESIGN AND SYNTHESIS OF NOVEL CHROMOPHORES FOR APTAMER BASED IMAGING

by

Jacob Michael Robison

A thesis submitted in partial fulfillment
of the requirements for the degree

of

Master of Science

in

Chemistry

MONTANA STATE UNIVERSITY
Bozeman, Montana

November 2015

ACKNOWLEDGMENTS

I would like to thanks my committee members, Dr. Mensur Dlakic, Dr. Mary Cloninger, and Dr. Rob Walker for the help and support in completing this thesis. They were an incredible help and this thesis and the work there in would not be possible without them. I would like to thank the MBRCT grant for their financial assistance for this work.

TABLE OF CONTENTS

LIST OF TABLES

Table Page

LIST OF SCHEMES

Scheme Page

LIST OF FIGURES

Figure Page

LIST OF FIGURES – CONTINUED

Figure Page

ABSTRACT

Fluorescent proteins are an incredibly versatile tool in biological imaging. Unfortunately, fluorescent proteins cannot be used to track small metabolites in vivo. The purpose of the work described herein was to create novel red-shifted RNA aptamer based probes for use in molecular imaging. All potential dyes were prescreened using molecular modeling and only the dyes that absorbed wavelengths longer than 500 nm were synthesized. The first aminothiophene based imidazolinone dyes (ATI-1 and ATI-2) were synthesized and their electronic properties were evaluated. SELEX was performed on ATI-2 to find several random RNA sequences that were capable of binding the chromophore and activating ATI-2 fluorescence. It is proposed that fluorescence activated cell sorting can be used to separate and isolate the sequences that form the brightest complexes with ATI-2.

CHAPTER ONE- INTRODUCTION

Since its initial discovery in *Aequorea Victoria,* green fluorescent protein (GFP) has proven to be invaluable in biological imaging[1]. GFP provides a robust, non-invasive, scaffold for imaging proteins. GFP consists of an 11 sheet β-barrel with an α-helix inside the barrel. The protein has a naturally high quantum yield. The chromophore, 4-hydroxybenzlidene imidazolinone(HBI), is surrounded by the β-barrel which provides a unique electronic environment for the chromophore. Upon proper folding of the protein scaffold the residues, Ser^{65}-Tyr^{66}-Gly^{67}, will undergo intramolecular cyclization and oxidation to form the internal fluorophore (see figure 1). [2,3]

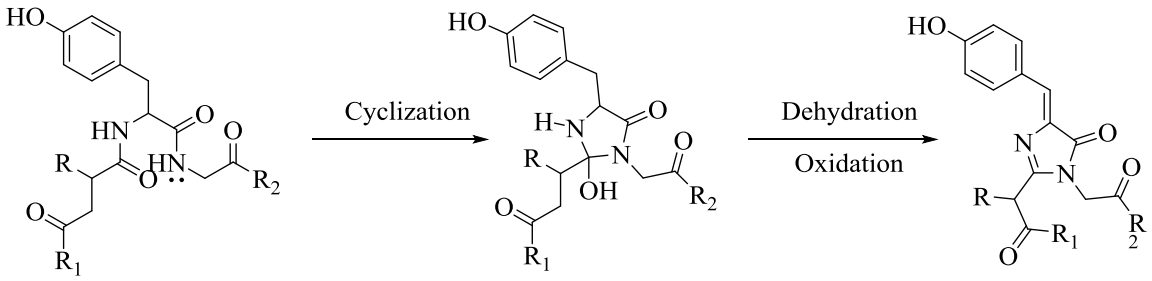

Figure 1-Formation of HBI inside GFP. R designates where the chromophore is attached to the protein.

Many proteins, most having high quantum yields, now comprise the family known as the fluorescent proteins (FP). The fluorophore inside GFP is isolated from most solvent effects and is in a unique electronic and sterically hindered environment.[1,4-7] If the electronic environment surrounding the fluorophore is changed, the overall absorption and emission profile can be bathochromically or hypsochromically shifted.[3] While the

GFP family typically contains HBI, the protein has been mutated by replacing the tyrosine residue with histidine. This point mutation resulted in blue fluorescent proteins which have an emission around 450 nm(see figure 2A).[3,8] The emission of fluorescent proteins can cover most of the visible spectrum. Red fluorescent proteins (RFPs) have subsequently been discovered and include mCherry, DsRed and mPlum. mPlum is one of the most red shifted fluorescent proteins discovered to date and has an excitation and emission of 590 nm and 649 nm respectively. The chromophores found in RFPs can vary widely depending on the individual protein. They are typically similar to HBI but the conjugation is extended beyond the imidazolinone core (see figure 2C).[3,8] While the individual electronic environment surrounding each protein can vary drastically, most fluorescent proteins depend on restricting the rotation and isomerization of the internal fluorophore.[5,6,9]

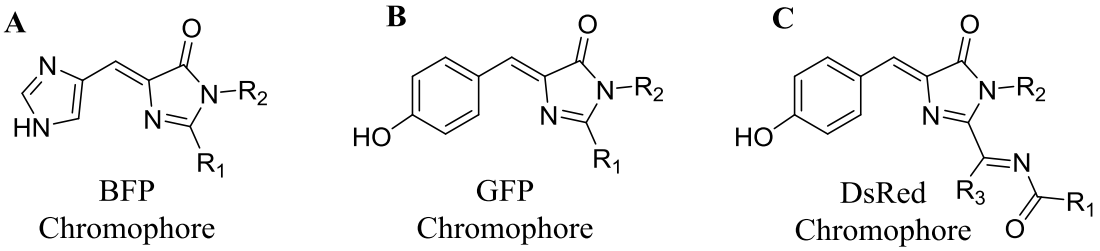

Figure 2-Chromophores of several common fluorescent proteins. The R groups designate where the chromophore is attached to the protein backbone.

GFP, as isolated from *Aequorea Victoria*, has a quantum yield of 0.80, while the free chromophore has a quantum yield of 10^{-3} and therefore is essentially non-fluorescent.[4,10] Investigations into this behavior have found that when rotation was

artificially restricted around the methylene, either by complexation with -BF_2 , Zn^{+2}, hydrogen bonding or inside the protein, HBI becomes fluorescent (see figure 3C).[6,10-14] When HBI is not conformationally locked, it is theorized that it undergoes a rapid, volume conserving isomerization upon excitation known as a “hula twist" (see figure 3C).[5] When bound, suppression of the hula twist mechanism, along with possible cis-trans isomerization, favors fluorescence. This viscosity and rotational dependence of fluorescence is not just specific for HBI and related imidazolinones, it is an incredibly common phenomenon across a variety of dye classes.[15-21]

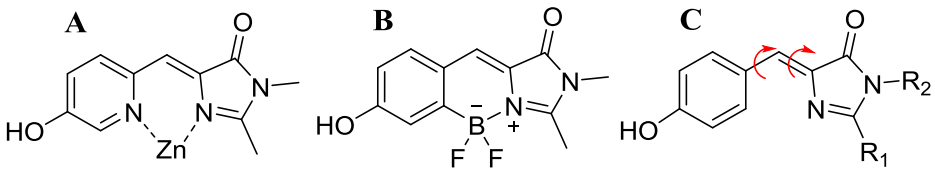

Figure 3-A.) A zinc binding imidazolinone derivative; B.) A -BF2 locked HBI adduct; C.) The hula twist (adapted from references 14 and 22)

In order to describe this effect, some basic physics of photoluminescence must be examined. When a dye absorbs a photon of the appropriate wavelength, an electron gets excited and moves from the highest occupied molecular orbital (HOMO) to the lowest unoccupied molecular orbital (LUMO) or to an allowed electronic excited state. The strongest excitation that occurs (λ_{max}) is related to the relative transition dipole moment (μ_{ge}) for each of the possible ground (g) to excited (e) state transitions. This is determined by molecular structure, as it relates to the molecular orbital electronics. The energy difference between the HOMO and LUMO (ΔE_{ge}) is called the band gap. ΔE_{ge} can be

expressed in terms of energy (eV - the energy of a photon), or in terms of wavelength (λ - nm) and frequency (ω – Hz). Band gap determines the "color" of the dye, and the absorption/emmision spectral location.

Once in the excited state, a dye molecule can relax back to the ground state via a variety of pathways including fluorescence, non radiatave decay, intersystem crossing to a triplet state, or quenching.[22] In order to be competitive, the timescale at which each process occurs (~ 10^{-7} – 10^{-9} seconds for fluorescence) must be comparable. In the case of conditional fluorescence, the specifics of dye structure, and the physical and/or electronic nature of the microenvironment in which the dye is embedded, combine to alter the relative favorability (timescale) of radiative versus nonradiative decay processes. By suppressing nonradiative decay, radiative decay is favored, increasing the number of photons emitted relative to the number of photons absorbed (fluorescence quantum yield, Φ_F). In some cases, a pronounced dependence of fluorescence quantum yield on viscosity is observed. This "viscometric" effect is due to it being more difficult for the exited state to lose energy through molecular motion (vibrational decay). However, in many cases, this "viscometric" effect is less apparent. This difference is due to the complicated nature of exctied state processes.

While the restricted rotation of HBI and HBI derivatives will readily induce fluorescence, another important factor that should not be overlooked is the specific hydrogen bonding present in the pocket of GFP. Hydrogen bonding is a major factor in the spectral tuning of fluorescent proteins. H-bonding of the carbonyl of the imidazolinone on the chromophore has been shown to red-shift the absorbance.[23,24]

Hydrogen bonding in the natural protein also accounts for excited state proton transfer (ESPT). ESPT causes HBI to be deprotonated to the phenolate form upon excitation at 395 nm. The phenolate form emits at 508 nm.[3,13,14,23,24.] This is to be expected due to the increased electron donating ability (reduced ionization potential) of the anion of structure B in figure 2, leading to an increase in HOMO energy and a corresponding reduction in ΔE_{eg}. If the pathway for ESPT is removed and HBI stays in the protonated phenol form the emission is expected to be hypsochromically shifted.[3]

Fluorescent proteins have become an extremely valuable tool in biochemistry. It is possible to track proteins and many cellular processes using them. In fact, GFP was first coupled to the neurons in *C. elegans.*[1] However, it can be difficult to track small cellular metabolites such as adenosine triphosphate (ATP), S-adenosylmethionine (SAM), or glutathione (GSH) without the use of recombinant techniques.[2,19,25-28] Metabolites are even more difficult to track when there are no obvious Förster resonance energy transfer (FRET) based sensors.

Recently, Jaffery and coworkers have developed a working dye-aptamer complex for use in cellular imaging.[2] An aptamer is an oligonucleotide that is capable of binding smaller analytes with high specificity. The dye-aptamer complex "Spinach" has since been used for the detection of ADP, SAM, cyclic-di guanine monophosphate (cdiGMP), RNA transcription, and protein expression.[2,25-27] The Spinach aptamer is 98 nucleotides long, binds 2,5-difluoro-4- hydroxybenzylimidazolinone (DFHBI), has a quantum yield of 0.72, and has a blue-green emission around $\lambda \sim 500$ nm. Figure 4 illustrates the proposed structure of Spinach. The dye is found bound in the large pocket at the base of

stem-loops 2 and 3 (figure 4).[2] Using X-ray crystallography, it was found that DFHBI was bound by a G-quadruplex. The fluorescence of the complex increased as the concentration of potassium increased. It is thought that K^+ helps stabilize the G-quadreplex along with Mg^{+2} [29]. The Spinach complex has been found to be more resistant to photo bleaching than GFP.[2] It is thought that if DFHBI is photochemically degraded or isomerizes it will be rapidly exchanged with fresh chromophore from solution due to the non-covalent nature of chromophore binding.[30] A new form of Spinach called Spinach2 has been optimized for better folding and tighter binding of the chromophore. It is markedly brighter and more stable than the original.

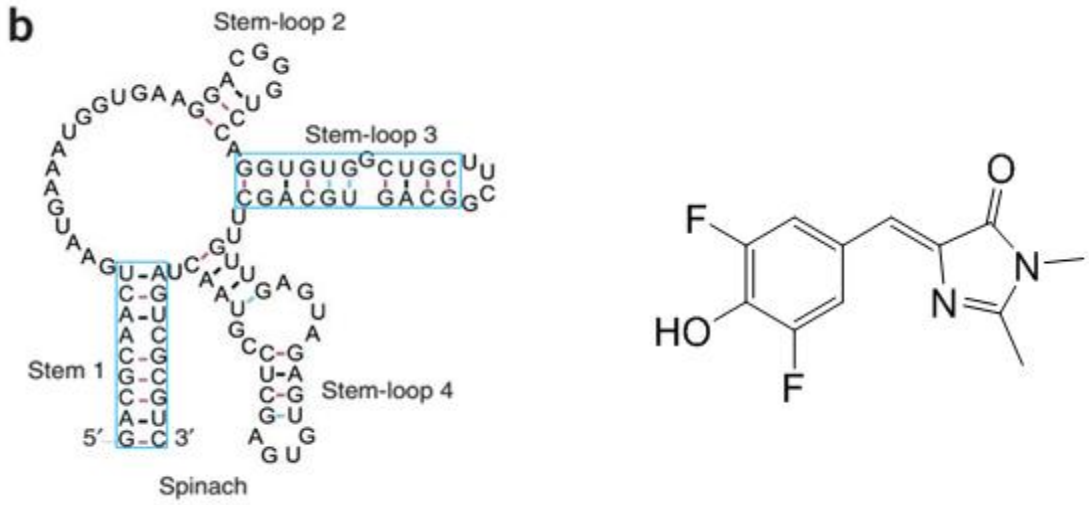

Figure 4-The Spinach Aptamer with DFHBI (adapted from reference 2).

Jaffery and coworkers explored several other dye aptamer complexes before discovering Spinach. Among these, there are several features worth noting. Some dyes, like 3,5-dimethoxy-4-hydroxybenzylimidazolinone (DMHBI), HBI or DFHBI, are pH dependent. There is a noticeable shoulder in the UV-Visible spectrum of DMHBI caused

by the phenolate form (see figure 4). This shoulder can even be seen in aptamer 17-3. It was found that some aptamers selected for DMHBI preferentially bound the phenolate only[2].

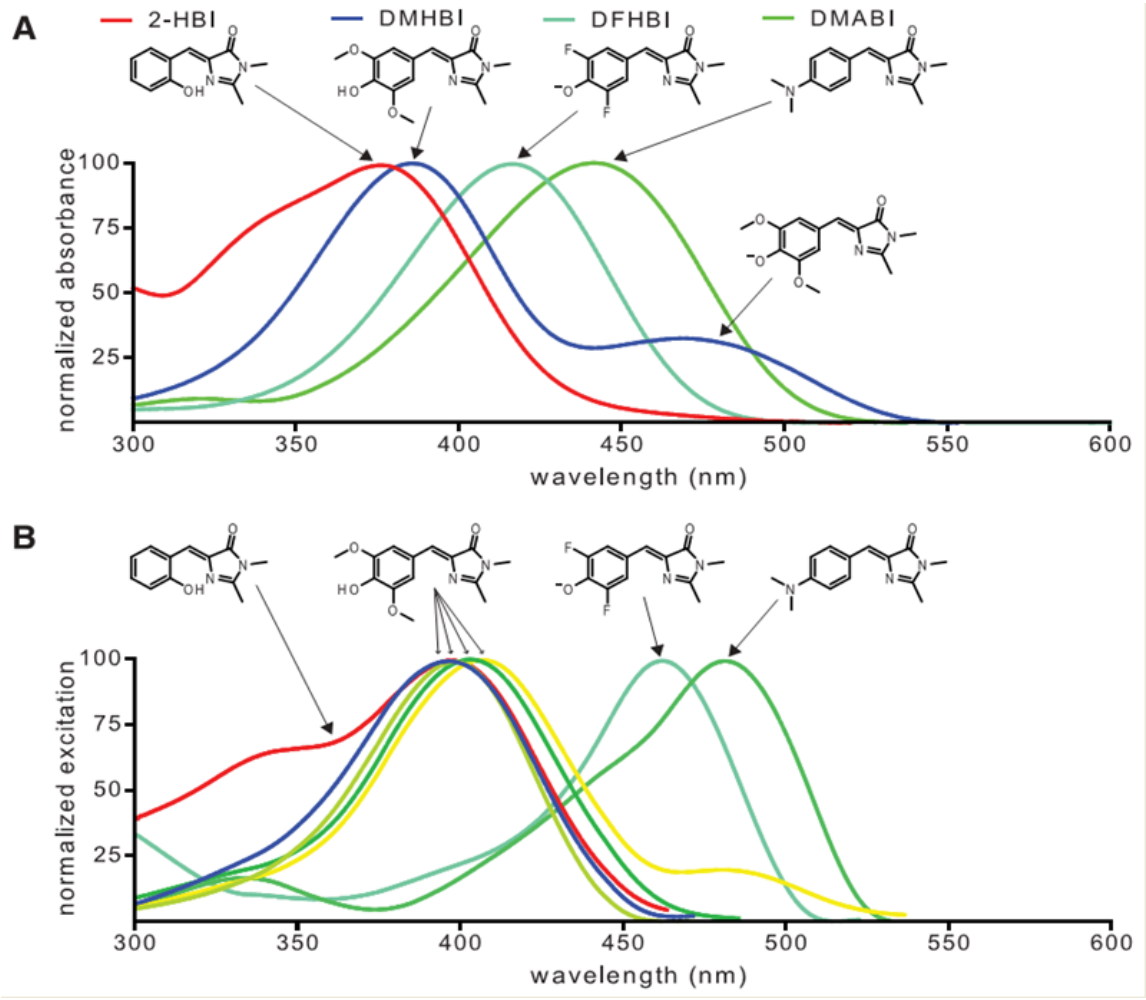

Figure 5-(A) The absorption several imidazolinone type dyes. (B) The excitation of several dye-aptamer complexes. DMHBI has several apatmers that bind the dye each with a unique spectral signature. The colors represent the approximate color of fluorescence for each complex (Adapted from reference 1).'

This pH dependence was one cause of the low brightness of some of the aptamers. The dye that absorbed the longest wavelength was 4-dimethylaminobenzylimidazolinone

(DMABI). Even when bound with an aptamer, the excitation maximum does not exceed 500 nm for any of the dye choices. For most of the dyes, aptamer binding causes a 50-75 nm red shift.[2] It would be beneficial to find new dyes that are not dependent on pH and had a maximum absorption (λ_{max}) of 500 nm or longer.

Recently the spectral properties of Spinach and Spinach2 have been tuned to enable the use of current YFP and GFP filter cubes in confocal microscopy. Slightly modified versions of DFHBI were screened against the aptamer in an effort to slightly red shift the emission. This "Edisonian" guess-and-check approach has allowed the emission of Spinach be red-shifted from $\lambda \sim 500$nm to $\lambda \sim 505$nm and $\lambda \sim 523$nm when the appropriate chromophores are used.[31]

Along with the "plug and play" chromophores, Jaffery and coworkers also discovered the aptamer "Broccoli." Broccoli was isolated using fluorescence activated cell sorting (FACS) and SELEX and has significantly decreased the magnesium dependency relative to Spinach or Spinach2[32]. Broccoli is also much smaller while having a higher thermal stability than either of the previous aptamers but is just as bright as Spinach2.[32]

For a historical note, the first dye-aptamer complex found was the malachite green RNA aptamer. As suggested, this aptamer binds the dye malachite green along with crystal violet, tetramethylrosamine, or pyronin Y, which are all structurally similar.[33] This complex has seen very limited use in vivo due to the high toxicity of malachite green.[33] Like Spinach, this aptamer was found using the systematic evolution of ligands by exponential enrichment (SELEX).

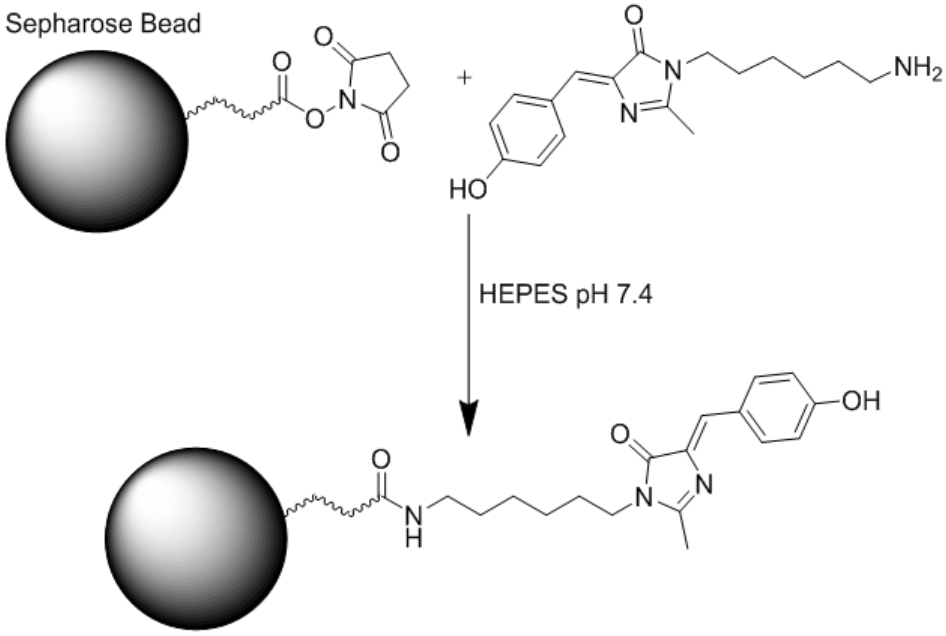

Figure 6-The functionalization of HBI to a NHS-activated sepharose bead

SELEX enables the selection of DNA or RNA oligonucleotides on the basis of their ability to bind small molecules with the highest affinity.[2,7,34-36]. SELEX has been used to select aptamers that could bind with green fluorescent protein, whole bacteria, carbohydrates, viral particles, and tissues. [2,7,34-36] SELEX is a cyclical process. With each round of selection, higher enrichment is achieved until eventually the tightest binding sequences are isolated. In order to perform SELEX, the chromophore must first be fixed to a solid support (see figure 6). Next, a previously prepared library of RNA aptamers is eluted through the column. Any RNA that does not bind is discarded. A solution of free dye is then eluted down the column to remove any sequences that have bound to the dye. RNA that does not bind selectively to the unbound dye stays adhered to the column. The eluted RNA is enriched with sequences that most tightly bind free dye in solution. The resulting RNA is converted to DNA-RNA duplex, which is then amplified using

polymerase chain reaction (PCR).[2] PCR enables exponential amplification so the eluted RNA is amplified with high fidelity.

Few of the aptamer probes discovered by Jaffery and coworkers have a λ_{max} at or below 500 nm. Other than the "plug and play" chromophores, the only probes that emit light below 500 nm are the malachite green aptamer and RNA Mango. Malachite green is largely unusable in vivo due to its high cytotoxicity and nonspecific binding interactions[33]. Mango is an aptamer dye complex that binds the dye thiazole orange with a very high affinity. It emits around 535 nm but has a relatively low quantum yield, ϕ=0.14, compared to Broccoli or Spinach2.[19] The "plug and play" chromophores are synthetically difficult and have a markedly decreased affinity to the Spinach2 aptamer. While the emission of both these complexes is below 500 nm there is still good portion of the visible spectrum that is not currently covered.

This thesis describes the design and investigation dyes that have a λ_{max} at or exceeding 500 nm in length. Longer wavelengths are less damaging to cells beacuse of their lower energy. They will cause less background fluorescence which in turn allows for a lower detection limit; and they can penetrate more deeply into tissue which could possibly allow for the imaging of tissue and not just individual cells. While SELEX can be difficult to control, the chromophore can be designed to fit our criteria.

Therefore, one significant goal of the work proposed here is to use conditional fluorophores to design a set of ratiometric RNA-aptamer based probes for the in vivo detection of cellular metabolites or antibiotics. Toward this goal, theory-guided molecular engineering techniques were used to prepare new dyes, with novel properties, via rational

design. Time-dependent density functional theory (TD-DFT) ab initio quantum mechanical computer simulations were employed to enable the predication of absorption and emission behavior. The modeled compounds were synthesized and characterized. Finally, SELEX coupled with FACS were used to select the best aptamer complexes

CHAPTER TWO- DESIGN AND SYNTHESIS OF CHROMOPHORES

In order for a dye to be useful for SELEX and detection in vivo it needs to fit several criteria. First and foremost, any dye needs to selectively fluoresce when bound by an aptamer. An ideal dye also needs to: have an appropriate excitation wavelength; be water soluble; be easily attached to sepharose (see figure 6); be easily synthesized from known (ideally commercially available) materials; and be non-cytotoxic. Currently, imidazolinone based dyes, such as DFHBI and HBI, fit the majority of the criteria. Therefore, rationally modified imidazolinone dyes were investigated here as first candidates. In order to help design a dye with an appropriate absorption, TD-DFT molecular modeling was performed on each proposed structural modification to predict the λ_{max}, prior to any in-lab synthesis work.

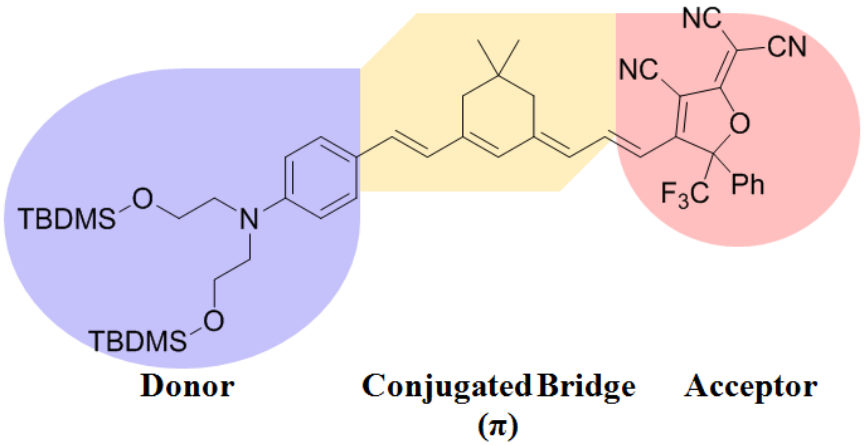

Figure 7-The Donor-π-Acceptor type dye YLD 124 (adapted from 39)

Typical small aromatic and/or conjugated structures show ΔE_{eg} such that ultraviolet light is strongly absorbed. In order for a dye to absorb visible wavelengths of light, ΔE_{eg} between the HOMO and LUMO needs to be smaller. There are several ways to modify a dye in order to decrease the band gap.[20,37-39] For D-π-A type dyes (see figure 7), the identity of the donor, conjugated bridge, and acceptor portions of the dye determine the electronics of the dye and ΔE_{eg}.[38,39]A longer conjugated bridge will lower the band gap but reduce solubility in water, so different donor-acceptor combinations will primarily be considered. As figure 5 demonstrates nicely, there is an observable trend between donor strengths. A donor is simply an electron donating group and will, upon excitation, transfer electrons to the acceptor. A stronger donor more easily gives up electrons and upon addition to a dye is most closely associated with an increase in the energy of the HOMO. Generally, phenols are better donors than methoxy substituted phenyl rings and phenolates are better still. Substituted amines, like the dimethylamine in DMABI, tend to be better donor than phenolates.[2]

Likewise, a good acceptor will accept electron density from the donor, and addition to the dye is most closely associated with a reduction in LUMO energy. 1,2-Dimethylimidazolinone functions as an acceptor though, 2-dicyanomethylene-3-cyano-4,5,5-trimethyl-2,5-dihydrofuran (TCF) is much stronger. The CF_3- Ph-TCF (see figure 7) is more strongly withdrawing than TCF, and a TCP (3-methyl-4-cyano-5-dicyanomethylene-2-oxo-3-pyrroline) acceptor is one of the strongest currently known.[38,39] Due to the fact that imidazolinones are not the "strongest" acceptors, some very good donors are considered in order to achieve the level of ΔE_{eg} reduction desired

here. It has been observed that amino substituted heteroaryl compounds like 2-aminothiophene, and 2-aminopyrroles are some of the best currently known donors. [39-41]

With this idea of tuning electron donors in mind, several structures were proposed as initial candidates, as shown in Table 1. All potential dyes were screened using ab initio TD-DFT calculations using a B3LYP functional and the 6-31G* basis set. DMHBI was run initially and the λ_{max} was predicted to be 381nm while the experimental was found to be 380 nm (see Appendix B Figure 15). Several interesting trends can be observed. First, adding a phenyl group to DMABI, structure 4, at the R4 position of the imidazolinone (See figure 8 structure 5) was calculated to cause a red shift to the absorption by about 50 nm. If the phenyl group is in plane with the chromophore it should effectively increase the overall conjugation. Next, the 2-aminothiopheneimidazolinones (ATI) and 2-aminopyrrolimidazolinones (API), structures 1-3, and 6 and 7 respectively, were modeled. It was predicted that adding a phenyl group to API, (structure 7 figure 8) would shift the absorbance by about 100 nm. When ATIs, which were by far the most red-shifted imidazolinones in this set, were modeled the phenyl modification once again red shifted the absorbance by about 50 nm. To test whether or not the conjugation was truly extended structure 3 was modeled. While the absorptivity was predicted to be larger, the λ_{max} for structures 2 and 3 was very close. Based on analysis of all of the results from the modeling studies structure 2 or a derivative there of was chosen as the synthetic target.

Table 1-Electron Donor Candidates for Imidazolinone based dyes

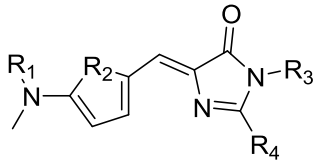

	R_1	R_2	R_3	R_4
1	CH_2CH_2OH	S	Me	Me
2	CH_2CH_2OH	S	Me	Ph
3	CH_2CH_2OH	S	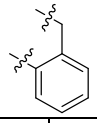	
4	Me	CH=CH	Me	Me
5	Me	CH=CH	Me	Ph
6	Me	NMe	Me	Me
7	Me	NMe	Me	Ph

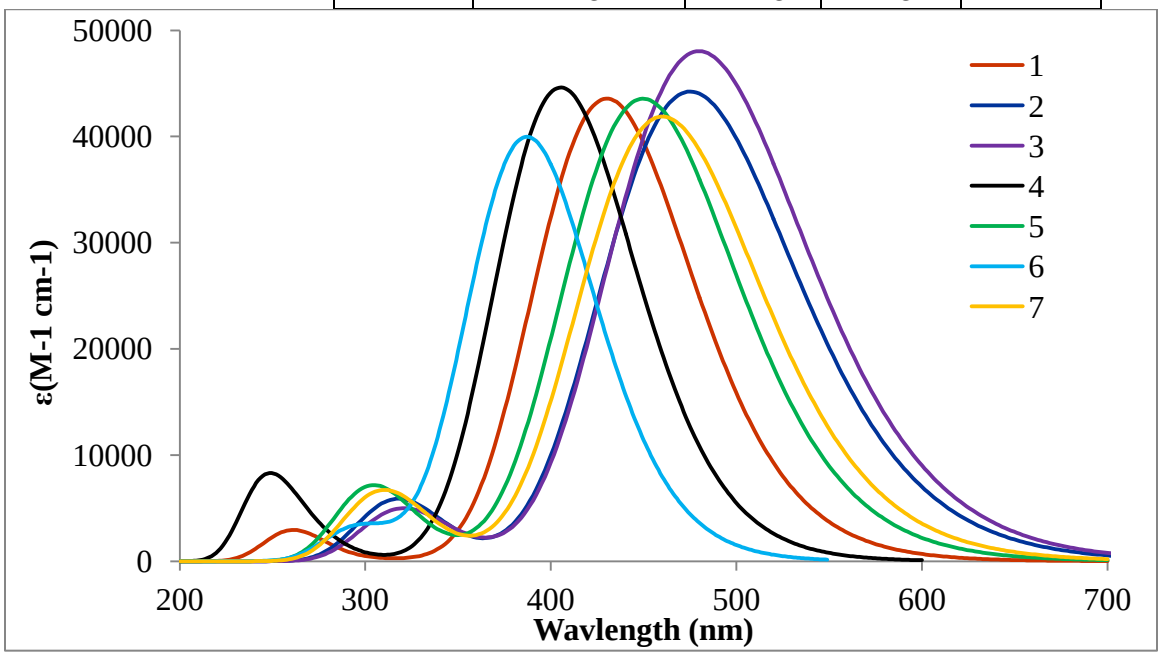

Figure 8-Theoritical UV-Vis for chromophores shown in Table 1

Synthesis of Imidazolinone Chromophores

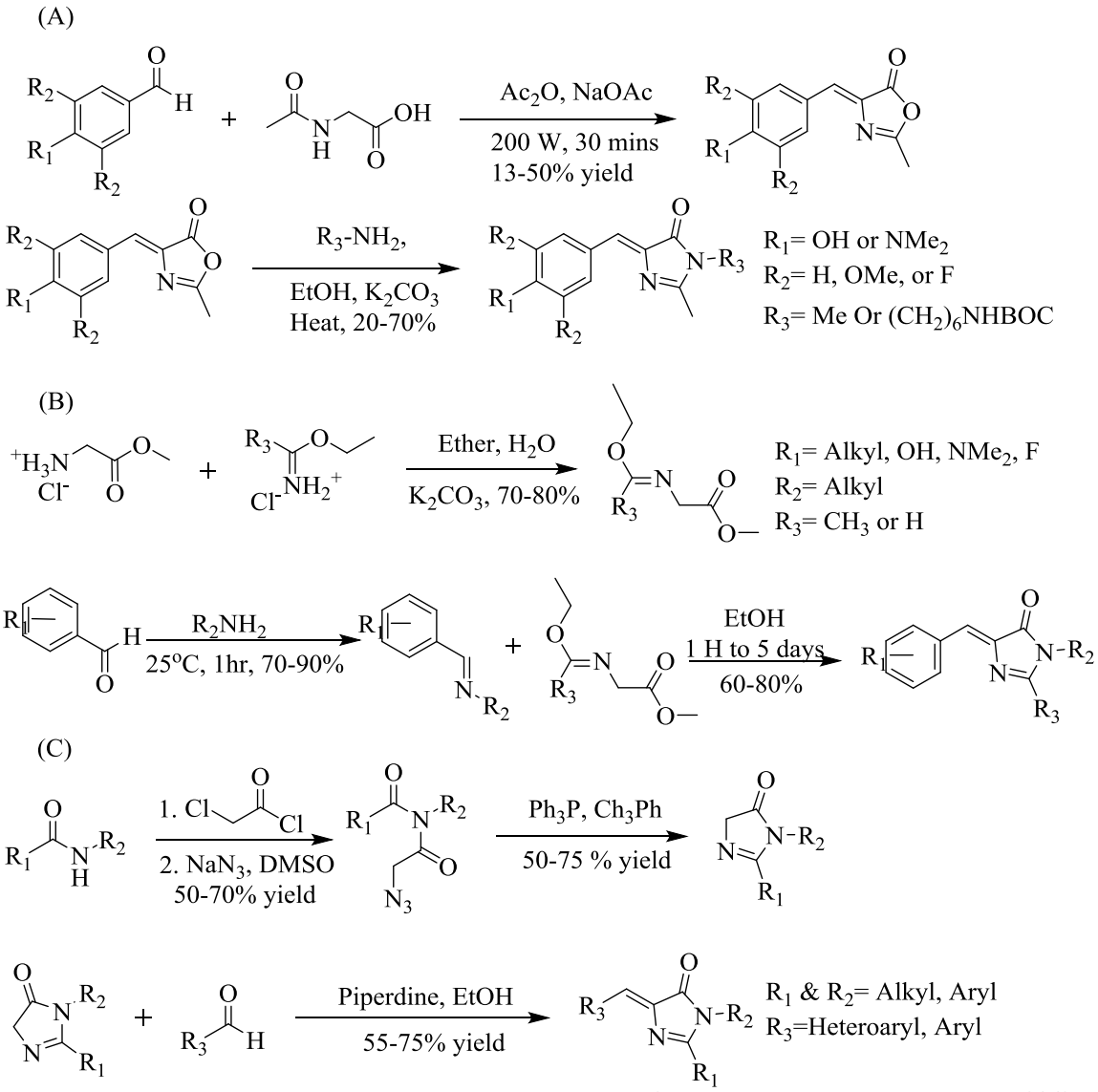

Scheme 1-(A) the Erlenmeyer Aza-lactone Synthesis[2]. (B) The [2+3] cycloaddition[24,42]. (C) The Intramolecular Aza-Wittig[6]

Several methods have been explored to synthesize imidazolinones. The three main methods include the Erlenmeyer aza-lactone synthesis, as used by Paige et al[2]., a [2+3] cycloaddition commonly employed by Tolbert et al[43]., and finally an intramolecular Aza-Wittig (see scheme 1A, 1B, and 1C respectively).[6] The Erlenmeyer synthesis requires only two steps. The first step is the formation of an oxoazolinone through an Erlenmeyer condensation reaction. The yields are poor for even simple aromatic aldehydes like 4-hydroxybenzaldehyde, and this reaction does not tolerate heteroaryl aldehydes such as pyrrole.[6] The second step can have yields ranging from 12-75% depending on the substrate. This method offers very little synthetic control and poor tolerance of sensitive functional groups.[6,24] Therefore, at best, this method is functional in that it allows access to the product in many cases, but yields are highly variable (generally poor) and purification of the resulting products is time-consuming. To make the version of the dye to be functionalized to sepharose (see figure 5) the intermediate oxoazolinone is reacted with tert-butyl 6-aminohexylcarbamate. The t-butyl carbamate (BOC) is then cleaved with in 1:1 trifluoroacetic acid: dichloromethane. The reaction plus subsequent deprotection afforded a 12% yield for the HBI derivative.

The [2+3] cycloaddition synthetic route offers more synthetic control and better yields than the Erlenmeyer synthesis.[42,43]The synthesis is combinatorial (modular) and the yields are typically moderate to high. The biggest weakness of the synthesis is the lack of synthetic ease by which to functionalize the R_3 position of the imidazolinones.[44] Only a few imidates are commercially available, and synthesis of alternatives can be challenging. In order to functionalize R_3 with something other than a methyl (a

potentially desirable modification as suggested by computer simulations) an imidate would need to be synthesized.[44] There is no precedent for being able to functionalize R_3 with a phenyl using this method.[24,39,42,43] It has been observed that some compounds such as the Schiff base of 2-formylpyridine cannot readily undergo cylclization.[24]

The final method for imidazolinone synthesis considered was an intramolecular Aza-Wittig. It allows for good synthetic variability using commercially available starting materials, and seemed, by inspection, likely to be straightforward and tolerant of various functionality. The aza-Wittig is selective and does not readily form side products and the yields are typically 60-70%. Following synthesis of the acceptor (imidazolinone), a Knoevenagel condensation is used to form the finished dye. The linker version of any dye can be readily synthesized without the need for any protecting groups[6,45]The major downside is the inability to make any small imidazolinones like 1,2-dimethylimidazoline without a significant risk of explosion due to the organic azide intermediate. This procedure was successfully and safely used to synthesize the first thiophene based imidazolinone dye called ATI-1 (see Scheme 2).

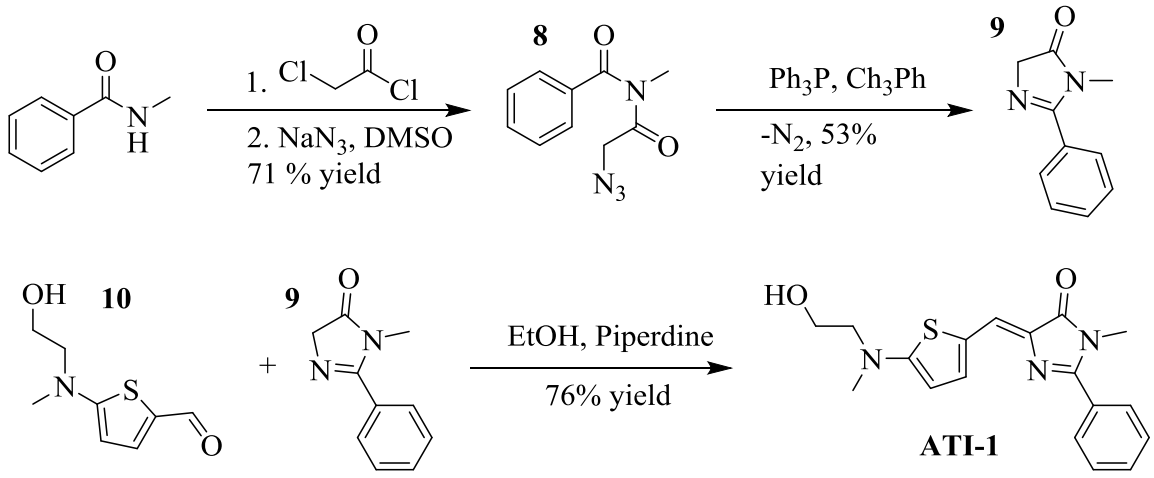

Scheme 2-The synthesis of ATI-1

ATI-1 was chosen as our first target due to the favorable absorption (see dye 2 figure 8) and the relative ease by which it could be synthesized. The α-azidoimide, 8, was formed in 71% yield which is in agreement with the literature preperation.[6] The imidazolinone, 9, was isolated in 53% unoptimized yield because it adhered to the column, and some coeluted with triphenylphosphene oxide. The Knoevenagel condensation between 9 and 10 occurred readily in piperidine, and the final material was isolated by flash chromatography in 5% methanol/dichloromethane on SiO_2 as a metallic-red crystalline solid in a 76 % yield. The λ_{max} is 531 nm in water and the molar absorptivity is 53,800 $cm^{-1}M^{-1}$. The λ_{max} and molar absorptivities of HBI and DMHBI are 26,500 $cm^{-1}M^{-1}$ at 374 nm and 24400 $cm^{-1}M^{-}1$ at 380 nm, respectively. Ab initio DFT was performed on ATI-1 and the modeling estimates that the λ_{max} will be 472 nm in chloroform, which agrees well with the experimental value of 505nm in $CHCl_3$. ATI-1 is

fairly solvatochromic (see Appendix B Figure 16), the λ_{max} will hypsocrhomatically shift from 489 nm in diethyl ether to 531 nm in water.

Unfortunately, the alcohol substituent did not impart significant solubility in water, so the dye would be extremely difficult to use for SELEX. A completely different version of the imidazolinone containing an amine functionalizable linker would need to be synthesized to attach to sepharose. A small amount of ATI-1 synthesized with hexanoic acid at the R_2 position was isolated in very low yields. The amine terminated version was made with ethylene diamine, and it was subsequently attached to sepharose. Due to the poor solubility of ATI-1 this material was attached to sepharose but never used.

A slight modification was needed to impart greater water solubility and to make it easier to attach to sepharose, so ATI-2 was devised with a methyl ester attached at the R_2 position (see Scheme 3). This modification allowed the synthesis of the amine terminated dye for attachment to sepharose and a more soluble form from the same intermediate.

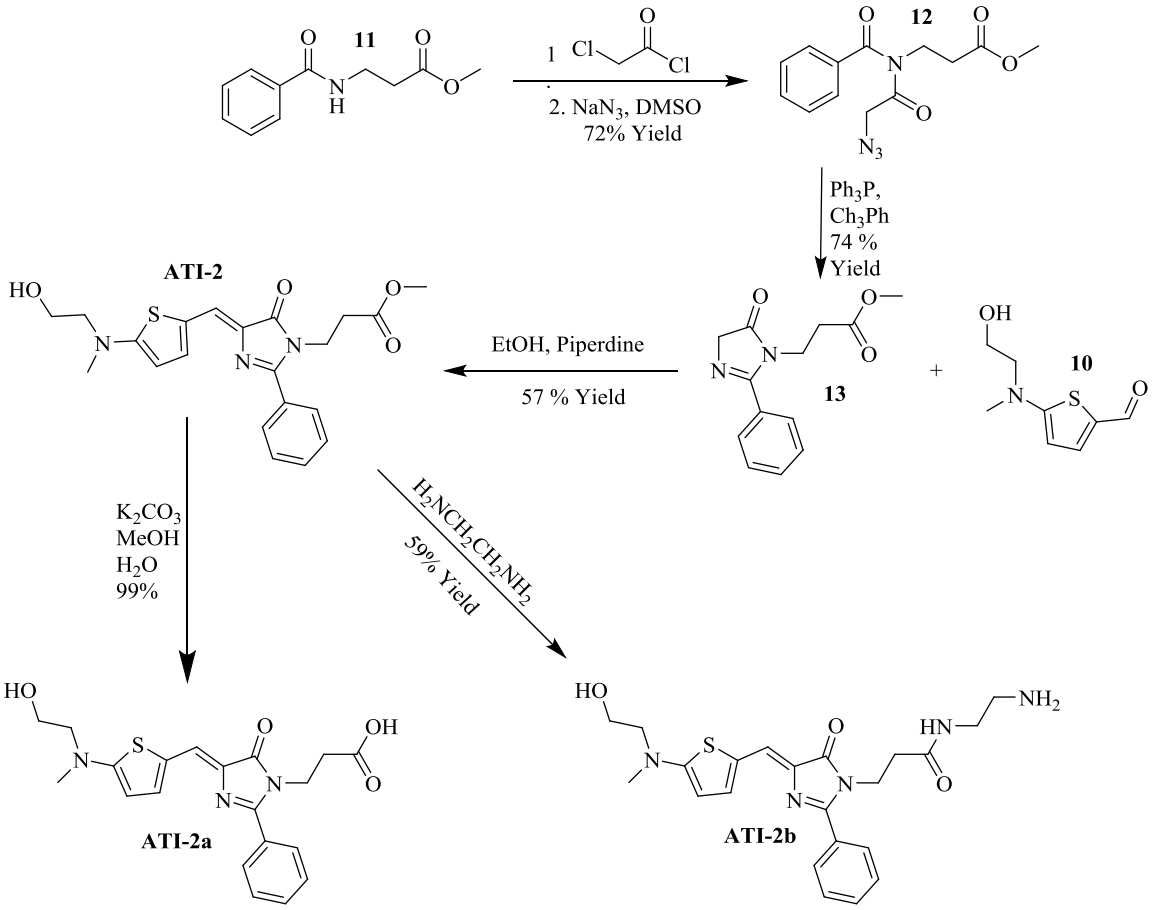

Scheme 3-The synthesis of ATI-2

11 was produced in 90 % yields by first esterifying β-alanine in methanol with $SOCl_2$ followed by amidation with benzoyl chloride.. [46] The α-azidoimide, 12, was typically synthesized in 50% yields but yields as high as 72% could be attained. The imidazolinone, 13, was found to unstable and degraded upon oxygen exposure. It was used immediately upon preparation. Compound 13 was not isolated; instead the toluene was removed, ethanol, piperdine and aldehyde were added and the reaction was stirred over night. The ATI-2 could be synthesized in about a 20 % yield from 12 in one pot. It was found that not isolating the imidazolinone and just performing the cyclization and

condensation in one pot saved considerable time and materials but resulted in 5% lower yields. The subsequent removal of the methyl ester from ATI-2 by hydrolysis and transamidation were very high yielding and the materials could be easily isolated and purified. The 4-aminothiophene-2-carbaldehyde (10) was synthesized in one step from commercially available starting materials.[47] Using this method a number of other dyes were produced.

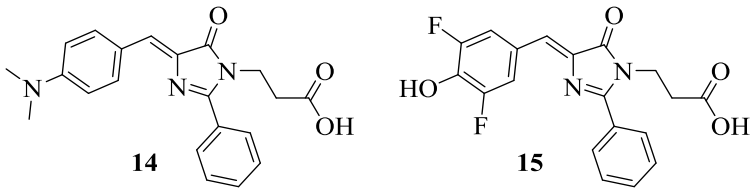

Figure 9- Several other imidazolinone chromophores

The chromophores synthesized were characterized using a number of techniques. Along with general techniques such as NMR and mass spectrometry(see Appendix C) most chromophores were characterized using Beer's law to calculate their molar absorptivity. Quantum yields were calculated for the key structures. It was found that ATI-2A had a molar absorptivity about twice that of DFHBI and was about 10 times more fluorescent. Though the quantum yield is higher than DFHBI; it is hypothesized that an ATI-2A binding aptamer would have a lower detection limit than Spinach. The phenyl substitution actually increased the quantum yield for all the tested chromophores. The Uv-Vis spectra for the chromophores are shown in figure 12. While the λ_{max} for dye 2 is about 50 nm off of the λ_{max} of ATI-1 and ATI-2A the modeling was still very useful

for screening potential chromophores and selecting the best target. The Uv-Vis spectra also show that ATI-1 and ATI-2A are not significantly different electronically.

Table 2-Spectrospcopic properties of imidazolinone chromophores

	$\lambda_{max\ abs}$ (nm)	$\varepsilon(M^{-1}\ cm^{-1})$	$\lambda_{max\ em}$ (nm)	φ^{a}
DFHBI	418	30,100	500	0.0007[2]
ATI-2A	527	57,000	567	0.0067±0.0001
14	468	37,000	558	0.0035±0.0001
15	443	32,500	536	0.0016±0.0001

[a] DFHBI as standard in 0.1 M HEPES (pH 7.4)

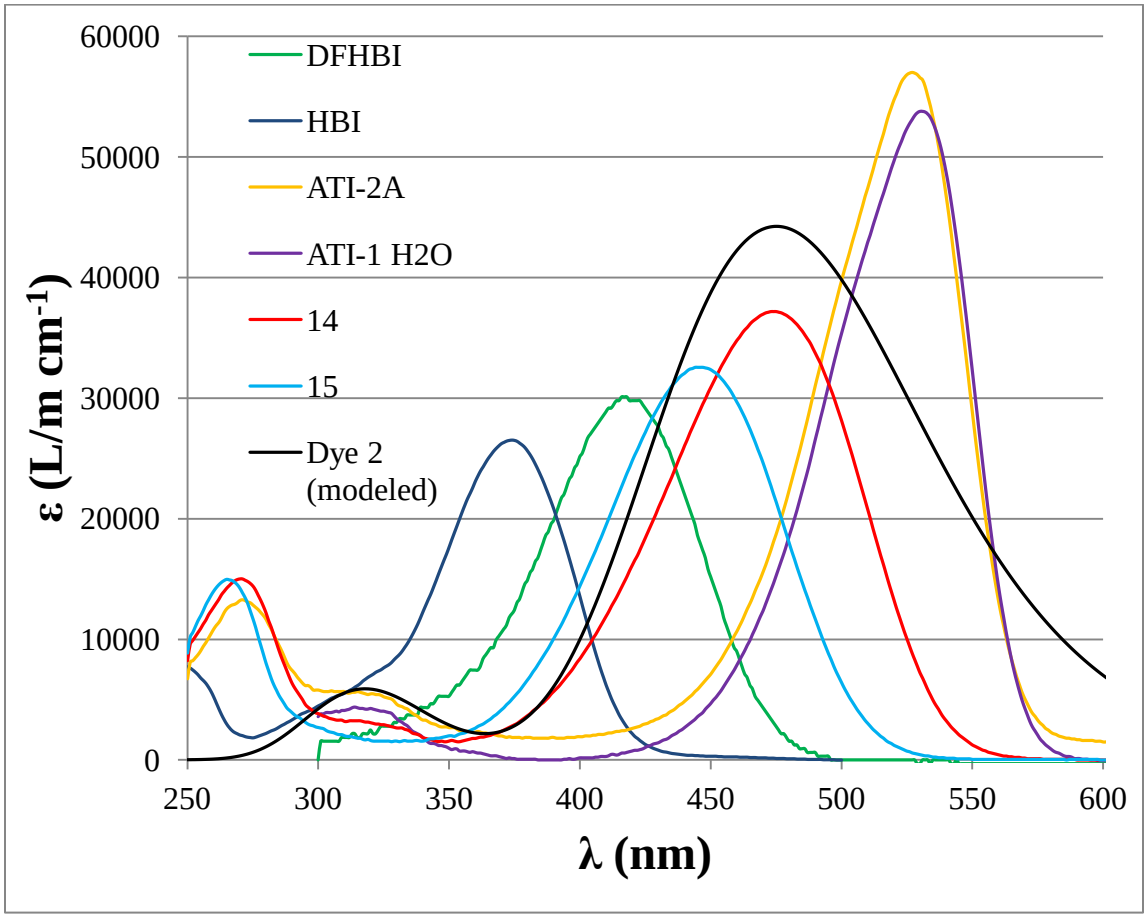

Figure 10-The UV-Vis of several Imidazolinone chromophores

Alternate Chromophores

While only ATI-2 and HBI were ultimately used for SELEX the synthesis of several other chromophores were explored. Unfortunately, due to a variety of reasons such as low yields and degradation of starting materials, none of the following chromophores proved to be practical. In order to demonstrate the usefulness of the aza-Wittig synthesis, several other chromophores were attempted. The first is the API based chromophores.

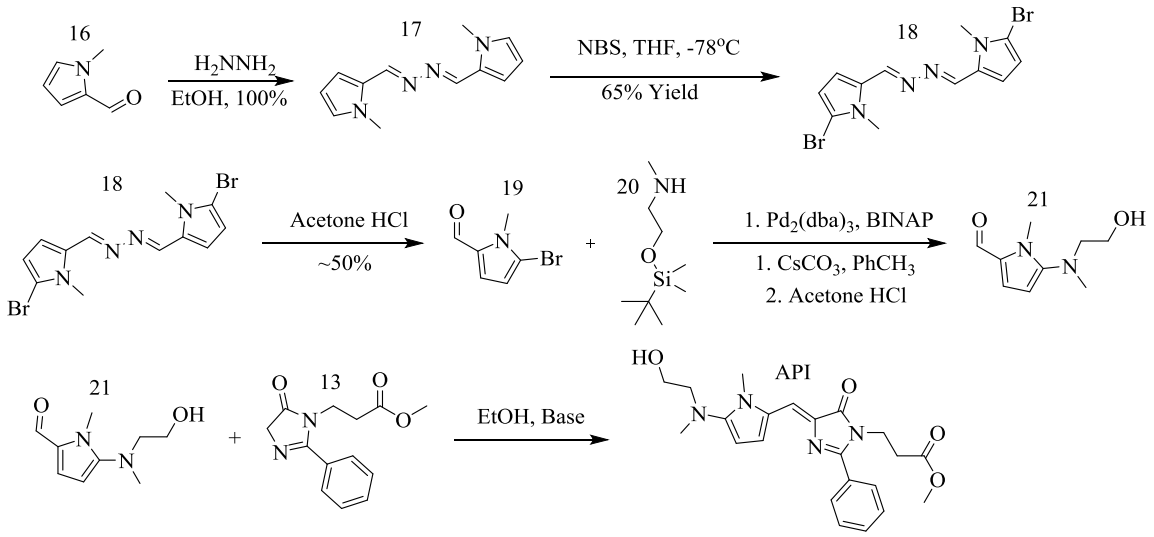

Scheme 4-The synthesis of API

The synthesis, as shown in scheme 4, was fairly straight forward. The 4-bromopyrrole-2-carboxaldehyde could be synthesized in moderate yields from commercially available starting materials. The Buchwald-Hartwig reaction protocol tolerated cyclic secondary amines such as piperidine but conditions could not be found where any appreciable material could be isolated when 20 was used as shown below. The pyrrole degraded readily under the reaction conditions and the purification of any material was difficult. While the molecular modeling predicted the λ_{max} to be around 450 nm (Figure 8 dye 7), the chromophore was expected to be highly solvatochromic. Pyrrole based chromophores have been shown to be highly influenced by a change in the electronic environment[39].

The other imidazolinone chromophore that seemed very promising was a 4,4'-diaminofluorenone based fluorophore. Molecular modeling predicted that the chromophore would have an absorbance around 600 nm or so, making it the most red

shifted chromophore for this application to date (see Appendix B Figure 17). The idea was that 2 electron donating groups would make for a very red shifted donor. Unfortunately, there were some difficulties in the synthesis of the compound.

It was possible to make the 4,4'-dibromofluoreneone from phenanthraquinone in very low yields. The double Buchwald proved to be unfeasible so Ullman conditions were attempted using CuI as a catalyst. The disubstitution was believed to be feasible due to the fact that a double Sonogashira was performed on the same substrate[48]. While some of the mono addition product was isolated under most attempted conditions the double addition was only observed with piperdine as the amine and with high catalyst loadings (20%). As soon as 20, as seen in scheme 4, was used very little product was isolated. The alcohols are desired to help impart a higher water solubility and prevent aggregation. It is thought that the barrier to this reaction was the solubility of the starting material. A large excess of piperdine did not produce more product, and a large amount of starting material remained present in suspension. The dibromofluoreneone is not soluble in most common solvents, including DMSO and toluene, which were both tried.

Recent literature has illustrated that the dibromofluorenone needs to be extremely pure for reaction and can be purified by tituration with acetone, followed by sublimation twice, soxhlet extraction, and finally recrystallization. The phenanthraquinone impurity will bind the palladium catalyst used in the Buchwald reaction. The more pure the fluorenone starting material, the higher the yields.[48,49] With more time and funding, it appears that the diaminofluorenone might still be a very good target. The terminal alkynol is reactive towards active methylene compounds such as malononitrile.[50]

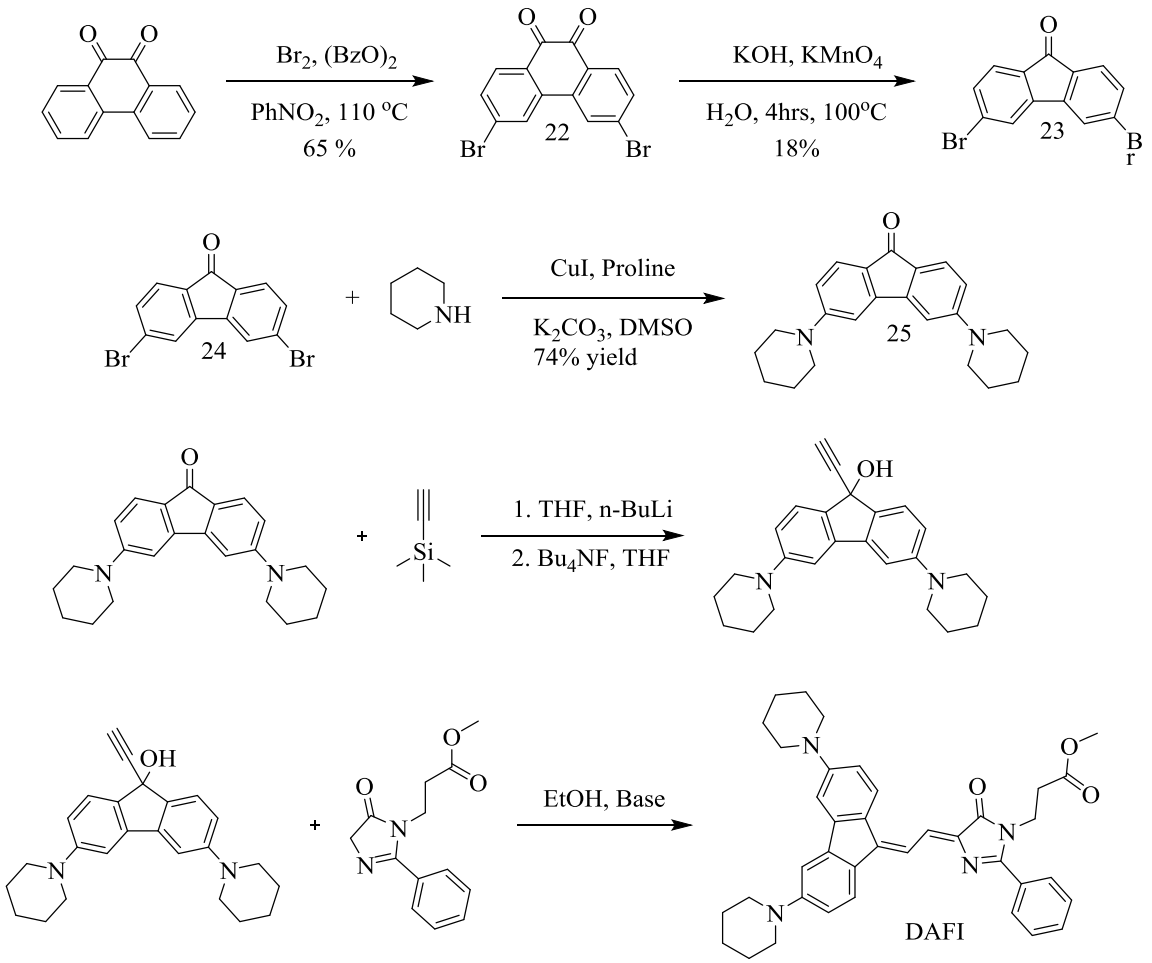

Scheme 5-The synthesis of a 4,4'-diamionfluorenone based dye

The last dye considered was a TCP based chromophore. It has an absorbance around 650 nm and is very easily synthesized from commercially available materials (see scheme 6).[38] The main issue is that the chromophore is extremely insoluble in all common solvents. The dye, 27, was alkylated at the pyrolline nitrogen by ethyl bromoacetate to form 28. In order to remove the acetate group to form 29, the dye was exposed to K_2CO_3 in methanol. Unfortunately, the material degraded and no useable material could be isolated. TCP based chromophores are not well characterized but there is no precedence for any fluorescence from this dye.[38] The toxicity of this family of dyes

is also unknown. While the only dye that will be used for aptamer selection is ATI-2 and HBI there are still plenty of potential targets for a hypsochromatically shifted chromophore. In spite of the synthetic challenges, the diaminofluorenone based dyes still show great promise.

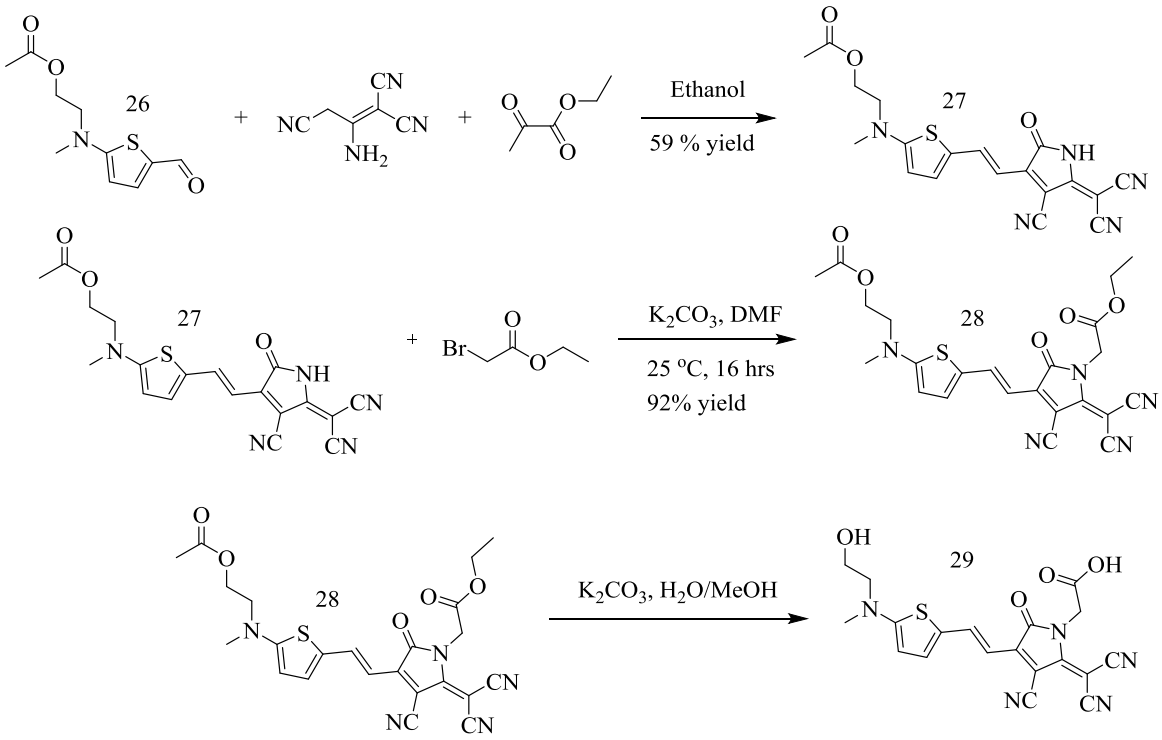

Scheme 6-The synthesis of a thiophene based TCP chromophore.

CHAPTER THREE- SELEX AND FACS

In order to use a chromophore in vivo an RNA aptamer that binds the dye must be identified. The goal of SELEX is to select an aptamer that is capable of binding the chromophore and will hopefully activate fluorescence. SELEX will select for an aptamer capable of tightly binding the dye but it will not select for the brightest fluorescence.[19,32] Fluorescence activated cell sorting (FACS) will be used to select for the brightest complexes.

Some initial work has been performed on HBI and ATI-2 in order to find aptamers that bind the dyes. The approximate RNA sequence for SELEX is as follows: GGGAGAAGCTTCTAGATGAA-$(N)_{26}$-CTGCTTCGGCAG-$(N)_{26}$-TGAATTCCTGGATCCGTCAC. N designates a random nucleotide. The stem loop, the 12 bp sequence in middle, helps ensure good folding so the random sequence will have a higher chance of binding the dye. Figure 12 below shows the amount of RNA recovered after each of selection for HBI. The exponential enrichment is expected. The reason the amount starts to plateau is that the best binders have been found further rounds of SELEX might remove one or two sequence from the pool but will no longer provide as much enrichment. There are still a significant number of sequences present and separating an individual sequence or two can be very challenging.[19]

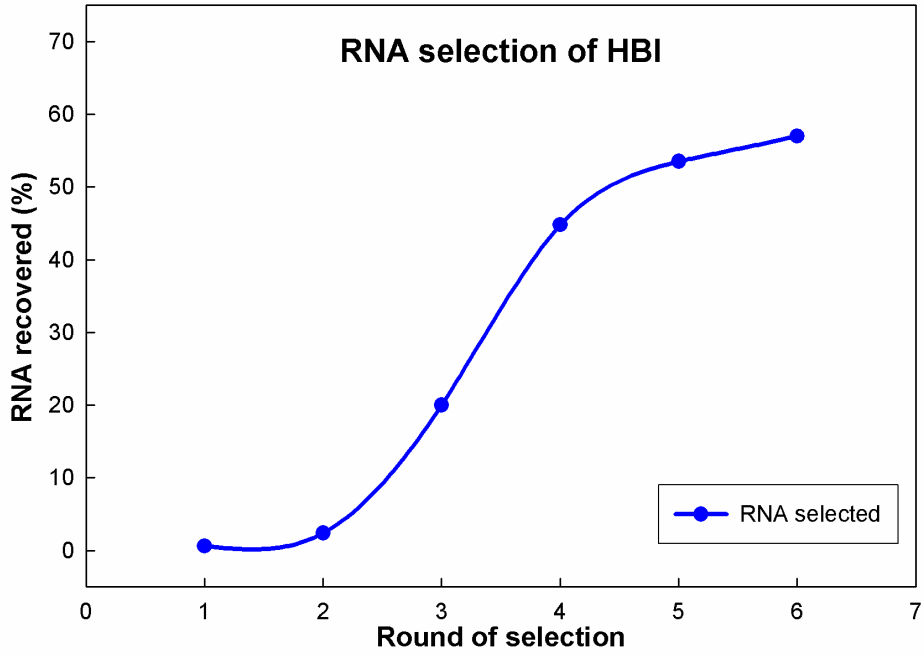

Figure 11-The amount of RNA recovered from each round of SELEX

Figure 13 shows the relative fluorescence enhancement with each corresponding round of SELEX. While SELEX selects for the tightest and best binders, it does not select for the brightest complex. In spite of this, a significant amount of fluorescent enhancement is still observed. It should be noted that any aptamers that are excited at any wavelength significantly different than 360 nm or emit at anything different from 528 nm will not be observed. If an aptamer preferentially binds the phenolate form of HBI, it will probably not be observed. This is largely an artifact of the instrument used.

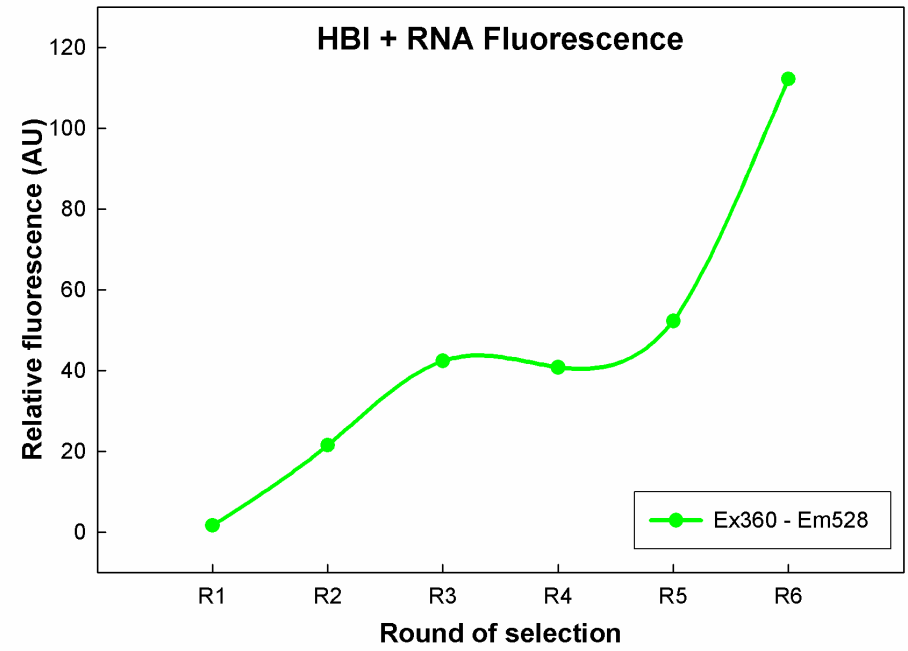

Figure 12-The relative fluorescence enhancement of HBI-Aptamer complexes during SELEX.

Figure 14 shows the fluorescence enhancement of ATI-2 aptamer complexes during SELEX. While the free chromophore emits at 567 nm at pH7.4, it should be noted that the exact fluorescence wavelength that most ATI-2 aptamer complexes is not known. Depending of the electronics of aptamer binding it is expected that the fluorescence could shift 50 to 100 nm from the free chromophore. Studies to discover this wavelength for several sequences were unsuccessful. It is expected that ATI-2 would have a higher initial fluorescence due to the fact that it is more fluorescent than HBI. However, in spite of the difficulties, a decent amount fluorescence enhancement is still observed.

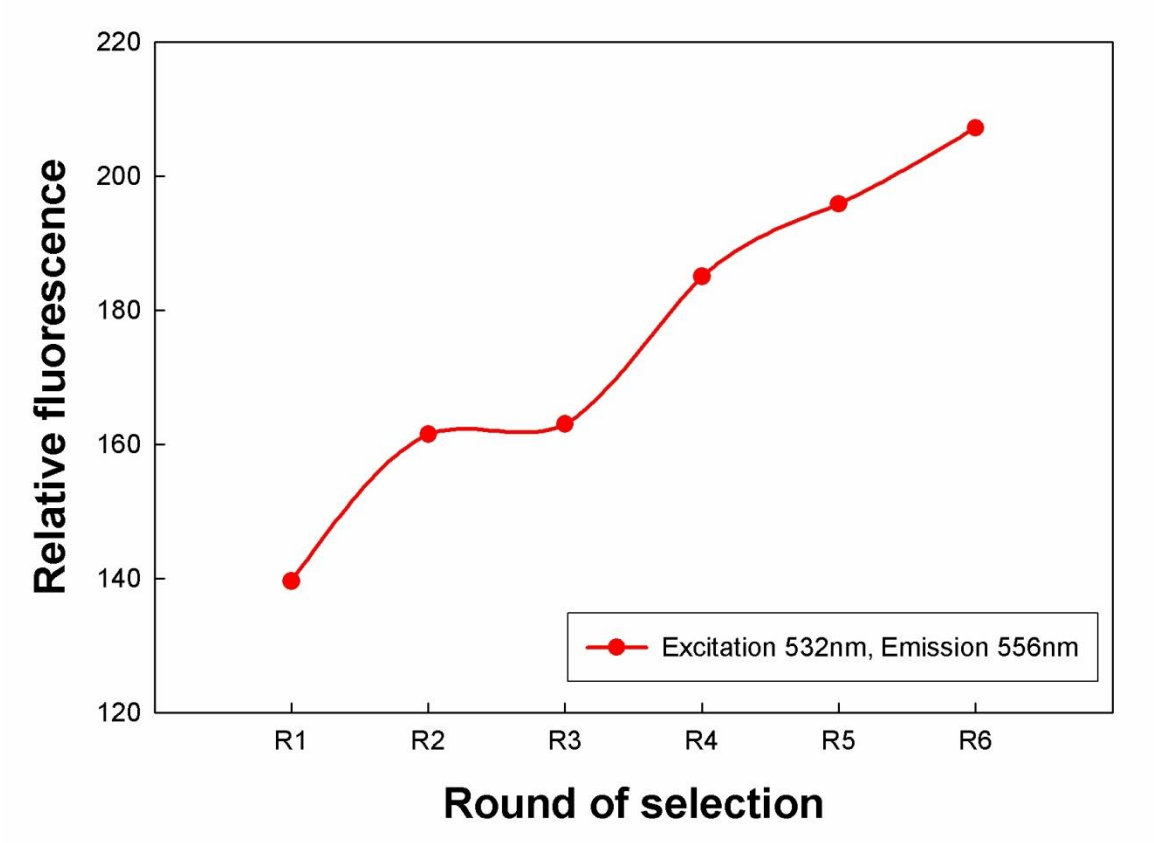

Figure 13-The relative fluorescence enhancement of ATI-2-Aptamer complexes during SELEX.

In order to select the brightest individual sequences FACS will be used. Attempts have made to clone round 4 and 5 of HBI and ATI selection into specially designed Duet plasmids (figure 15). Each plasmid in encoded with a fluorescent protein as a positive control. For HBI mCherry is used, while ATI-2 uses Venus. The aptamers are inserted into the plasmids using EcoR1 and Spe 1 restriction sites. E. Coli expression is controlled by lactose and kanamycin is used as a transfection control for ATI-2. The HBI plasmid still uses lactose to control expression but ampicillin is used as the transfection control

instead. Unfortunately, there have been some difficulties transfecting E. coli with the plasmids. The reason for this difficulty is currently unknown.

The goal is to express a small library of dye binding apatmers into E. coli. Once successfully expressed the population of e. coli will be sorted using FACS. This should, hopefully, isolate the aptamers that make brightest complexes. This SELEX coupled FACS was used to select the Broccoli aptamer much more quickly than Spinach.[32] Once individual aptamer sequences are isolated they will be characterized.

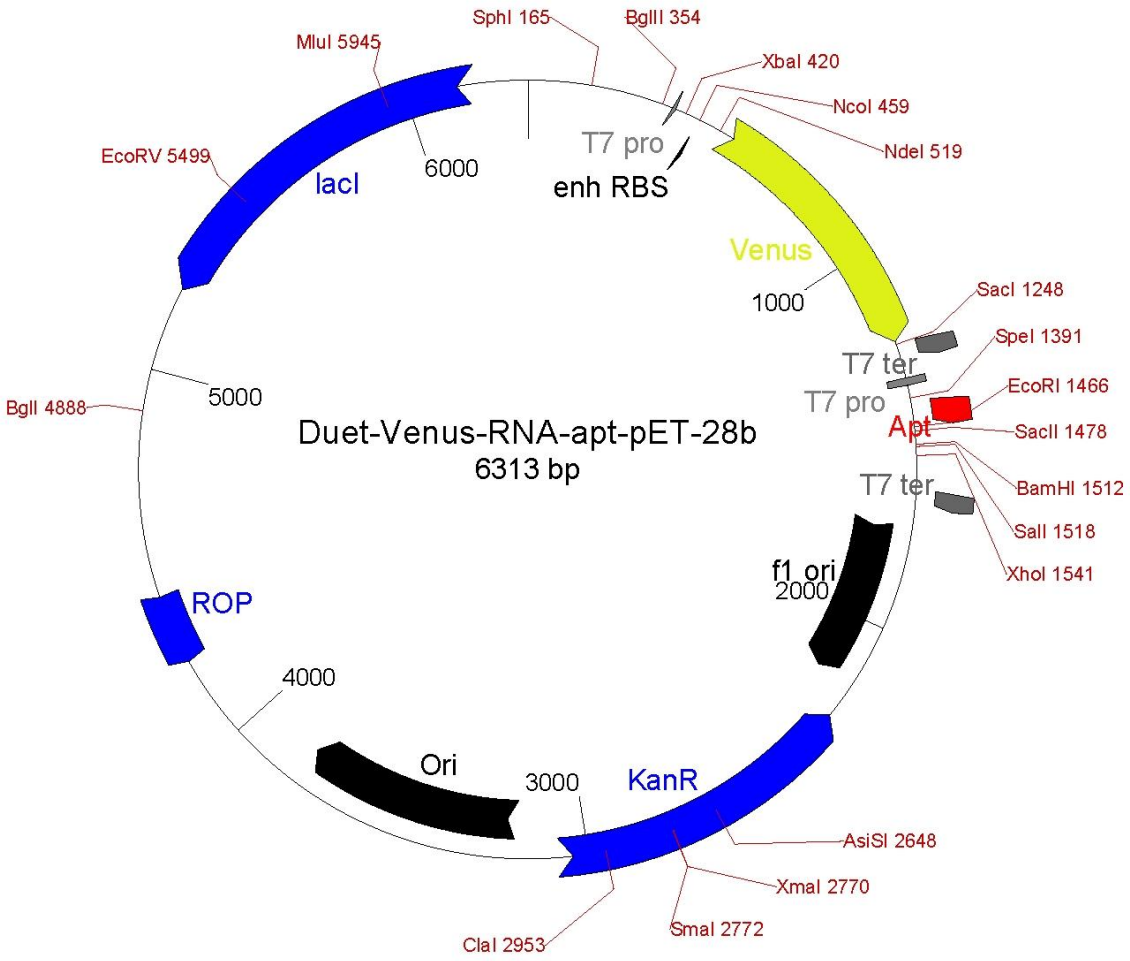

Figure 14-The Venus ATI-2 Duet plasmid

CHAPTER 4-CONCLUSION

In summary, several potential chromophores were evaluated using molecular modeling studies, and the most hypsochromatically shifted chromophores were synthesized. ATI-1 and ATI-2 are new chromophores that will be used for SELEX , and several chromophores also showed promise. While the λ_{max} of most uncharged chromophores can be easily approximated, several of the criteria cannot be easily predicted. The four biggest factors that can immediately disqualify a dye for consideration are if the dye is too fluorescent, is very cytotoxic, has any nonspecific binding interactions in vivo that cause fluorescence, or is not soluble enough in aqueous solution.

While ATI-2 has a very low quantum yield the in vivo properties are currently unknown. Like most imidazolinone chromophores, it is not expected to be overly cytotoxic but there is no literature data on a thiophene based imidazolinone dyes.[2] In spite of the lack of data, ATI-2 is still the most promising chromophore for SELEX. The fluorenone based dyes might intercalate DNA due to their large planer structure. The DAFI dyes might also be too large for the small aptamer sequences to bind adequately.

Ultimately, the dye-aptamer probes will be used to track small metabolites or antibiotics in vivo[2,26,34]. One goal is to design a ratiometric aptamer system so two interrelated metabolites could be tracked at the same time. Spinach and a hypothetical ATI-2 binding aptamer could potentially be used. Metabolite pairs that could be tracked include ATP/ADP or glutathione/ glutathione disulfide. These aptamers could valuable insight into living cells. Another goal is to track antibiotics in pseudomonas aeruginosa

biofilms. The depth of antibiotic penetration into the biofilm could be detected and the localization of antibiotics or metabolites could also be imaged in vivo using confocal microscopy.

APPENDICES

APPENDIX A

EXPERIMENTALS

General Procedures

All reagents used were purchased from commercial vendors and were used as received unless otherwise noted. All reactions were carried out under nitrogen in flame-dried glassware. Dichloromethane (DCM) and tetrahydrofuran (THF) were dried by distillation from CaH_2 and sodium benzophenone ketyl respectively. Toluene was dried by fractional distillation and storage over 4Å molecular sieves. All solvents used for chromatography, filtrations, and transfers were ACS reagent grade.

Thin-layer chromatography was performed on Sorbent Technologies silica XG TLC plates. Visualization was accomplished with UV light (254 nm), 2,4-dinitrophenyl hydrazine in 2 M HCl, and/or 0.2 M 4-dimethylaminobenzaldyhyde in ethanol with piperdine. Normal-phase flash chromatography was performed using Sorbent Technologies standard grade silica gel 60 Å, 40-63 μm (230 x 400 mesh). Pierce NHS-activated sepharose was functionalized according to a literature procedure.[2]

^{1}H and ^{13}C NMR spectra were recorded at 25 ^{o}C on a Bruker DRX 500 MHz spectrometer operating at 500 MHz for ^{1}H and 125 MHz for ^{13}C. Chemical shifts (δ) are reported in ppm, employing the solvent as the internal standard. Splitting patterns are designated as s (singlet), d (doublet), t (triplet), q (quartet), dd (doublet of doublets), m (multiplet), or bs (broad singlet). Infrared spectra (IR) were recorded using a Jasco FT/IR-4100 using sodium chloride plates coated in a neat film. UV-Vis spectra were recorded on a Shimadzu UV-2101PC UV-Vis Scanning spectrophotometer. All

florescence spectra were recorded on a Varian Cary Eclipse fluorescence spectrophotometer. All fluorescence lifetime data were recorded using a 96 well plate reader equipped with dual laser source emitting at 355/533 nm and the emission was collected at 474 nm or 556nm. All melting point transitions were collected on a TA instruments Discovery Series Differential Scanning Calorimeter and recorded as the onset temperature. High resolution mass spectroscopy (HRMS) was obtained by the Mass Spectrometry and Proteomics Facility at the University of Notre Dame.

Quantum Yields

All steady state fluorescent studies were recorded on a Varian Cary Eclipse fluorescence spectrophotometer. The slit widths were set at 5nm and 20 nm for excitation and emission respectively. All samples were tested in 100 mM HEPES at pH 7.4. The relative quantum yields were obtained using the area under the corrected emission spectra of the test sample compared to that of the standard DFHBI which has a quantum yield of 0.0007 in 100 mM HEPES at pH 7.4 according to literature[2,31,51]. Quantum yields of fluorescence were obtained from multiple trials (N=3) using the following equation:

$$\varphi_x = \varphi_{st}\left(\frac{I_x}{I_{st}}\right)\left(\frac{A_{st}}{A_x}\right)\left(\frac{\eta_x^2}{\eta_{st}^2}\right)$$

Where φ_{st} is the reported quantum yield of the reference, **I** is the integrated area of the fluorescence spectra, **A** is the absorbance of the sample at the excitation wavelength and **η** is refractive index of the solvent. X subscript denotes unknown and the st denotes the standard.

Procedures

(Z)-4-(4-Dimethylamino)benzylidene)-2-methyloxazol-5(4H)one

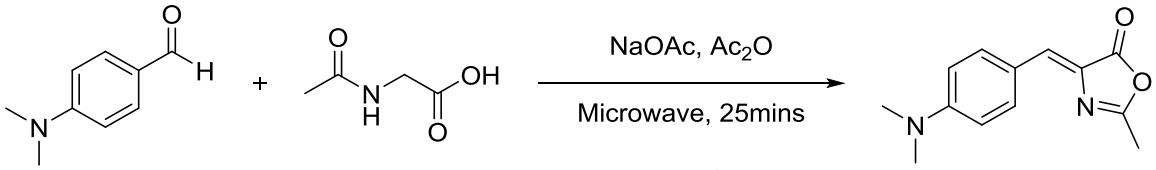

Prepared according to a previously reported procedure.[2] 4-(dimethylamino) benzaldehyde (2.98, 20mmol), n-acetylglycine (2.34g, 20 mmol), sodium acetate (NaOAc, 1.66 g, 20 mmol) and acetic anhydride (10ml), under dry nitrogen, were heated in a reaction microwave at 350 watts for 30 minutes. The reaction was cooled to 25^{o}C and flash chromatography of the crude product in DCM over SiO_2 gave 0.815 g (3.41mmol, 17.7%) of an orange solid. ^{1}H-NMR (500 MHz, $CDCl_3$): 8.01(d, 1H, J=9.17 Hz), 7.10 (s, 1H), 6.73 (d, 2H, J=9.17 Hz), 3.09 (s, 6H), 2.38 (s, 3H).

(Z)-4-(4-Dimethylamino)benzylidene)-1,2-dimethylimidazol-5(4H)one (DMABI)

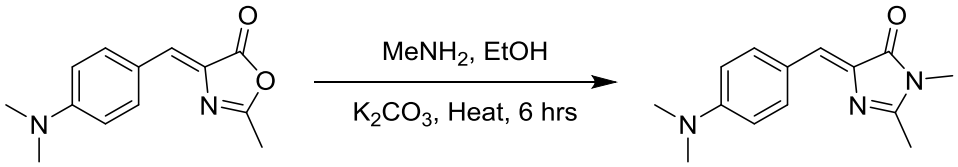

Prepared according to a previously reported procedure.[2] 0.702 g (3.11 mmol, 77.4% yield) as a red solid. ^{1}H NMR (500 MHz, $CDCl_3$) δ ppm 8.06 (2 H, d, *J*=8.80 Hz), 7.09 (1 H, s), 6.71 (2 H, d, *J*=8.80 Hz), 3.19 (3 H, s), 3.05 (6 H, s), 2.37 (3 H, s).

(Z)- 2,5-dimethoxy-4-((2-methyl-5-oxooxazol-4-(5H)-ylidene)methyl)phenyl acetate

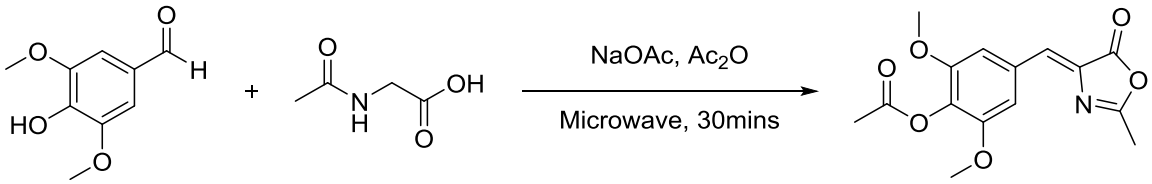

Prepared according to a previously reported procedure.[2] 2,5-dimethoxy-4-hydroxybenzaldehyde (1.82 g, 10mmol), n-acetylglycine (1.17 g, 10 mmol), NaOAc (0.83 g, 10mmol) and acetic anhydride (5 ml), under N_2, were heated in a reaction microwave at 350 watts for 30 minutes. The reaction was allowed to cool to 25^{o}C before -20^{o}C ethanol (30 ml) was added to the mixture. The resulting suspension was cooled to -20 ^{o}C, the resulting precipitate was isolated and washed with -20^{o}C ethanol (2 x 20ml), hot water (2 x 40 ml), and hexanes (2 x 40 ml) before drying in vacuuo which 1.79 g (5.8 mmol, 58.6%) of a yellow solid. ^{1}H-NMR (500 MHz, $CDCl_3$) δ ppm: 7.42 (s, 2 H), 7.04 (s, 1 H), 3.88 (s, 6 H), 2.40 (s, 3 H), 2.36 (s, 3 H)

Z-4-(4-hydroxy 3,5-dimethoxybenzylidene)-1,2-dimethyl-1H-imidazol-5(4H)-one

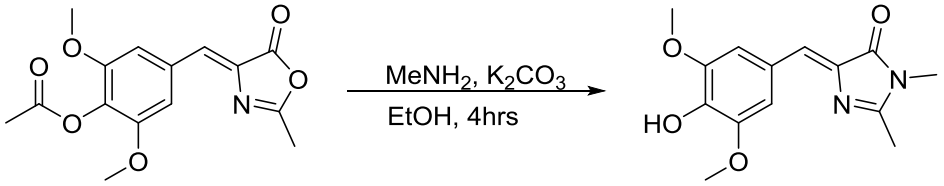

Prepared according to a previously reported procedure.[2] Isolated 0.228 g (1.25 mmol, 22.5 %) as a yellow solid ^{1}H-NMR (500 MHz, $CDCl_3$) δ ppm: 7.51 (s, 2H), 7.02 (s, 1H), 5.94 (b, 1 H), 3.95 (s 6H), 3.19 (s, 3 H), 2.37 (s, 1 H)

(Z)-4-((2-methyl-5-oxooxazol-4-(5H)-ylidene)methyl)phenyl acetate

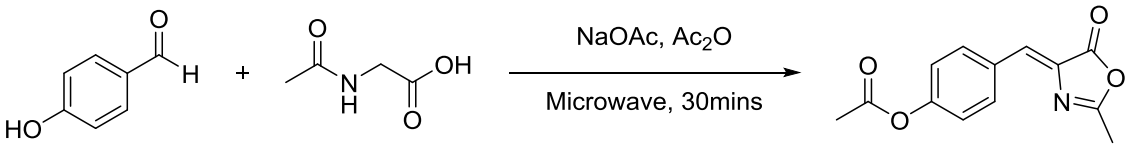

Prepared according to a previously reported procedure.[2] 4-hydroxybenzaldehyde (5.0 g, 41mmol), n-acetylglycine (4.79g, 41 mmol), NaOAc (3.40 g, 41mmol) and acetic anhydride (25 ml), were heated in a reaction microwave at 350 watts for 30 minutes. The reaction was allowed to cool to 25^{o}C before 4^{o}C water (120 ml) was added to the mixture. The precipitate was isolated and washed with -20 ^{o}C 70% ethanol (50 ml) before during in vacuuo isolating 6.06 g (24.6 mmol, 60.3%) of a yellow solid. ^{1}H-NMR (500 MHz, $CDCl_3$) δ ppm: 8.12 (2 H, d, *J*=8.80 Hz) 7.19 (2 H, d, *J*=8.80 Hz) 7.12 (1 H, s) 2.41 (3 H, s) 2.33 (3 H, s)

Z-4-(4-hydroxybenzylidene)-1,2-dimethyl-1H-imidazol-5(4H)-one (HBI)

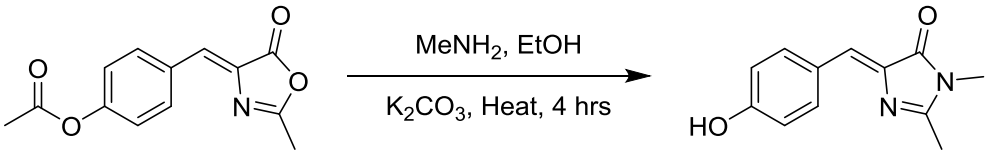

Prepared according to a previously reported procedure.[2] 0.230 g (1.09 mmol, 26.1%) as a yellow solid. ^{1}H NMR (500 MHz, DMSO-d_6) δ ppm 8.05 (2 H, d, *J*=8.44 Hz), 6.96 (1 H, s), 6.85 (2 H, d, *J*=8.80 Hz), 4.54 (1 H, br. s.), 3.10 (3 H, s), 2.38 (3 H, s)

tert-butyl 6-aminohexylcarbamate

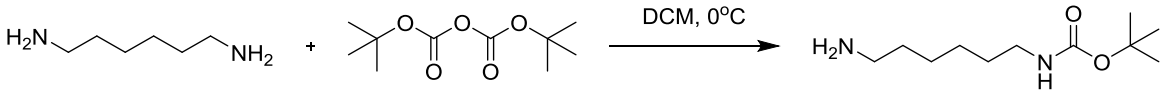

Prepared according to a previously reported procedure.[52]1.89g (8.7 mmol, 87%) as a colorless oil. ^{1}H NMR (500 MHz, $CDCl_3$) δ ppm: 4.59 (1 H, bs), 3.08 (2 H, bs), 2.66 (2 H, t, *J*=6.97 Hz), 1.52 - 1.06 (17 H, m).

Z-4-(4-hydroxybenzylidene)-1-(6-aminohexyl)-2-methyl-1H-imidazol-5(4H)-one (HBI-Hex)

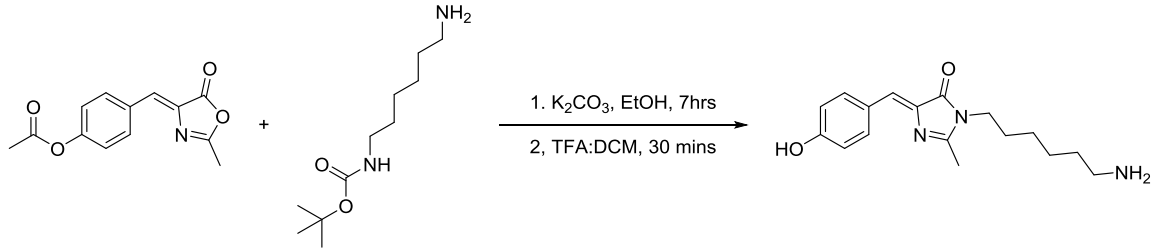

Prepared according to a previously reported procedure.[2] A supension of (Z)-4-((2-methyl-5-oxooxazol-4-(5H)-ylidene) methyl)phenyl acetate (1.00 g, 4.40 mmol), tert-butyl 6-aminohexylcarbamate and K_2CO_3 (0.564, 4.08 mmol), in ethanol (10 ml) was heated to reflux at 75°C. Reflux was maintained for 7 hrs before cooling the mixture to 25°C. The solution was poured into water (40 ml) and acidified to pH 3.0 with HCl. The precipitate was isolated by filtration and triturated with ethyl acetate. The precipitate was suspended in 1:1 TFA/DCM and stirring was maintained for 30 minutes. The reaction was concentrated in vacuuo. Flash chromatography was performed on of the residue eluting a polar gradient from 1:9:0.1 methanol/DCM/triethylamine to acetone over SiO_2 gave 0.160 g (0.53 mmol, 12%) of a yellow solid. ^{1}H NMR (500 MHz, DMSO-d_6) δ ppm 8.05 (2 H, d, *J*=8.98 Hz), 7.77 (1 H, br. s.), 6.87 (1 H, s), 6.80 (2 H, d, *J*=8.55 Hz), 3.53 (2 H,

t, *J*=7.27 Hz), 3.02 (2 H, m), 2.34 (3 H, s), 1.78 (2 H, s), 1.49 - 1.56 (2 H, m), 1.38-1.24 (6 H, m).

2,5-difluoro-4-hydroxybenzaldehyde

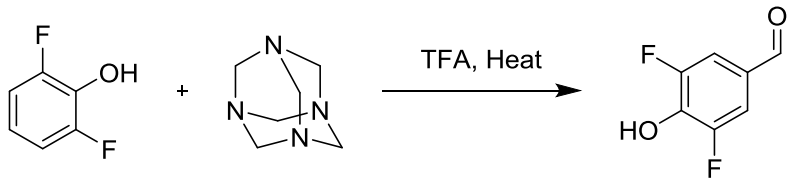

Prepared according to a previously reported procedure. [53] 75.6% yield (0.920 g, 5.81 mmol) of a cream colored solid. ^{1}H NMR (500 MHz, $CDCl_3$) δ ppm: 9.83 (1 H, s), 7.50 (2 H, d, *J*=7.70 Hz), 5.74 (1 H, bs)

(Z)- 2,5-difluoro-4-((2-methyl-5-oxooxazol-4-(5H)-ylidene)methyl)phenyl acetate (JMR1062)

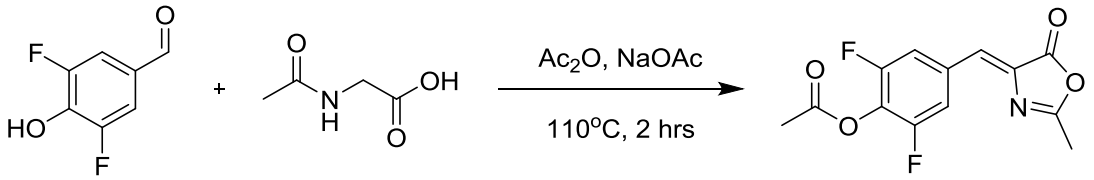

Prepared according to a previously reported procedure[2]. 55.4% yield (0.616 g, 2.19 mmol) as a yellow solid. ^{1}H NMR (500 MHz, $CDCl_3$) δ ppm: 7.77 (2 H, d, *J*=8.44 Hz), 6.97 (1 H, s), 2.43 (3 H, s), 2.40 (3 H, s)

Z-4-(4-hydroxy-3,5-difluorobenzylidene)-1,2-dimethyl-1H-imidazol-5(4H)-one (DFHBI)

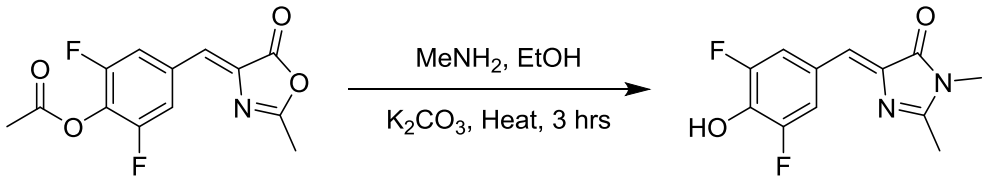

Prepared according to a previously reported procedure.[2] 53.5% yield (0.239 g, 0.95 mmol) as a bright yellow solid. ^{1}H NMR (500 MHz, DMSO-d_6) δ ppm 10.92 (1 H, bs), 7.97 (2 H, d, *J*=9.17 Hz), 6.90 (1 H, s), 3.09 (3 H, s), 2.36 (3 H, s)

8 (N-(2-azidoacetyl)-N-methylbenzamide)

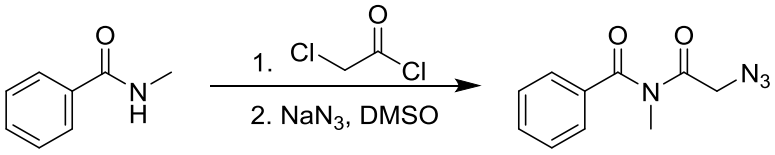

Prepared according to a previously reported procedure.[41] 3.10g (14.2 mmol, 71.1%) as a white solid. ^{1}H NMR (500 MHz, $CDCl_3$) δ ppm: 7.59 (3 H, m), 7.51 (2 H, t, *J*=7.00 Hz), 4.40 (2 H, s), 3.24 (3 H, s)

9 (1-methyl-2-phenyl-1H-imidazol-5(4H)-one)

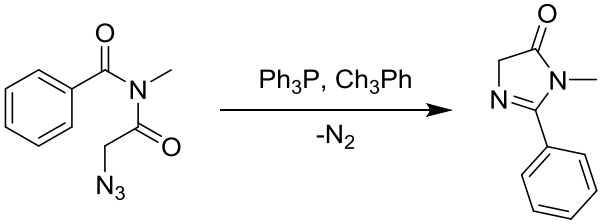

Prepared according to a previously reported procedure.[41] 0.927g (5.3mmol, 53%) of a red solid. ^{1}H NMR (500 MHz, $CDCl_3$) δ ppm: 7.62 (2 H, d, *J*=6.97 Hz), 7.55 (1 H, m), 7.51 (1 H, d, *J*=7.34 Hz), 4.28 (2 H, s), 3.14 (3 H, s)

10 (N-(hydroxyethyl)-N-methyl-5-aminothiophene-2-carboxaldehyde) (JMR1101)

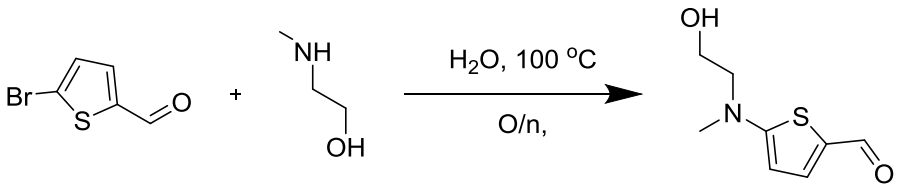

Prepared according to a previously reported procedure.[50] 1.33g (7.14 mmol, 68%) of a brown solid isolated. ^{1}H NMR (500 MHz, $CDCl_3$) δ ppm: 9.44 (1 H, s), 7.46 (1 H, d, *J*=4.40 Hz), 5.98 (1 H, d, *J*=4.40 Hz), 3.90 (2 H, t, *J*=5.50 Hz), 3.57 (2 H, t, *J*=10.60 Hz), 3.17 (3 H, s) ^{13}C NMR (126MHz ,DMSO-d_6) δ = 179.3, 167.2, 141.5, 124.7, 103.2, 57.8, 56.9, 40.8

ATI-1

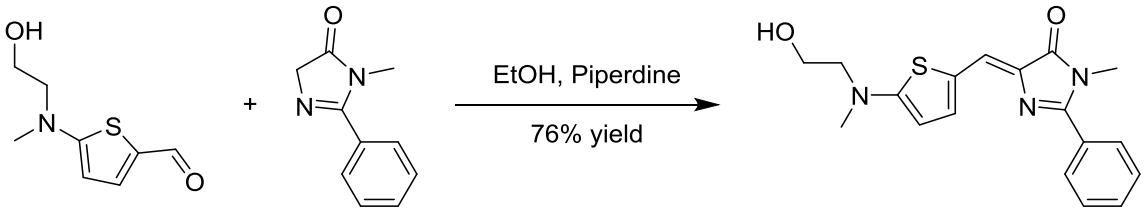

N-(hydroxyethyl)-N-methyl-5-aminothiophene-2-carboxaldehyde (0.556 g, 3 mmol) and 1-methyl-2-phenyl-1H-imidazol-5(4H)-one (0.522g, 3.0 mmol) were stirred in piperidine (15 ml) overnight. The solution was concentarted in vacuuo and the resulting red residue was subjected to flash chromatography on SiO_2 eluting with 5% MeOH/DCM which yielded 0.775 g (2.268 mmol, 76 %) of a metallic red solid. M.P. =161 °C; ^{1}H NMR (500 MHz, DMSO-d_6) δ ppm: 7.85 (2 H, d, *J*=3.67 Hz) 7.56 (3 H, d, *J*=3.67 Hz) 7.49 (1 H, s.) 7.32 (1 H, s) 6.11 (1 H, d, *J*=4.40 Hz) 4.87 (1 H, br. s.) 3.64 (2 H, d, *J*=4.40 Hz) 3.49 (1 H, t, *J*=11.00 Hz) 3.25 (3 H, s) 3.12 (3 H, s). ^{13}C NMR (126MHz ,DMSO-d_6) δ = 168.8, 168.6, 140.5, 130.4, 130.0, 128.8, 128.3, 124.1, 103.7, 79.3, 58.1, 57.0, 40.9, 28.6 $\lambda_{max\ abs}$

515nm (ε= 32,413 $M^{-1}cm^{-1}$), $\lambda_{max\ emiss}$566 nm, in EtOH; MS (ESI) m/z calcd for $(M+H)^+$ $C_{18}H_{20}N_3O_2S$ 342.13; found 342.13

Standard Procedure 1

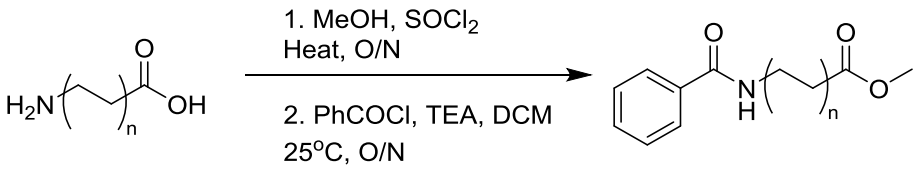

Prepared according to a previously reported procedure.[46] Thionyl chloride (3 eq.) was added drop wise to a stirring solution of amino acid (1 eq.) in methanol (10 eq) at 0°C over the course of 1 hr. The resulting solution was heated to 65°C in an oil bath and the heat was maintained 12 hrs. The solution was cooled to 25°C and the solvent was removed in vacuuo. The resulting solid was suspended in dry DCM (0.3 M) to which triethylamine (2.05 eq) was added. The resulting solution was cooled to 0°C and benzoyl chloride (1.05 eq) was added drop wise over 1 hour. The suspension is allowed to warm to room temperature overnight. The organic layer was washed with water (20 ml), 1.0 N HCl (2 x 30 ml), saturated $NaHCO_3$ (2 x 30 ml), and brine (1 x30 ml). The solution was dried over $MgSO_4$ before the solvent was removed in vacuuo.

methyl 6-benzamidohexanoate

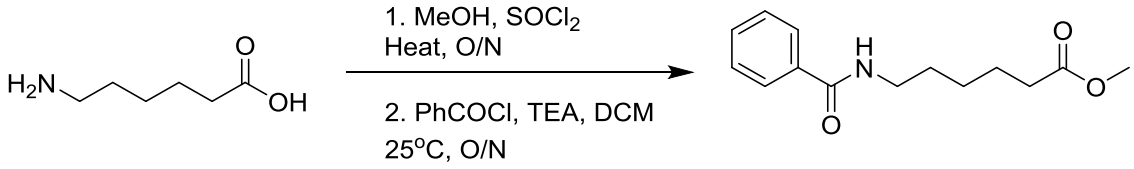

Prepared according to Standard Procedure 1. To a stirring suspension of 6-aminohexanoic acid (6.56 g, 50 mmol), in methanol (20.2 ml, 500 mmol) at 0°C, thionyl chloride (10.1 ml, 150 mmol) was added drop wise over 1 hour. The resulting solution was heated to

65^{o}C and allowed to reflux overnight. Upon cooling to room temperature the solvent was removed in vacuuo. The white solid was added to DCM (166 ml) followed by triethylamine (14.3 ml, 102.5 mmol). The solution was cooled to 0^{o}C and benzoyl chloride (6.1 ml, 52.5 mmol) was added drop wise over 1 hour. The solution was allowed to stir overnight at 25^{o}C before washing with water (20 ml), 1.0 N HCl (2 x 30 ml), saturated $NaHCO_3$ (2 x 30 ml), and brine (1 x30 ml). The solution was dried over $MgSO_4$ before the solvent was removed in vacuuo isolating 14.50 g (50 mmol, 100%) of a colorless oil. ^{1}H NMR (500 MHz, $CDCl_3$) δ ppm 7.77 (2 H, d, *J*=7.34 Hz), 7.49 (1 H, t, *J*=7.3 Hz), 7.42 (2 H, t, *J*=7.70 Hz), 6.29 (1 H, bs), 3.66 (3 H, s), 3.46 (2 H, q, *J*=6.97 Hz), 2.33 (2 H, t, *J*=7.34 Hz), 1.72-1.59 (4 H, m), 1.42 (2 H, m, *J*=7.70 Hz)

methyl N-(2-chloroacetyl)-6-benzamidohexanoate

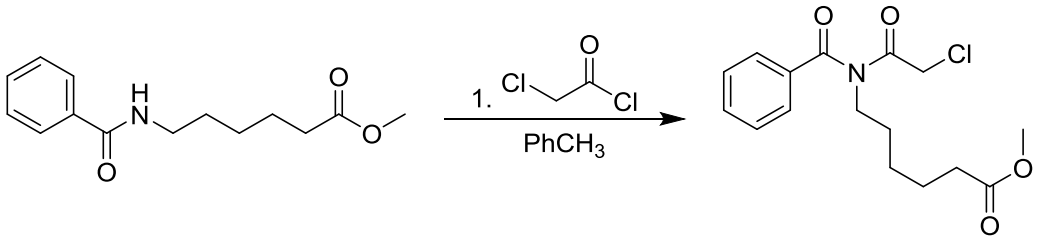

To a stirring solution of methyl 6-benzamidohexanoate (14.50g, 50mmol) in toluene (166 ml) was added chloroacetyl chloride (6.21 g, 55 mmol) drop wise. The mixture was heated to 110^{o}C and the heat was maintained for 11 hours. The reaction mixture was allowed cooled to 25^{o}C and the solvent was removed in vacuuo. Flash chromatography on the crude residue with DCM on SiO_2 yielded 6.40 g (19.65 mmol, 39.3%) of a colorless oil. ^{1}H NMR (500 MHz, $CDCl_3$) δ ppm: 7.63 (2 H, d, *J*=6.97 Hz), 7.59 (1 H, d, *J*=7.34 Hz), 7.50 (2 H, t, *J*=8.10 Hz), 4.41 (2 H, s), 3.73 (2 H, t, *J*=7.70 Hz), 3.64 (3 H, s), 2.24 (2 H, t, *J*=7.34 Hz), 1.57 (4 H, m, *J*=11.40 Hz), 1.23 (3 H, m, *J*=7.70 Hz)

N-(2-azidoacetyl)-6-benzamidohexanoate

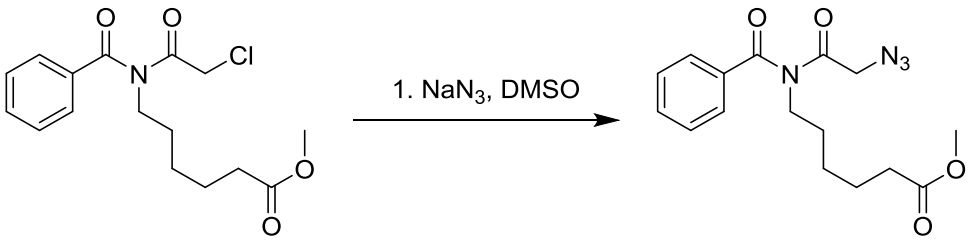

To a stirring solution of methyl N-(2-chloroacetyl)-6-benzamidohexanoate (6.404g, 19.6 mmol), in DMSO (40 ml), was added sodium azide (2.60g, 40 mmol) in one portion. The reaction was stirred for 45 minutes before pouring into water (160ml). The aqueous solution was extracted with ethyl acetate (3 x 30ml). The organic solution was washed with water (30 ml) and brine (30 ml) before drying over $MgSO_4$ and removing the solvent under reduced pressure. Flash chromatography on the residue with EtOAc on SiO_2 yielded 5.65 g (16.95 mmol, 86.7 %) of a yellow oil. ^{1}H NMR (500 MHz $CDCl_3$) δ ppm: 7.57 (3 H, m), 7.47 (2 H, t, *J*=7.30 Hz), 4.17 (2 H, s), 3.71 (2 H, t, *J*=7.70 Hz), 3.61 (3 H, s), 2.21 (2 H, t, *J*=7.34 Hz), 1.52 (4 H, m), 1.18 (2 H, m, *J*=7.70 Hz). ^{13}C NMR (126MHz ,$CDCl_3$) δ ppm: 174.1, 173.7, 171.6, 135.6, 134.3, 132.6, 128.9, 128.1, 77.3, 54.3, 51.4, 46.9, 33.6, 28.4, 26.1, 24.2

11 (methyl 3-benzamidopropionate)

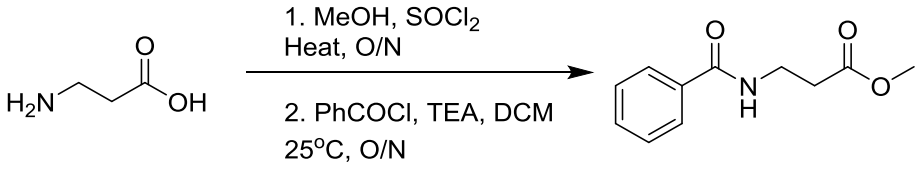

Prepared according to Standard Procedure 1. To a stirring suspension of β-alanine (4.45g, 50 mmol), in methanol (20.2 ml, 500 mmol) at 0°C, thionyl chloride (10.1 ml, 150 mmol) was added drop wise over 1 hour. The resulting solution was heated to 65°C and the

reflux was maintained for 12 hrs. The mixture was allowed to cool to 25^{o}C and the solvent was removed in vacuuo. The white solid was added to DCM (166 ml) followed by triethylamine (14.3 ml, 102.5 mmol). The solution was cooled to 0^{o}C and benzoyl chloride (6.1 ml, 52.5 mmol) was added drop wise over 1 hour. The solution was allowed to stir overnight before washing with H_2O (20 ml), 1.0 N HCl (2 x 30 ml), saturated $NaHCO_3$ (2 x 30 ml), and brine (1 x30 ml). The solution was dried over $MgSO_4$ before the solvent was removed in vacuuo isolating 9.63 g (48 mmol, 96%) of a waxy solid ^{1}H NMR (500 MHz, $CDCl_3$) δ ppm 7.77 (2 H, d, *J*=6.97 Hz), 7.49 (1 H, t, *J*=7.70 Hz), 7.42 (2 H, t, *J*=7.70 Hz), 6.89 (1 H, bs), 3.74 (2 H, t, *J*=5.90 Hz), 3.71 (3 H, s), 2.66 (2 H, t, *J*=5.87 Hz). ^{13}C NMR (75MHz ,$CDCl_3$) δ = 173.0, 167.3, 134.2, 131.3, 128.3, 126.8, 51.6, 35.2, 33.5. MS (ESI) m/z calcd for (M+Na) $C_{11}H_{13}NO_3Na$=230.0778 found 230.0772.

12 (N-(2-azidoacetyl)-3-benzamidopropionate)

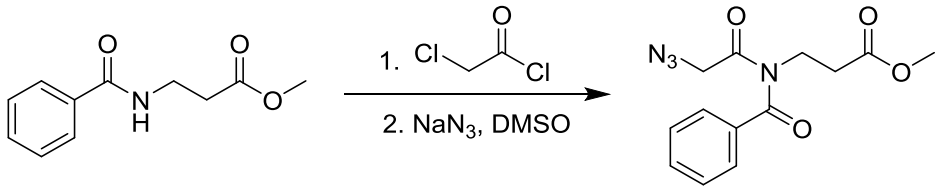

To a solution of methyl 3-benzamidopropionate (4.14g, 20 mmol), in toluene (66 ml), was added chloroacetyl chloride (2.48 g, 22 mmol) drop wise. The solution was heated to 110^{o}C and the reflux was maintained for 16 hrs. The reaction was cooled to 25^{o}C and the toluene was removed under reduced pressure. DMSO (40ml) was added to the brown residue before sodium azide (2.60 g, 40 mmol) was added in one portion. The solution was stirred for 15 minutes at 25 ^{o}C before pouring into water (120 ml). The cloudy

solution was extracted with ethyl acetate (3 x 30ml) and diethyl ether (1 x 30 ml). The organics were combined and washed with water (30 ml) and brine (30ml) before drying over $MgSO_4$ and concentrating under reduced pressure. Flash chromatography on the crude residue with 5% EtOAc/DCM on SiO_2 yielded 2.66 g (9.16 mmol, 45 %) of a colorless oil. ^{1}H NMR (500 MHz, $CDCl_3$) δ ppm: 7.64 (3 H, d, *J*=7.34 Hz), 7.60 (1 H, t, *J*=7.30 Hz), 7.50 (2 H, t, *J*=7.70 Hz), 4.20 (2 H, s), 4.02 (2 H, t, *J*=6.42 Hz), 3.62 (3 H, s), 2.69 (2 H, t, *J*=6.42 Hz), ^{13}C NMR (126MHz , $CDCl_3$) δ ppm: 173.7, 171.6, 171.4, 134.1, 132.9, 129.0, 128.5, 100.5, 77.3, 77.1, 76.8, 53.9, 51.8, 43.2, 32.6 MS (ESI) m/z calcd for (M+Na)$C_{13}H_{14}N_4O_4$=313.0907 Found 313.0887

13 (1-(methyl propionate)-2-phenyl-1H-imidazol-5(4H)-one)

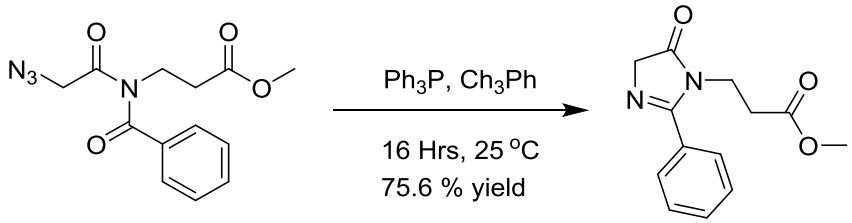

To a stirring solution of N-(2-azidoacetyl)-3-benzamidopropionate (2.10 g, 7.23 mmol) in dry toluene (25 ml) was added triphenyl phosphine (2.08g, 7.95 mmol) in one portion. After stirring for 16 hrs, 15 ml of hexanes were added and the precipitate was removed. The filtrate was concentrated under reduced pressure Flash chromatography on the red residue with 1:1 ethyl acetate/ dichloromethane on SiO_2 yielded 73.5 % (1.31 g, 5.32 mmol) of a colorless oil. ^{1}H NMR (500MHz ,$CDCl_3$) δ = 7.56 - 7.51 (m, 2 H), 7.51 - 7.44 (m, 3 H), 4.22 (s, 2 H), 3.84 (t, *J* = 7.5 Hz, 3 H), 3.54 (s, 5 H), 2.51 (t, *J* = 7.3 Hz, 3 H) ^{13}C NMR (126MHz ,$CDCl_3$-d) δ = 181.6, 170.6, 164.3, 130.9, 129.6, 128.8, 127.7, 77.2, 58.5, 51.6, 37.2, 32.4

ATI-2

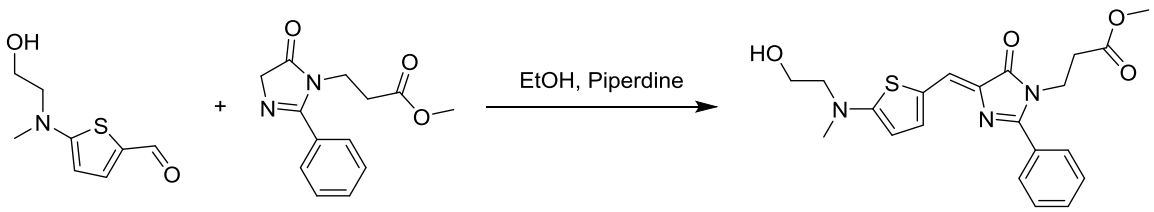

N-(hydroxyethyl)-N-methyl-5-aminothiophene-2-carboxaldehyde (0.58 g, 3.13 mmol) and 1--(methyl propionate)-2-phenyl-1H-imidazol-5(4H)-one (0.77g, 3.13 mmol) were stirred in piperdine (15 ml) for 16 hrs. The piperdine was removed in vacuuo and the redresidue was subjected to flash chromatography on $SiO_{2\ eluting}$ with 5% MeOH/DCM which yielded 57.4 % (0.740 g, 1.8 mmol) of a metallic red solid. ^{1}H NMR (500MHz ,DMSO-d_6) δ = 7.78 - 7.73 (m, 2 H), 7.58 - 7.53 (m, 3 H), 7.50 (br. s., 1 H), 6.11 (d, *J* = 4.4 Hz, 1 H), 4.89 (t, *J* = 4.4 Hz, 1 H), 3.96 (t, *J* = 7.3 Hz, 2 H), 3.66 - 3.59 (m, 2 H), 3.48 (s, 3 H), 3.11 (s, 2 H), 2.59 (t, *J* = 7.2 Hz, 2 H)^{13}C NMR (126MHz ,DMSO-d_6) δ = 170.8, 168.7, 168.5, 154.2, 140.7, 130.2, 130.1, 128.8, 128.6, 128.1, 124.3, 120.9, 103.7, 58.0, 56.9, 51.4, 40.7, 37.2, 32.7 MS (ESI) m/z calcd for $(M+H)^+$ $C_{21}H_{23}N_3O_4S$ 414.14; found 414.1482

ATI-2A

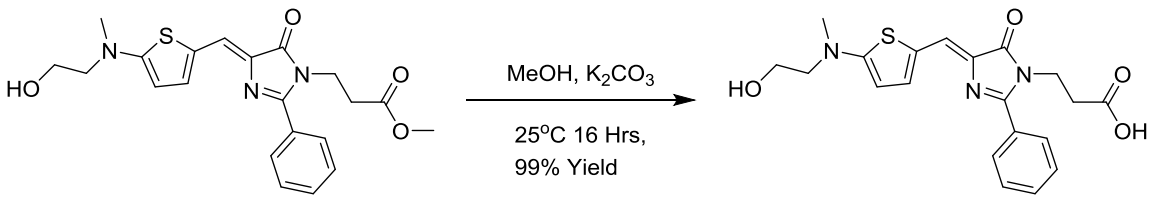

To a suspension of ATI-2 (1.247 g, 3.0 mmol) in 1:1 water/ methanol (15 ml) was added K_2CO_3 (0.833 g, 6.0 mmol). The reaction was stirred for 3 days at 25^oC before removing the methanol under reduced pressure. The solution was neutralized by the addition of glacial acetic acid to the pH of 3.0. The solution was chilled to 4^oC and the precipitate was isolated. The green solid was dried in vacuuo yielding 75% (2.2 mmol, 0.910 g). ^1H NMR (500MHz ,DMSO-d_6) δ = 7.75 (d, *J* = 5.1 Hz, 1 H), 7.59 - 7.52 (m, 2 H), 7.48 (br. s., 1 H), 7.31 (s, 1 H), 6.12 (d, *J* = 4.4 Hz, 1 H), 3.89 (t, *J* = 7.3 Hz, 2 H), 3.61 (t, *J* = 5.5 Hz, 2 H), 3.48 (t, *J* = 5.1 Hz, 2 H), 3.10 (s, 3 H), 2.44 (t, *J* = 7.0 Hz, 2 H)^{13}C NMR (126MHz ,DMSO-d_6) δ = 172.5, 168.7, 168.6, 154.4, 140.7, 130.2, 130.2, 128.8, 128.1, 124.2, 120.9, 103.8, 57.9, 56.9, 40.8, 37.6, 33.6; $\lambda_{max\ abs}$ 527nm (ε= 57,000 $M^{-1}cm^{-1}$), $\lambda_{max\ emiss}$566 nm; ϕ= 0.0067±0.0001. MS (ESI) m/z calcd for $(M+H)^+$ $C_{20}H_{22}N_3O_4S$ 400.13; found 400.1326

ATI-2B

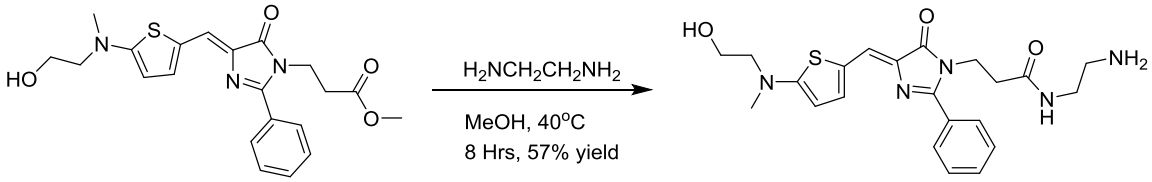

To a solution of ATI-2, in methanol (1 ml) was added ethylene diamine (1ml). The mixture was stirred at 40^o C for 8 hrs before cooling to 25 ^{o}C. The solvent was removed in vacuuo and the residue was solvated into a minimum amount of chloroform (1 ml) before adding to 1:1 hexanes/ diethyl ether. The suspension was cooled to 0 ^{o}C and the precipitate was isolated, washed with hexanes and dried in vacuuo yielding 59% (62 mg, 0.142 mmol) of a dark red powder. ^1H NMR (500MHz , DMSO-d_6) δ = 7.77 (br. s., 4 H),

7.55 (br. s., 6 H), 7.49 (br. s., 2 H), 7.31 (s, 2 H), 6.11 (d, *J* = 4.4 Hz, 2 H), 4.90 (br. s., 2 H), 3.89 (t, *J* = 7.5 Hz, 4 H), 3.62 (t, *J* = 5.0 Hz, 4 H), 3.48 (t, *J* = 4.8 Hz, 4 H), 3.33 (br. s., 7 H), 3.11 (s, 6 H), 2.99 - 2.93 (m, *J* = 7.0 Hz, 3 H), 2.40 - 2.34 (m, 4 H). ^{13}C NMR (126MHz ,DMSO-d_6) δ = 169.4, 168.7, 168.6, 154.4, 140.6, 130.2, 130.1, 128.8, 128.2, 127.9, 127.8, 124.1, 120.9, 103.7, 58.0, 56.9, 41.5, 40.7, 38.0, 34.5 MS (ESI) m/z calcd for $(M+H)^+$ $C_{22}H_{28}N_5O_3S$ 442.1907; found 442.1886

methyl 3-[(4*Z*)-4-(N,N-dimethyl-4-aminobenzylidene)-5-oxo-2-phenyl-4,5-dihydro-1*H*-imidazol-1-yl]propanoate

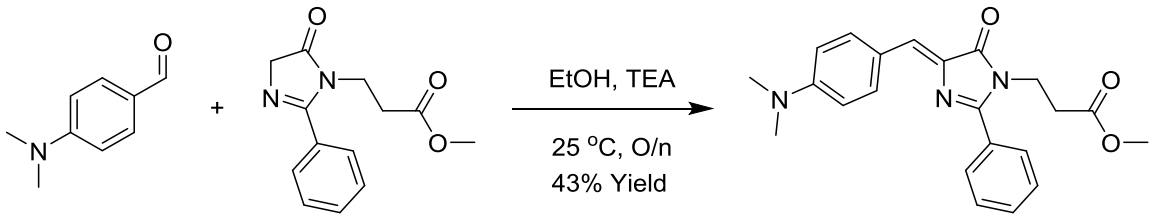

To a solution of 1-(methyl propionate)-2-phenyl-1H-imidazol-5(4H)-one (0.517 g, 2 mmol) (0.313 g, 2.00 mmol) in triethylamine (10 ml) and ethanol (2 ml) was added N,N-dimethyl 4-aminobenzaldhyde and the suspension was allowed to stir for 16 hrs at 25^{o}C. The mixture was cooled to -20 ^{o}C and the precipitate was isolated yielding 43% (0.327 g, 0.86 mmol) of an orange powder. ^{1}H NMR (500MHz ,$CDCl_3$) δ = 8.15 (d, *J* = 8.4 Hz, 2 H), 7.76 (d, *J* = 4.0 Hz, 2 H), 7.53 (s, 4 H), 7.23 (s, 1 H), 6.70 (d, *J* = 8.4 Hz, 2 H), 4.10 (t, *J* = 7.5 Hz, 2 H), 3.61 (s, 3 H), 3.05 (s, 6 H), 2.68 (t, *J* = 7.5 Hz, 2 H); ^{13}C NMR (126MHz , $CDCl_3$) δ = 171.2, 171.0, 158.4, 151.7, 134.7, 134.5, 130.8, 129.9, 128.8, 128.3, 122.2, 111.7, 51.7, 40.0, 37.5, 33.0 MS (ESI) m/z calcd for $(M+H)^+$ $C_{22}H_{24}N_3O_3$ 378.1812; found 378.1790

14 [methyl 3-[(4*Z*)-4-(N,N-dimethyl-4-aminobenzylidene)-5-oxo-2-phenyl-4,5-dihydro-1*H*-imidazol-1-yl]propanoic acid]

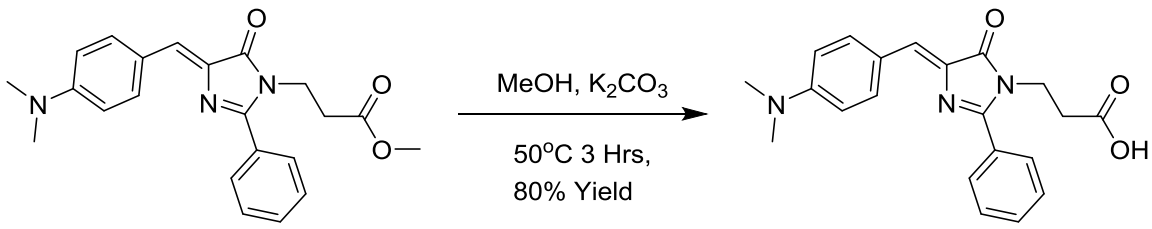

A suspension of methyl 3-[(4*Z*)-4-(N,N-dimethyl-4-aminobenzylidene)-5-oxo-2-phenyl-4,5-dihydro-1*H*-imidazol-1-yl]propanoate (0.100 g, 0.26 mmol) and K_2CO_3 (0.103g, 0.52mmol) in 3 ml of 1:1 methanol/ water was stirred for 3 days at 25 ^{o}C. Methanol (3 ml) was added and the suspension was heated to 50 ^{o}C for 3 hrs. The solution was allowed to cool to 25 ^{o}C. The solution was acidified to pH 3.0 with glacial acetic acid and extracted with methylene chloride (3 x 10 ml). The organic layers were combined, dried over $MgSO_4$, and concentrated under reduced pressure. The red residue was recrystallized in methanol yielding 80% (0.075 g, 0.21 mmol) of a red solid. $\lambda_{max\ abs}$ 474nm (ε= 37,000 $M^{-1}cm^{-1}$), $\lambda_{max\ emiss}$ 559 nm; ϕ= 0.0034±0.0001. ^{1}H NMR (500MHz ,DMSO-d_6) δ = 8.14 (d, *J* = 8.4 Hz, 2 H), 7.82 (d, *J* = 7.3 Hz, 2 H), 7.63 - 7.56 (m, 3 H), 7.07 (s, 1 H), 6.77 (d, *J* = 8.8 Hz, 2 H), 3.93 (t, *J* = 7.5 Hz, 2 H), 3.17 (s, 1 H), 3.07 - 2.99 (m, 7 H). MS (ESI) m/z calcd for $(M+H)^+$ $C_{21}H_{222}N_3O_3$ 364.1656; found 364.165

methyl 3-[(4*Z*)-4-(3,5-difluoro-4-hydroxybenzylidene)-5-oxo-2-phenyl-4,5-dihydro-1*H*-imidazol-1-yl]propanoate

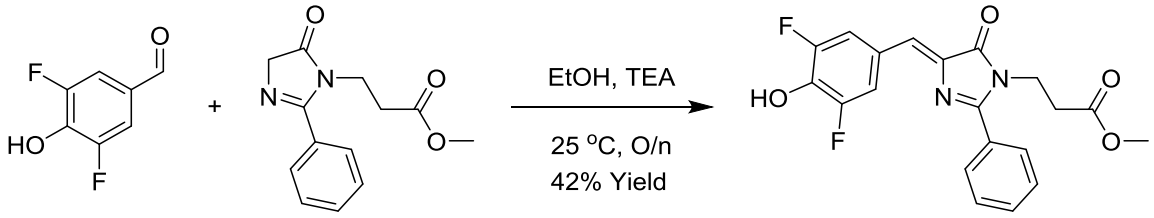

To a suspension of 1-(methyl propionate)-2-phenyl-1H-imidazol-5(4H)-one (0.543 g, 2.2 mmol) in triethylamine (10 ml) and ethanol (4 ml was added 3,5-difluoro-4-hydroxybenzaldhyde (0.350 g, 2.20 mmol). The reaction was allowed to stir for 16 hrs at 25 ^{o}C. The precipitate was isolated and subjected to flash chromatography with 2% MeOH/DCM on SiO_2 yielding 42% (0.360 g, 0.92 mmol) of a yellow powder. ^{1}H NMR (500MHz ,DMSO-d_6) δ = 8.03 (d, *J* = 8.4 Hz, 2 H), 7.84 (d, *J* = 7.7 Hz, 2 H), 7.68 - 7.58 (m, 3 H), 7.11 (s, 1 H), 3.97 (t, *J* = 7.2 Hz, 2 H), 3.49 (s, 3 H), 2.60 (t, *J* = 7.2 Hz, 2 H); ^{13}C NMR (126MHz ,DMSO-d_6) δ = 170.7, 170.2, 162.4, 152.8 (d, J=7.4Hz), 150.9 (d, J=7.4 Hz), 137.9, 137.9, 136.3 (t, J=16.6), 131.5, 129.1, 129.0, 128.4, 125.4, 124.5 (t, J=9.2 Hz), 115.6 (d, J=5.5 Hz), 115.5 (d, J=7.4 Hz), 51.5, 37.5, 32.20 MS (ESI) m/z calcd for $(M+NA)^{+}$ $C_{20}H_{16}F_2N_2O_4Na$ 409.0970; found 409.0969

15 [methyl 3-[(4*Z*)-4-(3,5-difluoro-4-hydroxybenzylidene)-5-oxo-2-phenyl-4,5-dihydro-1*H*-imidazol-1-yl]propanooc acid]

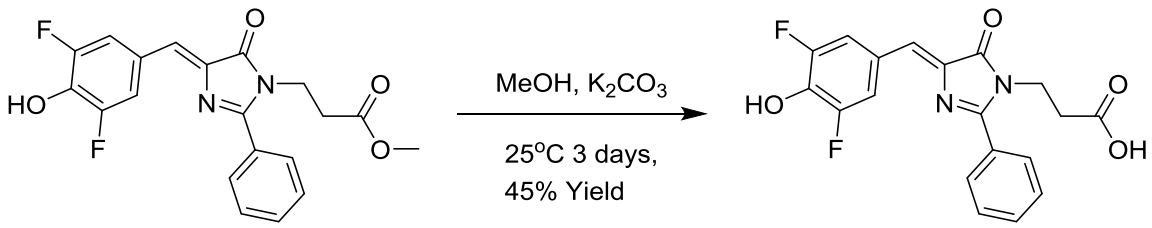

A suspension of methyl 3-[(4*Z*)-4-(3,5-difluoro-4-hydroxybenzylidene)-5-oxo-2-phenyl-4,5-dihydro-1*H*-imidazol-1-yl]propanoate (0.174 g, 0.45 mmol) and K_2CO_3 (0.124g, 0.90 mmol) in 3 ml of 1:1 methanol/ water was stirred for 3 days at 25 ^{o}C. The solution was acidified to pH 1.0 with HCl and extracted with ethyl acetate (3 x 10 ml). The organic layers were combined, dried over $MgSO_4$, and concentrated under reduced pressure. The yellow residue was subjected to flash chromatography on SiO_2 eluting with a polar gradient from 3% methanol/DCM to 10% methanol/DCM yielding 47% (0.078 g, 0.20 mmol) of a yellow solid. $\lambda_{max\ abs}$ 445nm (ε= 32,500 $M^{-1}cm^{-1}$), $\lambda_{max\ emiss}$537 nm; ϕ= 0.0016±0.0001 in 100mM HEPES @ pH 7.4. ^{1}H NMR (500MHz ,DMSO-d_6) δ = 8.01 (d, *J* = 8.4 Hz, 2 H), 7.84 (d, *J* = 8.1 Hz, 1 H), 7.66 - 7.57 (m, 3 H), 7.08 (s, 1 H), 3.93 (t, *J* = 7.2 Hz, 2 H), 2.52 (t, *J* = 7.7 Hz, 2 H). ^{13}C NMR (126MHz ,DMSO-d_6) δ = 171.9, 170.3, 162.6, 152.9 (d, J=7.4 Hz), 151.0 (d, J=7.4 Hz), 138.0, 136.4 (t, J=16.65 Hz), 131.6, 129.3, 129.0, 128.5, 125.4, 124.5 (t, d=9.2 Hz), 115.6 (dd, J=5.5 Hz), 37.6, 32.5. MS (ESI) m/z calcd for $(M+NA)^{+}$ $C_{19}H_{14}F_2N_2O_4Na$ 395.0814; found 395.0804

17 [(1E,2E)-1,2-Bis[(N-methylpyrrol-2-yl)methylene]hydrazine]

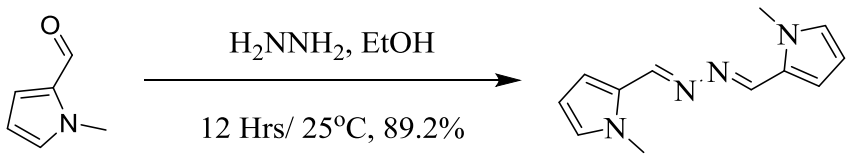

Prepared according to a previously reported procedure.[40] 12.375 g(57.75 mmol, 89%) of a yellow powder. ^{1}H NMR (500MHz ,$CDCl_3$) δ = 8.53 (s, 1 H), 6.80 (s, 1 H), 6.64(m, 1 H), 6.21 (td, *J* = 2.0, 4.0 Hz, 1 H), 4.00 (s, 3 H)

18 [(1E,2E)-1,2-Bis[(5-bromo N-methylpyrrol-2-yl)methylene]hydrazine]

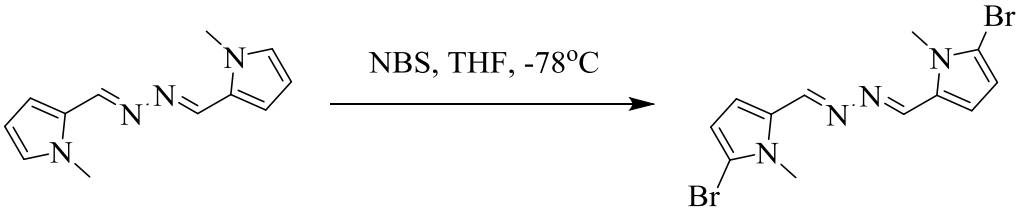

Prepared according to a previously reported procedure.[40] 2.97 g(7.9 mmol, 80%) of a yellow-green powder. ^{1}H NMR (500MHz ,$CDCl_3$) δ = 8.43 (s, 2 H), 6.60 (d, *J* = 2.9 Hz, 2 H), 6.29 (d, *J* = 4.0 Hz, 2 H), 4.07 - 3.92 (m, 6 H)

19 (5-Bromo N-methylpyrrole-2-carbaldehyde)

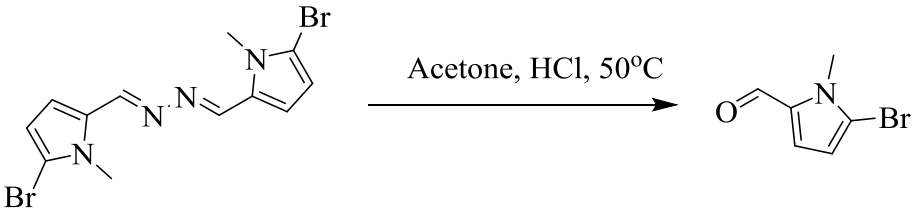

Prepared according to a previously reported procedure.[40] 5.70 g(30.3 mmol, 51%) of a yellow powder. ^{1}H NMR (300MHz ,CHLOROFORM-d) δ = 9.38 (s, 1 H), 6.89 (d, *J* = 4.2 Hz, 1 H), 6.33 (d, *J* = 4.2 Hz, 1 H), 3.97 (s, 3 H)

22 (3,6-dibromophenanthrenequinone)

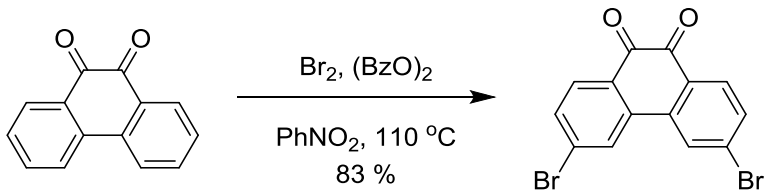

Prepared according to a previously reported procedure.[48,49] To a suspension of , 9,10-phenanthrenequinone (20.4 g, 98 mmol) and benzoyl peroxide (1.95 g, 8.0 mmol) in nitrobenzene was added bromine drop wise (10.2 ml, 199 mmol). The reaction was heated to 110 ^{o}C. The temperature was maintained for 16 hrs before allowing the reaction to cool to 25^{o}C. The precipitate was isolated, washed extensively with hexanes, and dried in vacuuo yielding 83% (29.76 g, 81.3 mmol) of a gold solid. ^{1}H NMR (500MHz ,$CDCl_3$) δ = 8.13 (s, 2 H), 8.08 (dd, *J* = 2.0, 8.3 Hz, 2 H), 7.68 (td, *J* = 1.9, 8.3 Hz, 2 H)

23 (3,6-Dibromo-9H-fluoren-9-one)

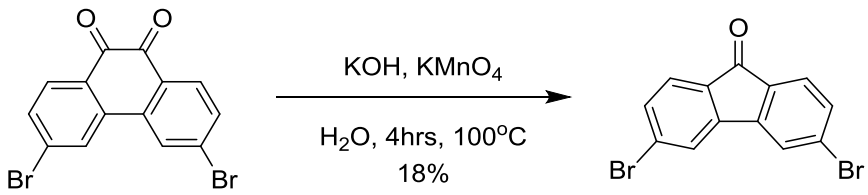

Prepared according to a previously reported procedure.[48,49] To a solution of KOH (144.7 g, 2.43 mols) in 405 ml H_2O was added 3,6 dibromophenanthrenequinone (28.86 g, 78.8 mmol). The suspension was allowed to stir for 3 hrs at 80 ^{o}C before $KMnO_4$ (64.23 g, 406.5 mmol) was added portion wise over the course of 1 hour. The temperature was increased to 110 ^{o}C and the temperature was maintained for 3 hours. The reaction was allowed to cool to 25 ^{o}C and the resulting suspension was filtered. The solids were resuspended in H_2O, heated to 80 ^{o}C and enough sodium metabisulfite was added to turn

the suspension pale yellow. The solids were isolated by filtration and lyophilized for 2 days to remove excess water. The solids were then subjected to soxhlet extraction in toluene for 3 days. The gold flakes were subsequently recrystallized in 1.0 l of toluene yielding 30.6 % (8.159 g, 24.1 mmol) of yellow flakes. ^{1}H NMR (500MHz ,DMSO-d_6) δ = 8.24 (s, 2 H), 7.66 - 7.63 (m, 2 H), 7.57 (d, *J* = 7.3 Hz, 2 H)

24 (3,6-(1-Dipiperidinyl)-9H-fluoren-9-one)

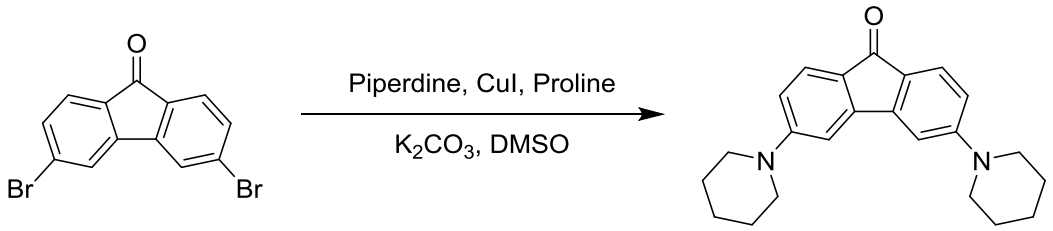

To a suspension of 3,6-Dibromo-9H-fluoren-9-one (0.338g, 1.0 mmol), CuI (40 mg, 0.20mmol), proline (30 mg, 0.26 mmol) and K_2CO_3 (0.580 g, 4 mmol) in DMSO (5 ml) was added piperdine (0.60 ml, 6.0 mmol). The reaction was heated to 100 ^{o}C and stirred for 12 hours before more piperdine (0.30 ml, 3 mmol), CuI (20 mg, 0.10 mmol) and proline (24 mg, 0.21 mmol) were added.The temperature was maintained for 16 more hours in till no sign of starting material remained (according to TLC). The reaction was cooled to 25 ^{o}C and poured into 1:1 ethyl acetate/ H_2O (50 ml). The layers were separated and the aqueous layer was extracted with ethyl acetate (2 x 25 ml). The organic layers were combined, dried over $MgSO_4$ and the solvent was removed under reduced pressure. Flash chromatography on SiO_2 eluting with 20 % ethyl acetate/hexanes yielded 62.4 % (0.216 g, 0.624 mmol) of red solid. ^{1}H NMR (500MHz ,$CDCl_3$) δ = 7.50 (d, *J* = 8.4 Hz, 2 H), 6.98 (s, 2 H), 6.65 (d, *J* = 8.4 Hz, 2 H), 3.45 - 3.34 (m, 8 H), 1.75 - 1.61 (m, 12 H)

2-amino-1,1,3-tricyano-1-propene

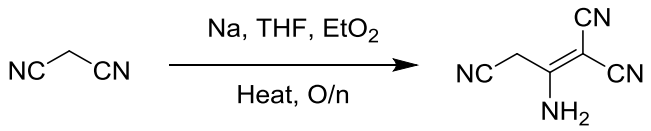

Prepared according to a previously reported procedure.[54] 8.6 g (65.1 mmol, 52 %) of a brown needles. ^{1}H NMR (500 MHz, DMSO-d_6) δ ppm 9.00 (2 H, d, *J*=22.37 Hz), 3.84 (2 H, s). ^{13}C NMR (126MHz ,DMSO-d_6) δ ppm: 164.8, 115.4, 114.7, 114.3, 22.2.

25 (N-(Actoxyethyl)-N-methyl-5-aminothiophene-2-carboxaldehyde)

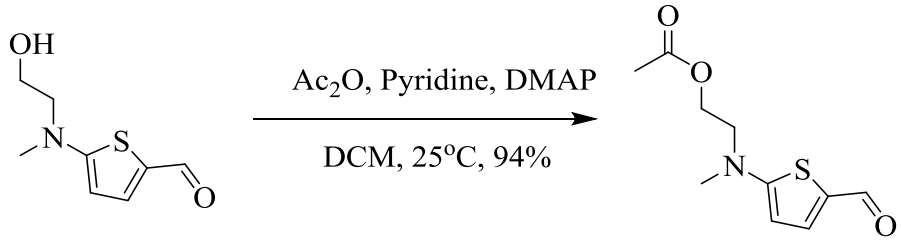

To a solution of 10 (0.926 g, 5.0 mmol), pyridine (0.44 ml, 5.5 mmol), 4-(N,N-dimethyl)aminopyridine (0.061 g, 0.5 mmol) in DCM (25 ml) was added acetic anhydride (0.52 ml, 5.5 mmol) drop wise. The reaction was allowed to stir for 3 days at 25 ^{o}C before washing with H_2O (2 x 25 ml), 0.1 M HCl (3 x 25 ml), saturated $NaHCO_3$ (1 x 25 ml) and saturated brine (1 x 25 ml). The reaction was dried over $MgSO_4$ and the solvent was removed under reduced pressure yielding 94% (1.03 g, 4.7 mmol) of a black oil. ^{1}H NMR (500MHz ,$CDCl_3$) δ = 9.51 (d, *J* = 1.8 Hz, 1 H), 7.48 (d, *J* = 4.4 Hz, 1 H), 5.98 (d, *J* = 4.4 Hz, 1 H), 4.31 (t, *J* = 5.5 Hz, 2 H), 3.65 (t, *J* = 5.7 Hz, 2 H), 3.13 (s, 3 H), 2.03 (s, 3 H)

26

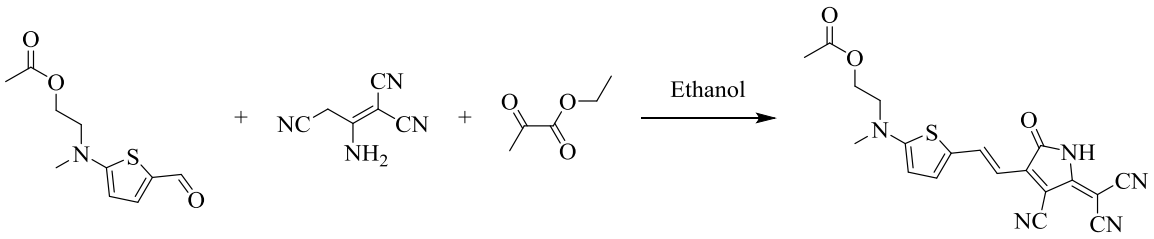

A solution of 2-amino-1,1,3-tricyano-1-propene**(** 0.85 g, 6.7 mmol) and ethyl pyruvate (1.55 g, 1.49 ml, 13.4 mmol) was heated in ethanol (4 ml) at 80 ^{o}C, under N_2 while stirring, for one hour before a solution of N-(actoxyethyl)-N-methyl-5-aminothiophene-2-carboxaldehyde (1.03 g, 4.7 mmol) in ethanol (2 ml) was added drop wise. The heating and stirring was continued for 3 hrs before cooling to -20 ^{o}C. The green precipitate was washed extensively with ethanol and allowed to air dry yielding 58.9 % (1.09 g, 2.77 mmol) of a virtually insoluble material. ^{1}H NMR (500MHz ,DMSO-d_6) δ = 8.60 (d, *J* = 9.2 Hz, 1 H), 8.03 (s., 1 H), 7.05 (s., 1 H), 6.14 (d, *J* = 11.0 Hz, 1 H), 4.35 (s, 1 H), 4.04 (s, 1 H), 3.43 (s., 3 H), 1.97 (s, 3 H)

27

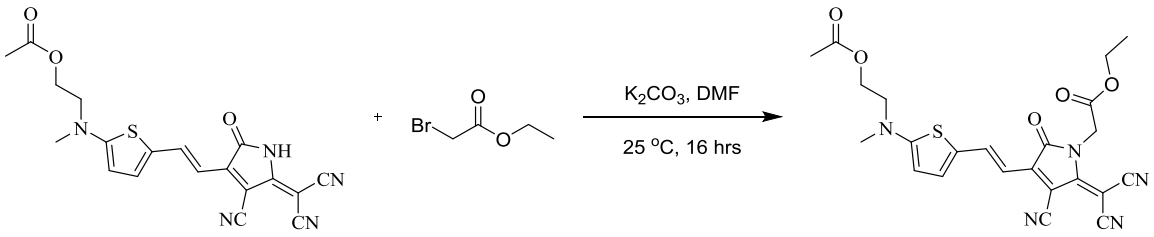

To a dry single neck round bottom flask was added JMR 2056 (0.100 g, 0.25 mmol), ethyl bromoacetate (0.046 g, 0.28 mmol), K_2CO_3 (0.0691 g, 0.28 mmol) and dry N,N-dimethyl formamide (1 ml). The reaction was allowed to stir at 25 ^{o}C for 16 hrs before 10 ml H_2O were added. The solution was extracted with DCM (3 x 20 ml), The organic

solution was washed with brine (10 ml) dried over $MgSO_4$. The solvent was removed under reduced pressure. The residue was dried in vacuuo yielding 91.7 % (0.11 g, 0.23) mmol of a slightly more soluble green solid. ^{1}H NMR (500MHz ,$CDCl_3$) δ = 8.50 (d, *J* = 13.2 Hz, 1 H), 7.47 (s., 1 H), 6.44 (d, *J* = 2.9 Hz, 1 H), 6.31 (d, *J* = 13.2 Hz, 1 H), 4.76 (s, 2 H), 4.39 (t, *J* = 5.3 Hz, 1 H), 4.28 (q, *J* = 7.0 Hz, 1 H), 3.88 (t, *J* = 5.1 Hz, 1 H), 3.37 (s, 3 H), 2.03 (s, 3 H), 1.31 (t, *J* = 7.2 Hz, 2 H)

APPENDIX B

UV- VISIBLE SPECTRA

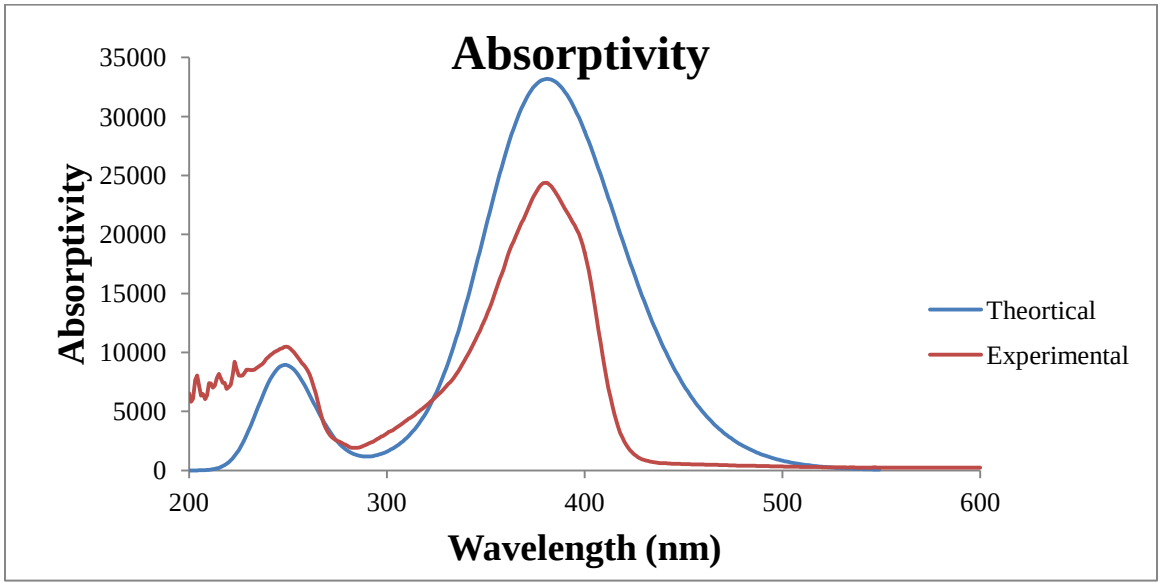

Figure 15-Absorptivity of DMHBI

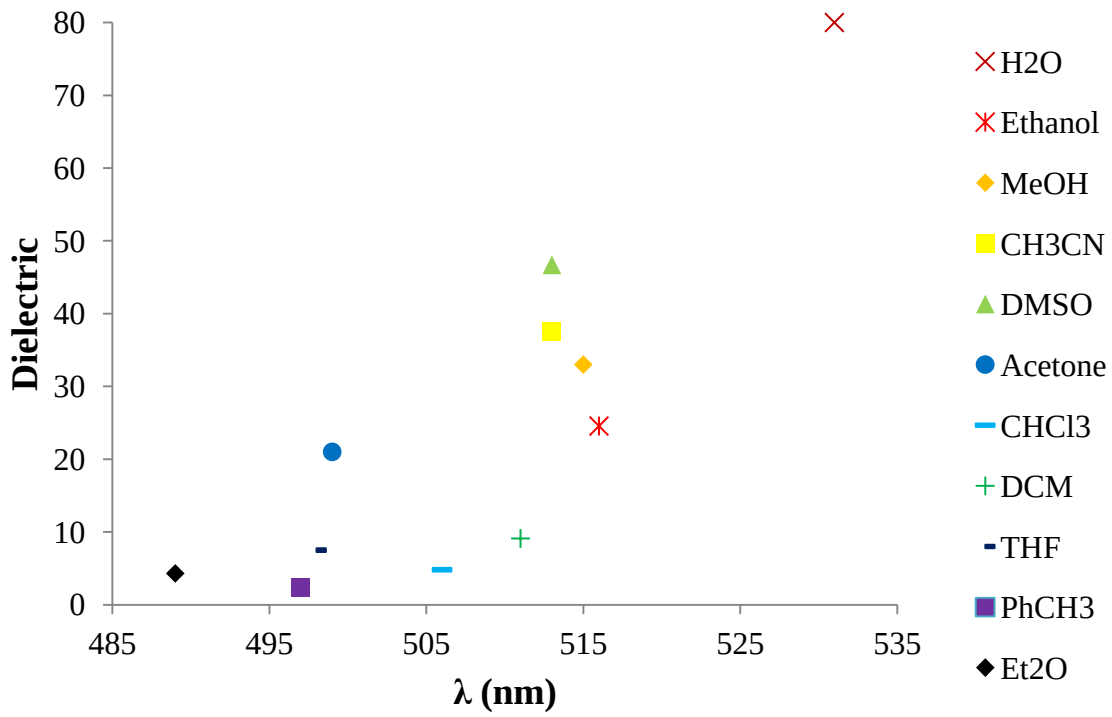

Figure 16-Solvatochromisim of ATI-1

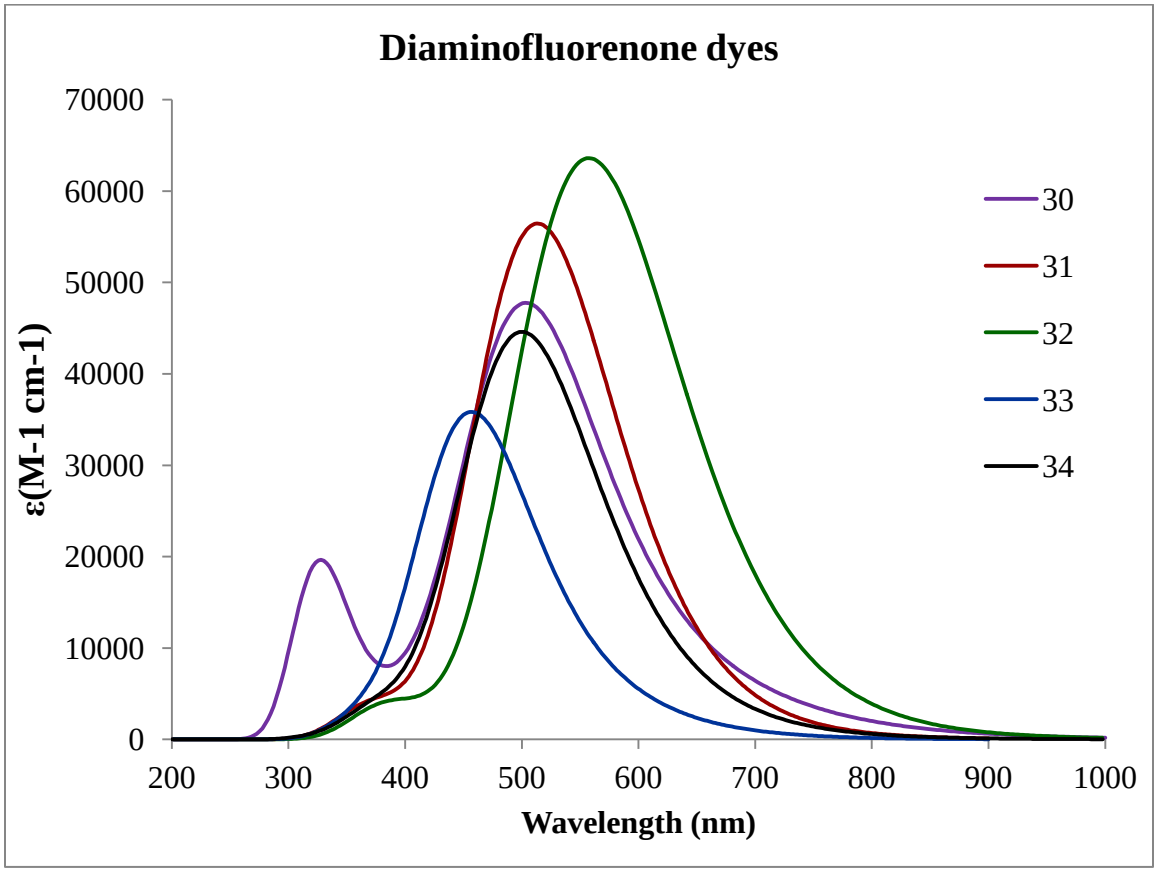

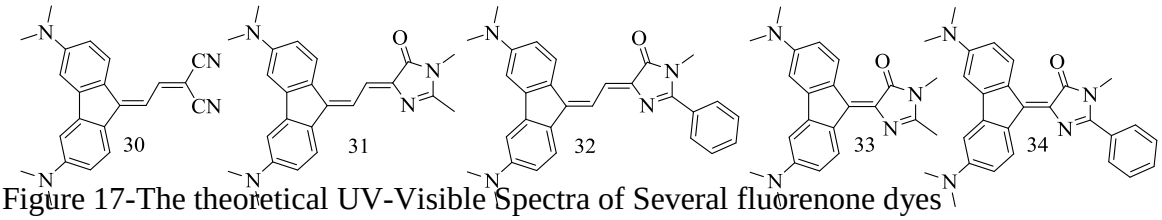

Figure 17-The theoretical UV-Visible Spectra of Several fluorenone dyes

APPENDIX C

^{1}H NMR AND ^{13}C NMR SPECTRA

^{1}H NMR of ATI-1

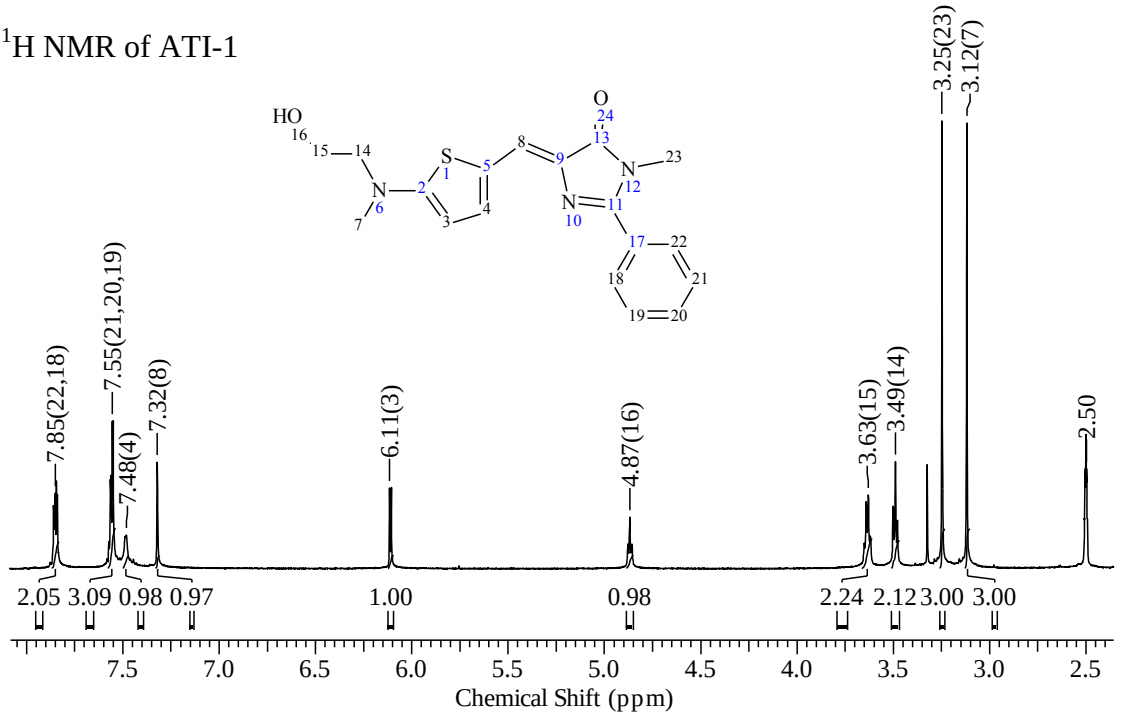

^{13}C NMR of ATI-1

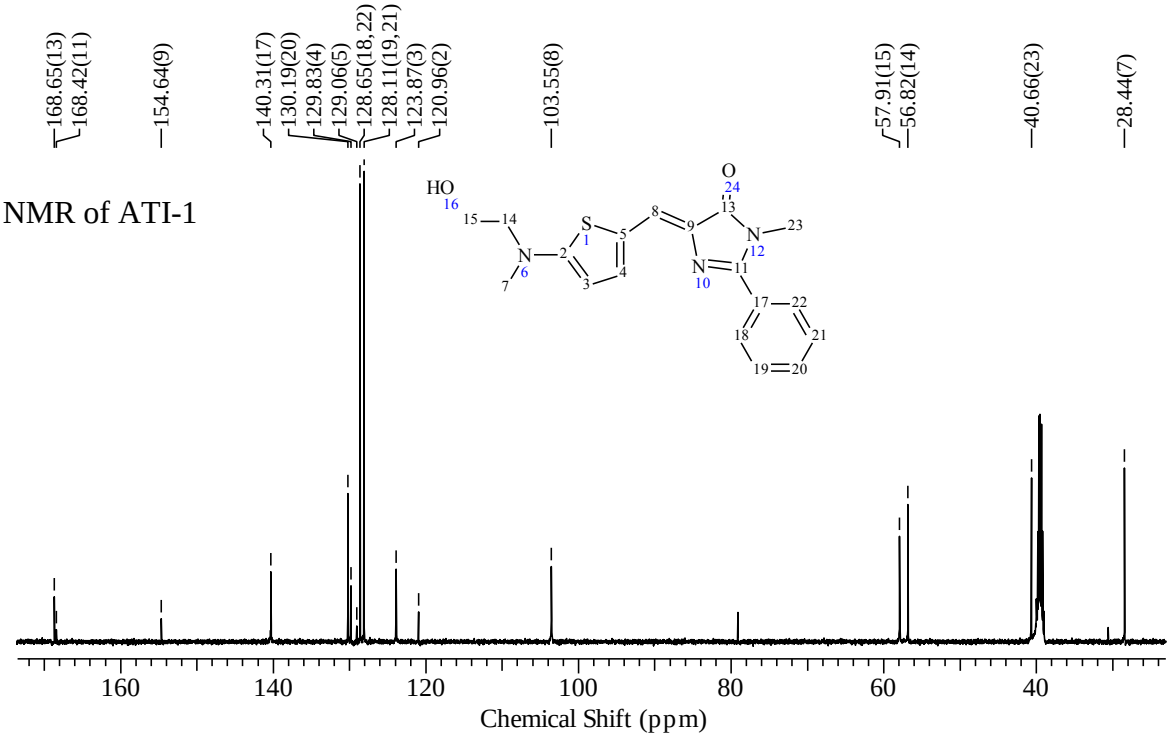

^{1}H NMR of 11

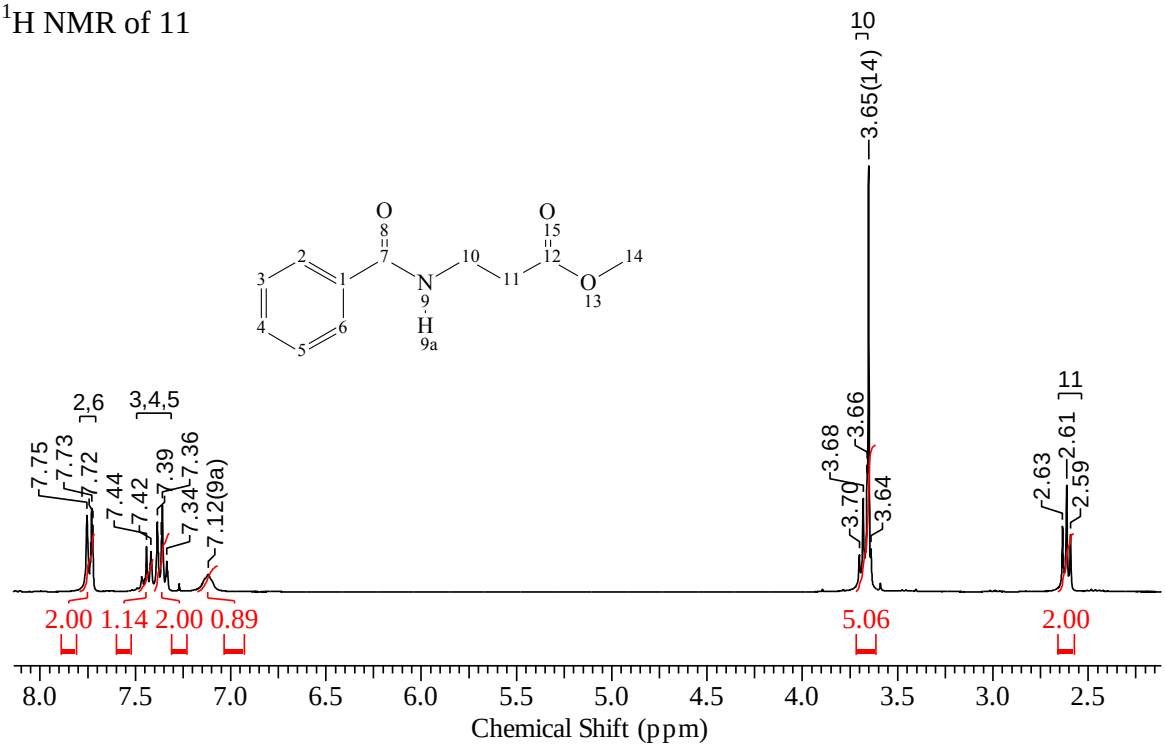

^{13}C NMR of 11

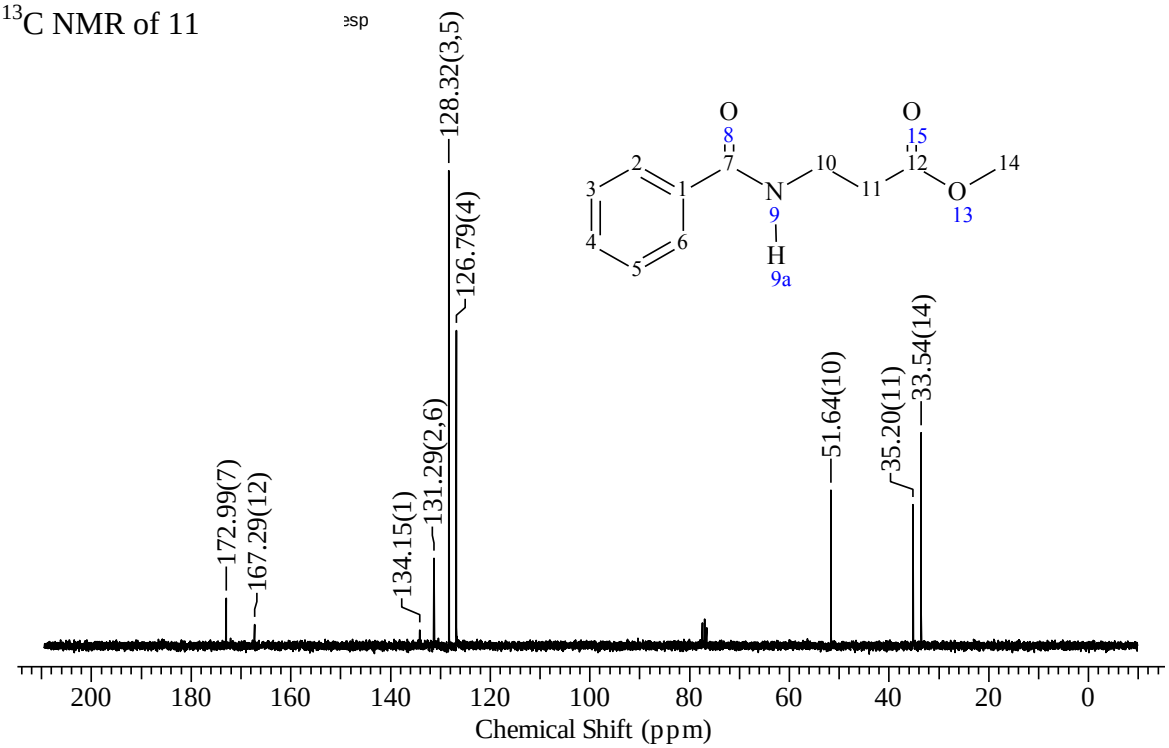

^{1}H-NMR of 12

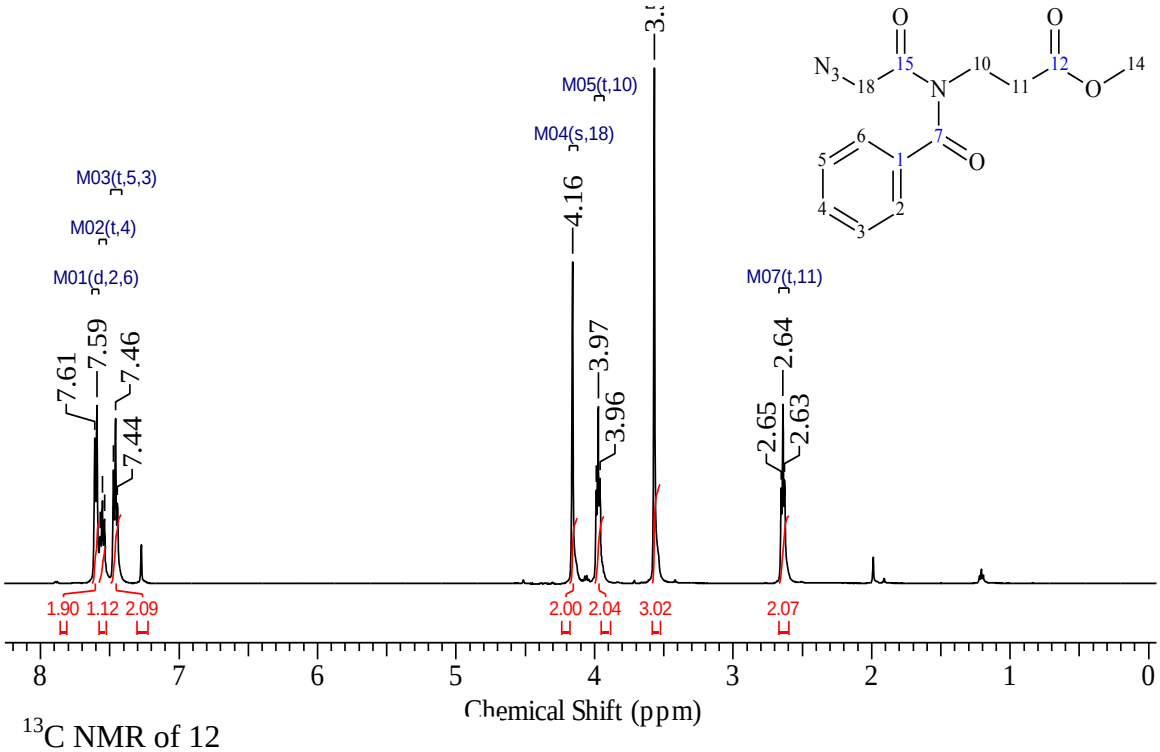

^{13}C NMR of 12

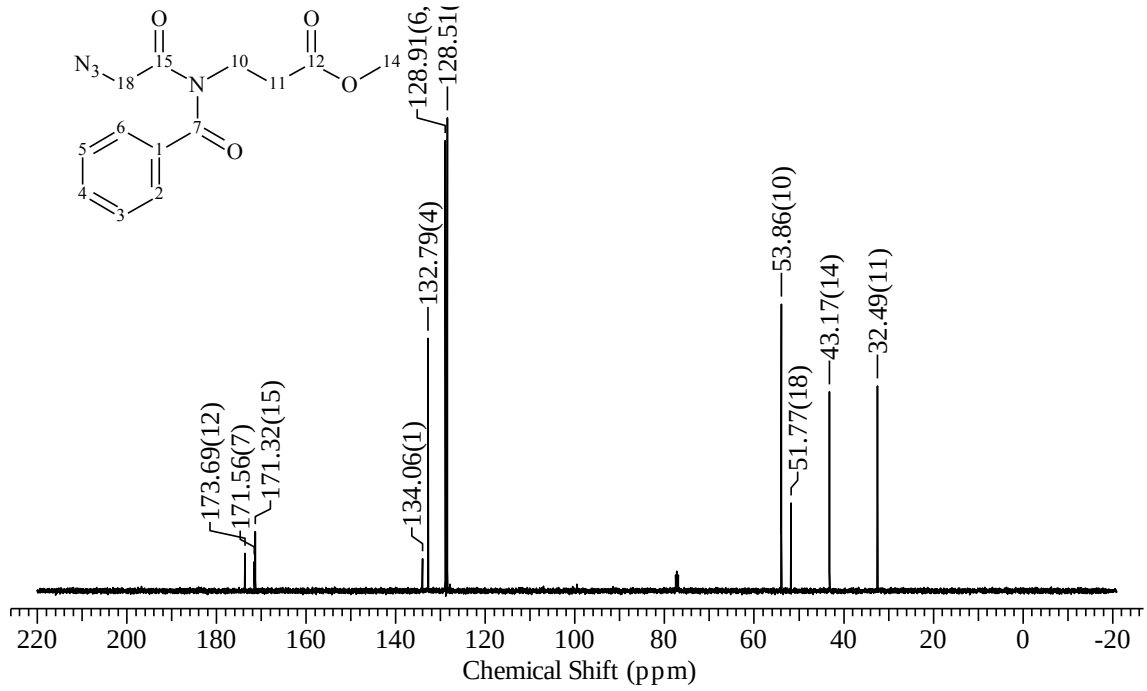

^{1}H-NMR of 13

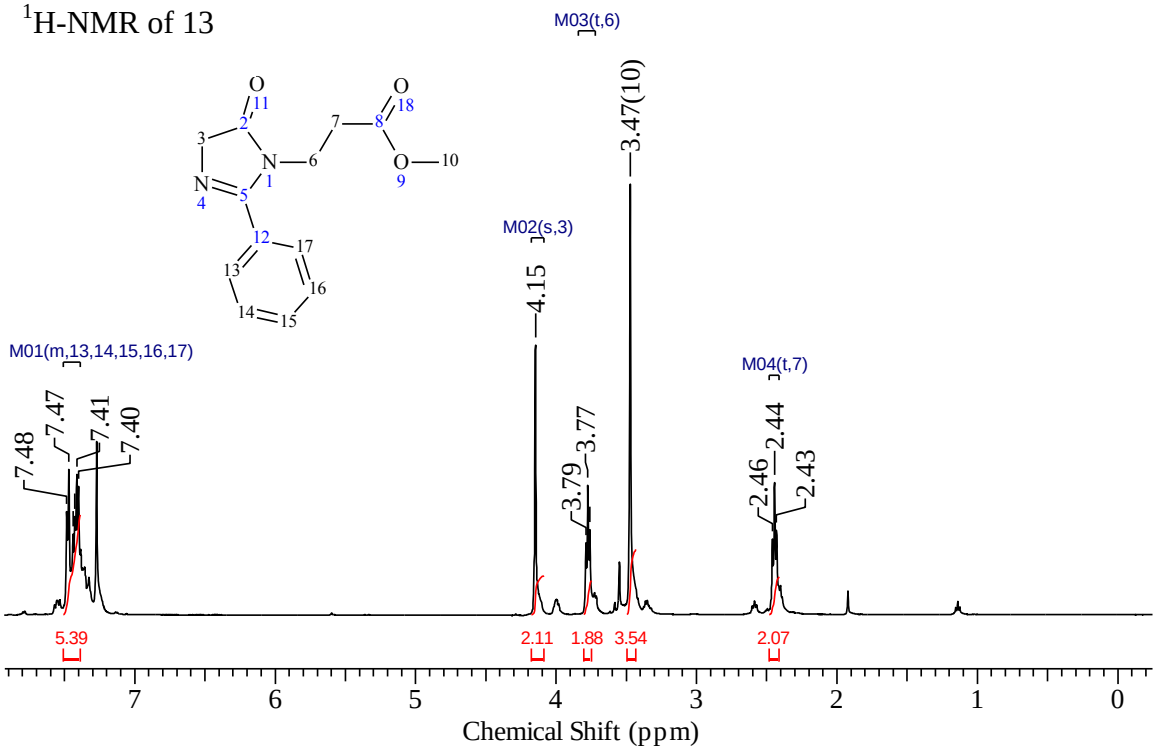

^{13}C-NMR of 13

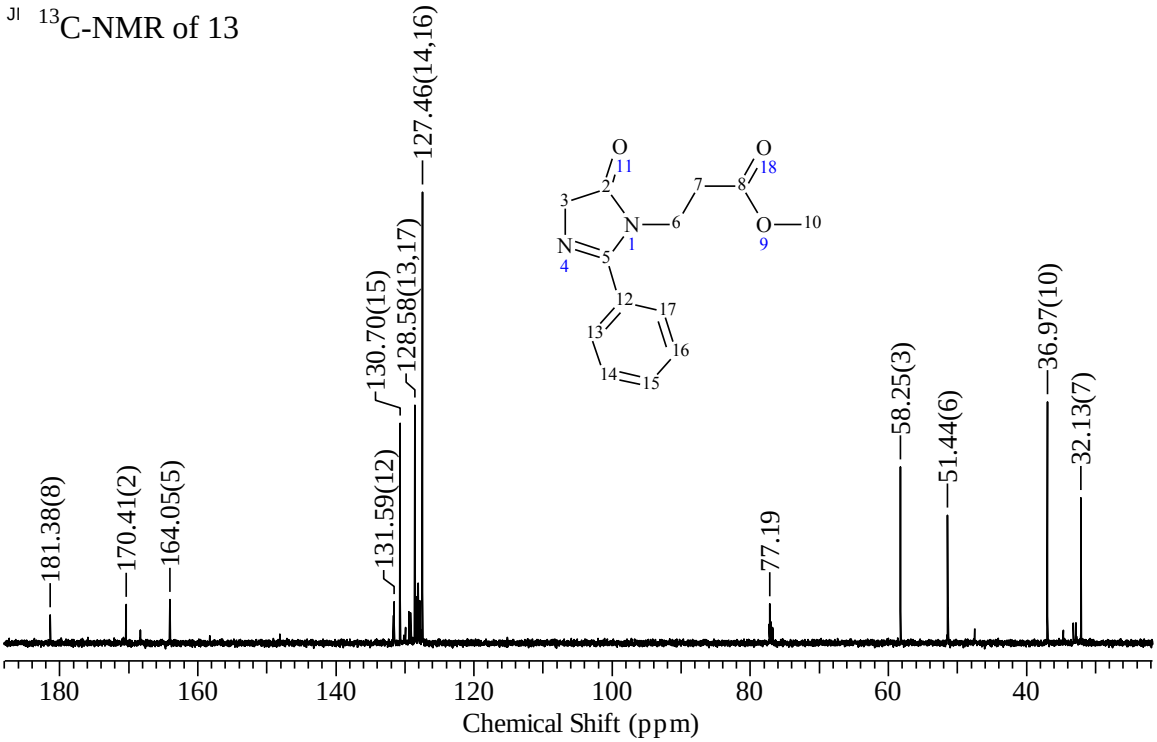

^{1}H-NMR of ATI-2

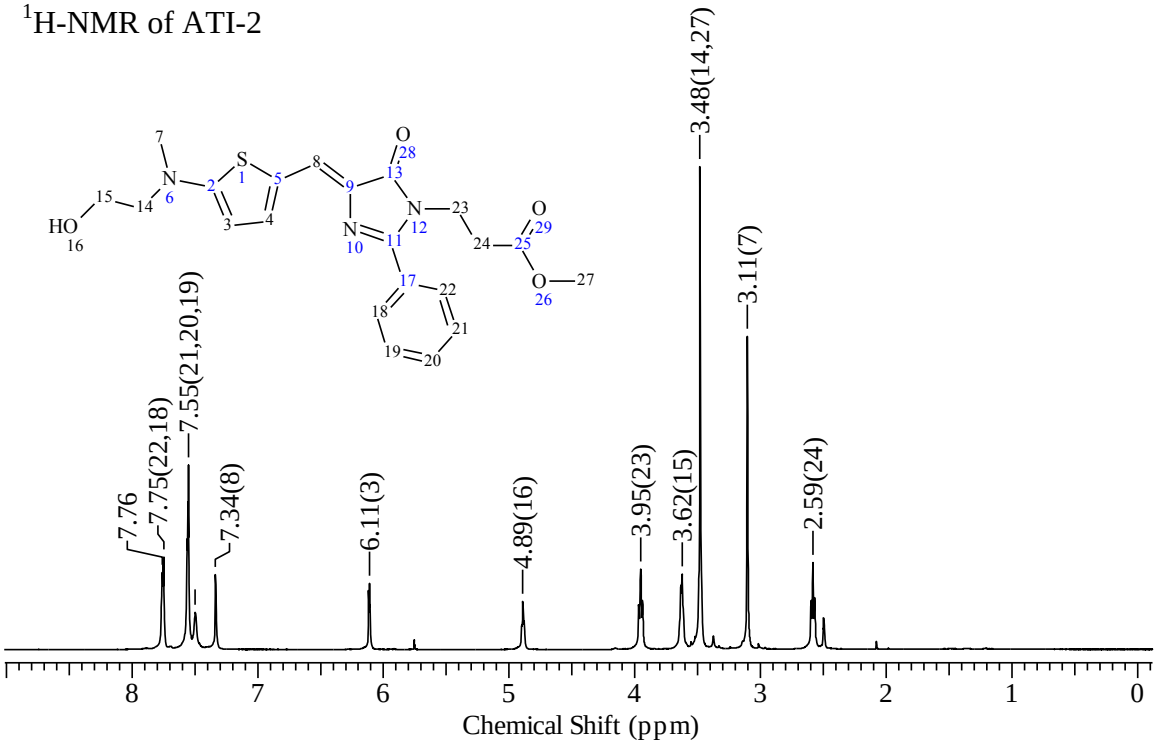

^{13}C-NMR of ATI-2

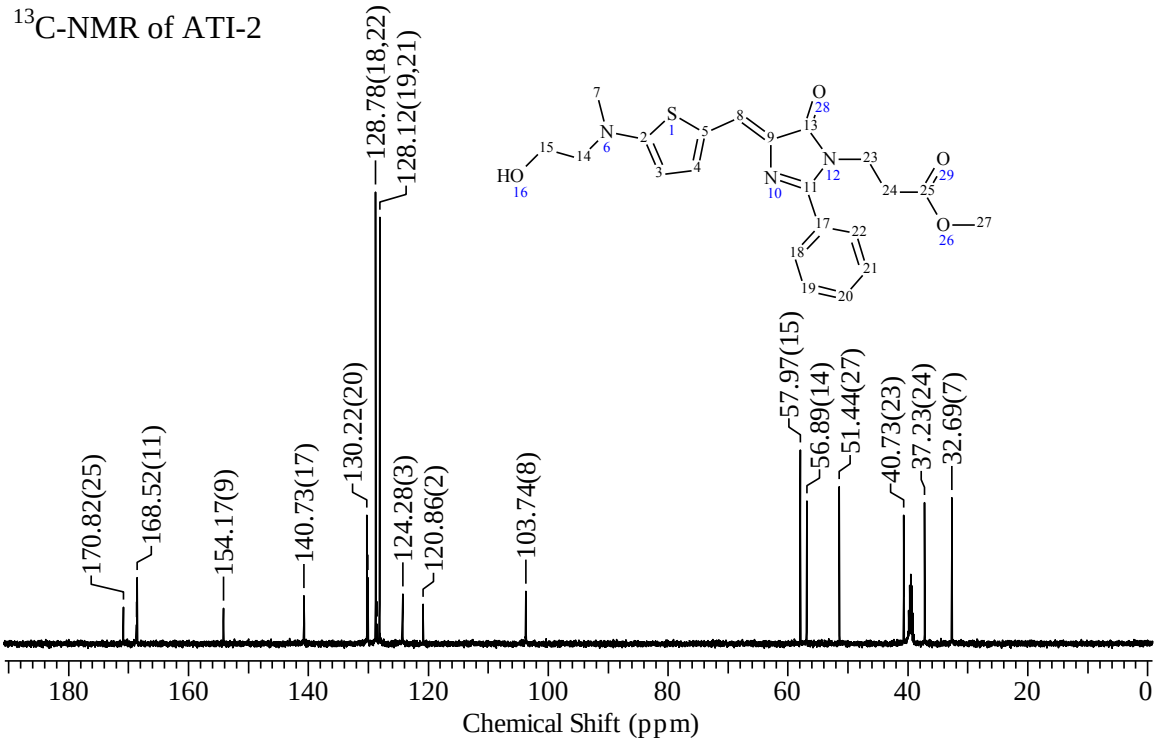

^{1}H-NMR of ATI-2A

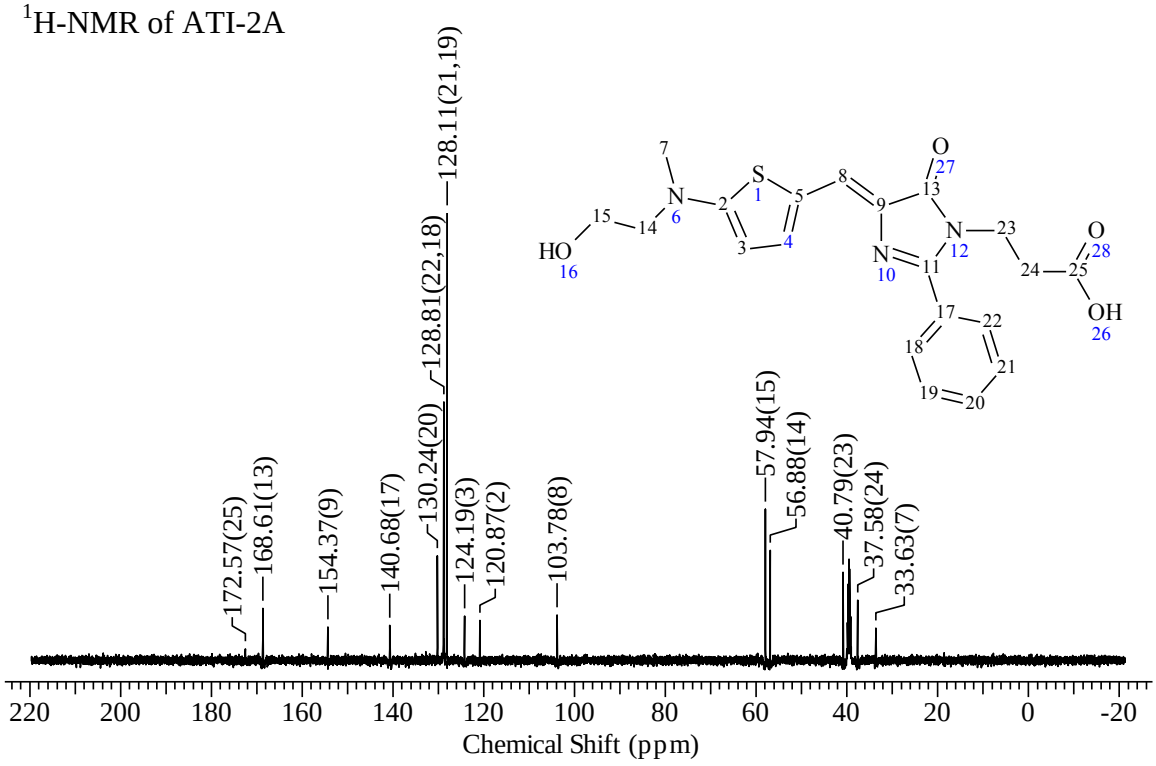

^{13}C-NMR of ATI-2A

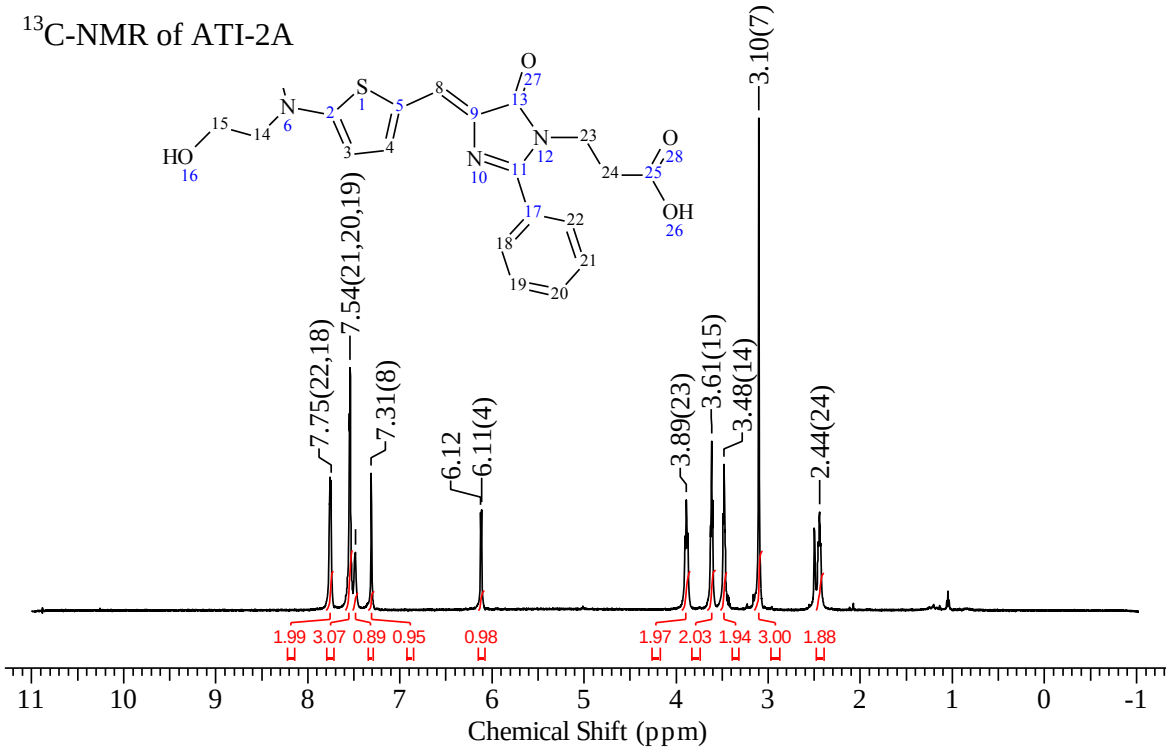

^{1}H-NMR of ATI-2B

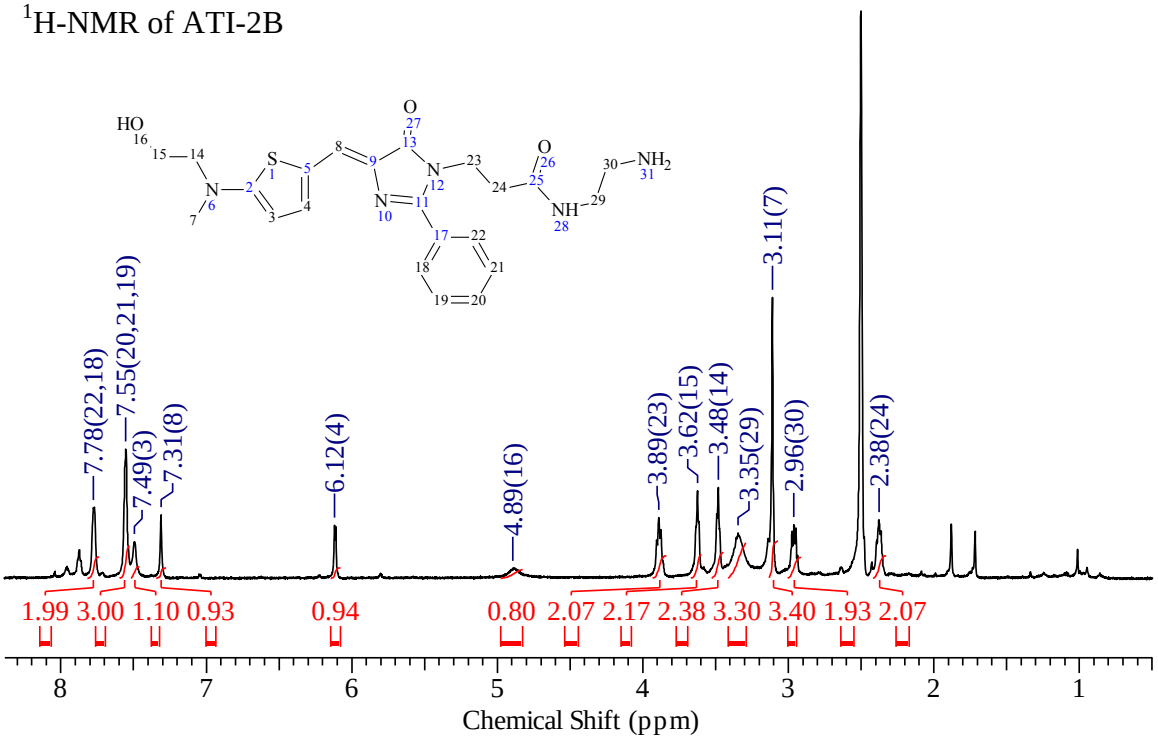

^{13}C-NMR of ATI-2B

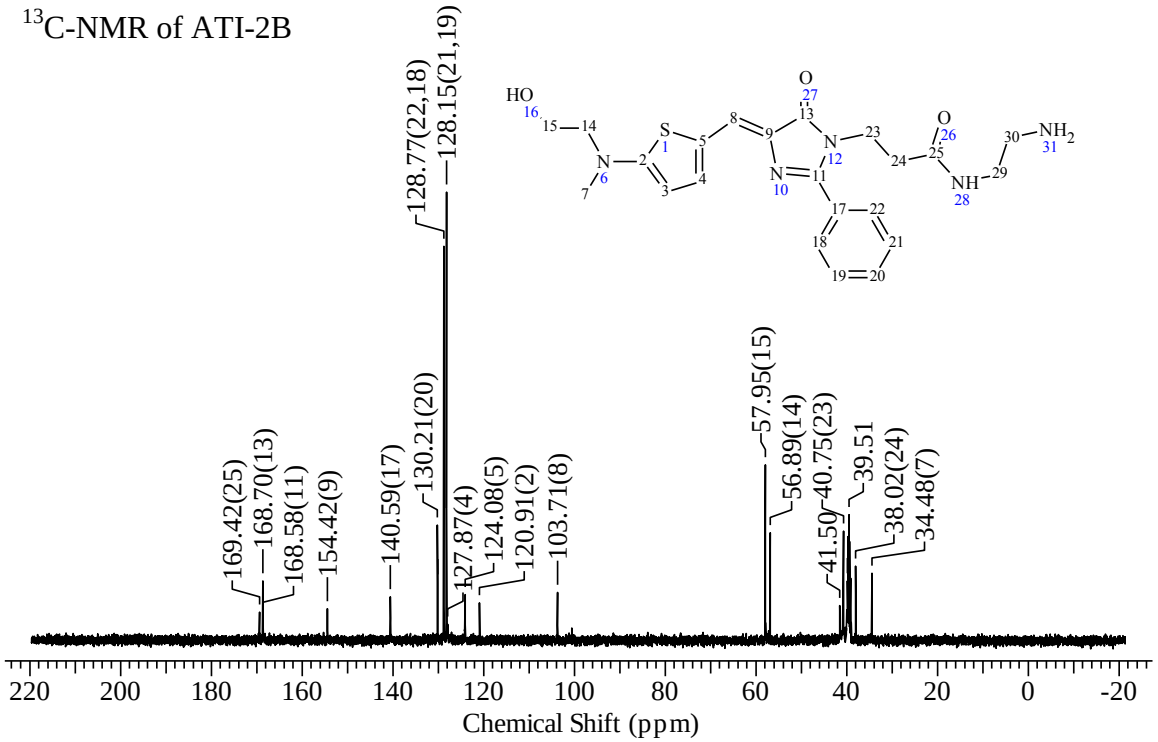

JMR1167-2014-07-07 H.esp

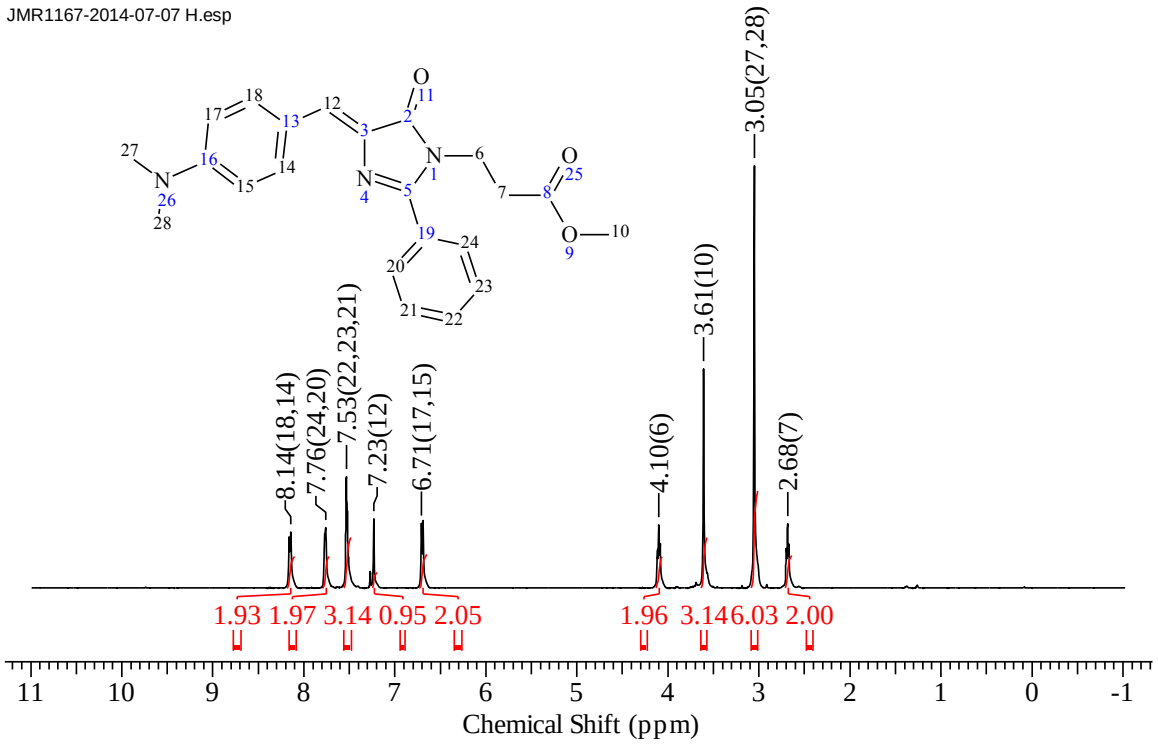

JMR1167-2014-07-07 Carbon.esp

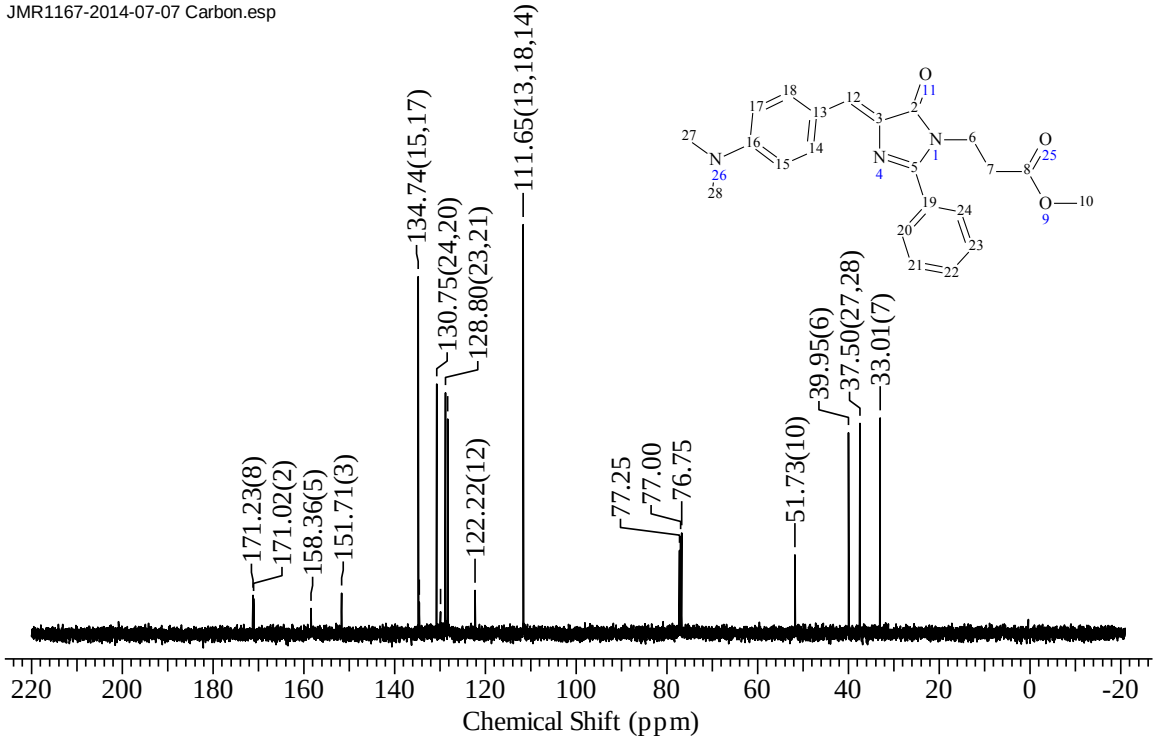

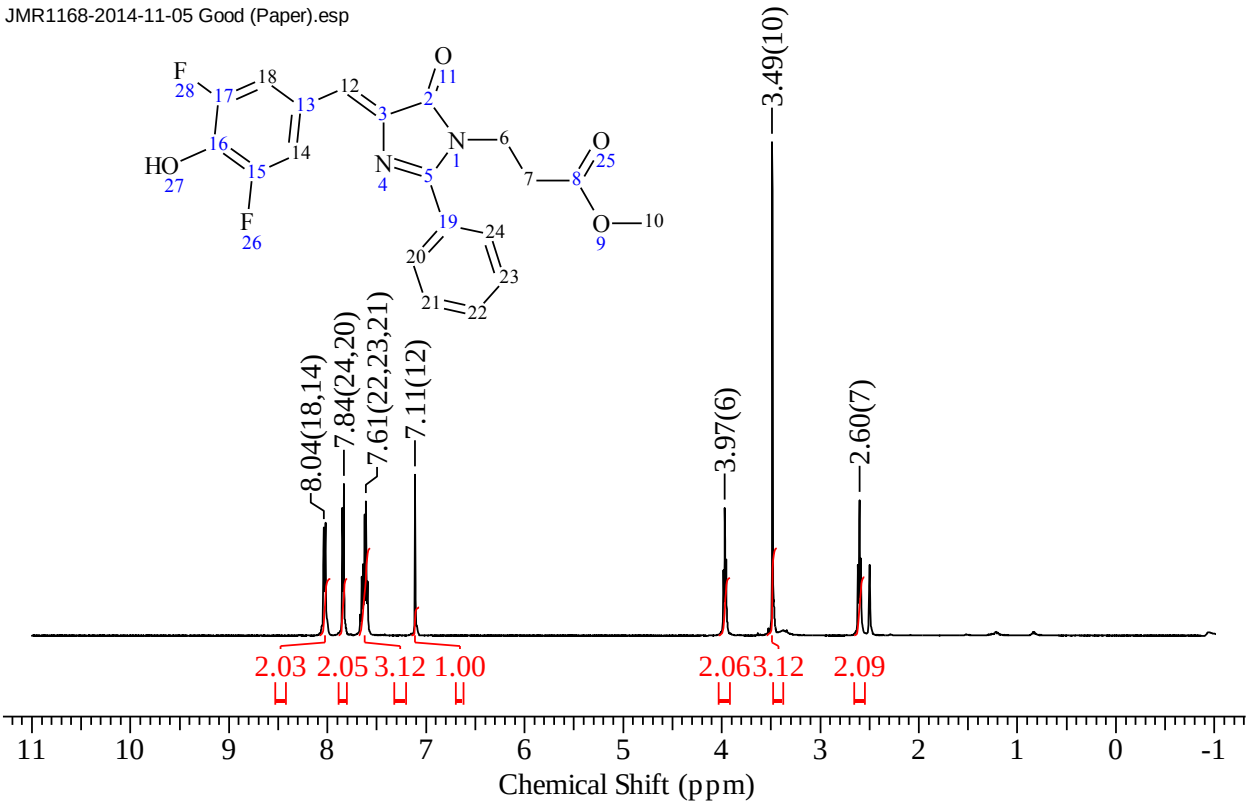
JMR1168-2014-11-05 Good (Paper).esp
8.04(18,14)
7.84(24,20)
7.61(22,23,21)
7.11(12)
3.97(6)
3.49(10)
2.60(7)
2.03 2.05 3.12 1.00
2.06 3.12 2.09
Chemical Shift (ppm)

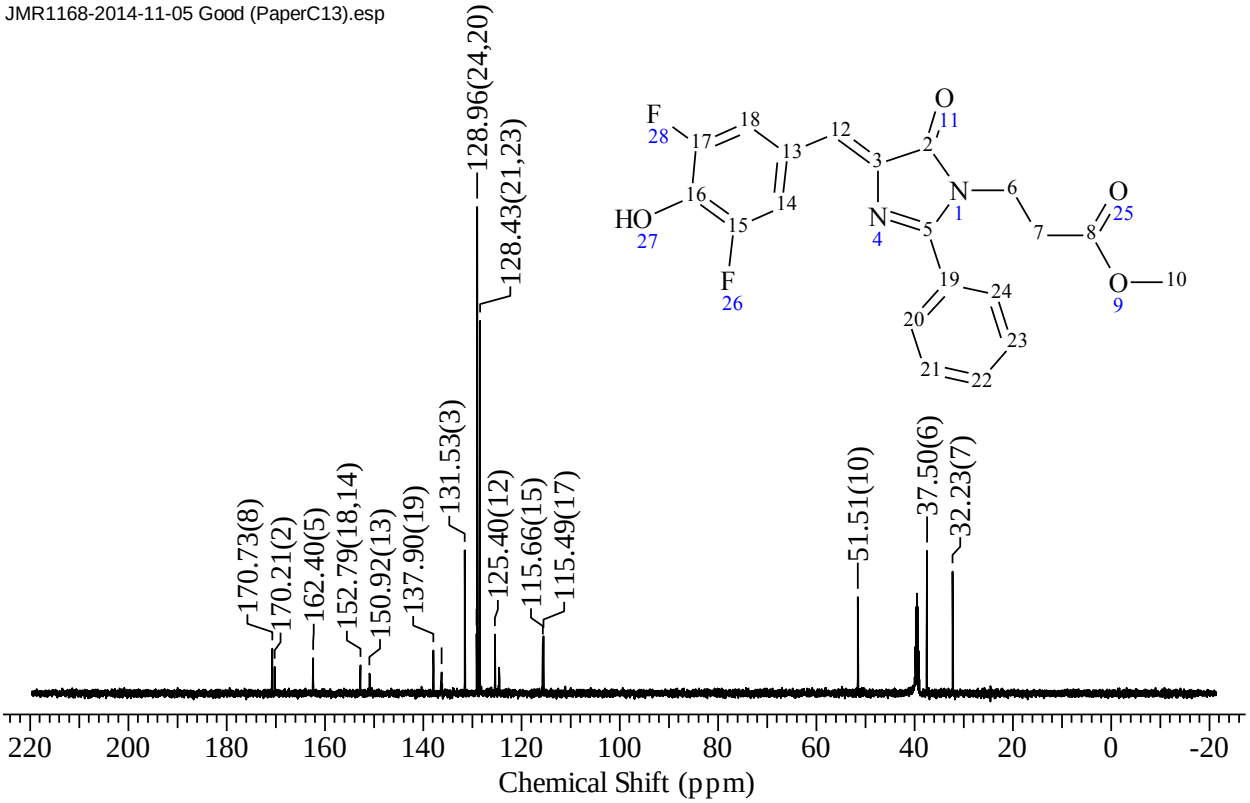
JMR1168-2014-11-05 Good (PaperC13).esp
128.96(24,20)
128.43(21,23)
131.53(3)
170.73(8)
170.21(2)
162.40(5)
152.79(18,14)
150.92(13)
137.90(19)
125.40(12)
115.66(15)
115.49(17)
51.51(10)
37.50(6)
32.23(7)
Chemical Shift (ppm)

^{1}H- NMR of 14

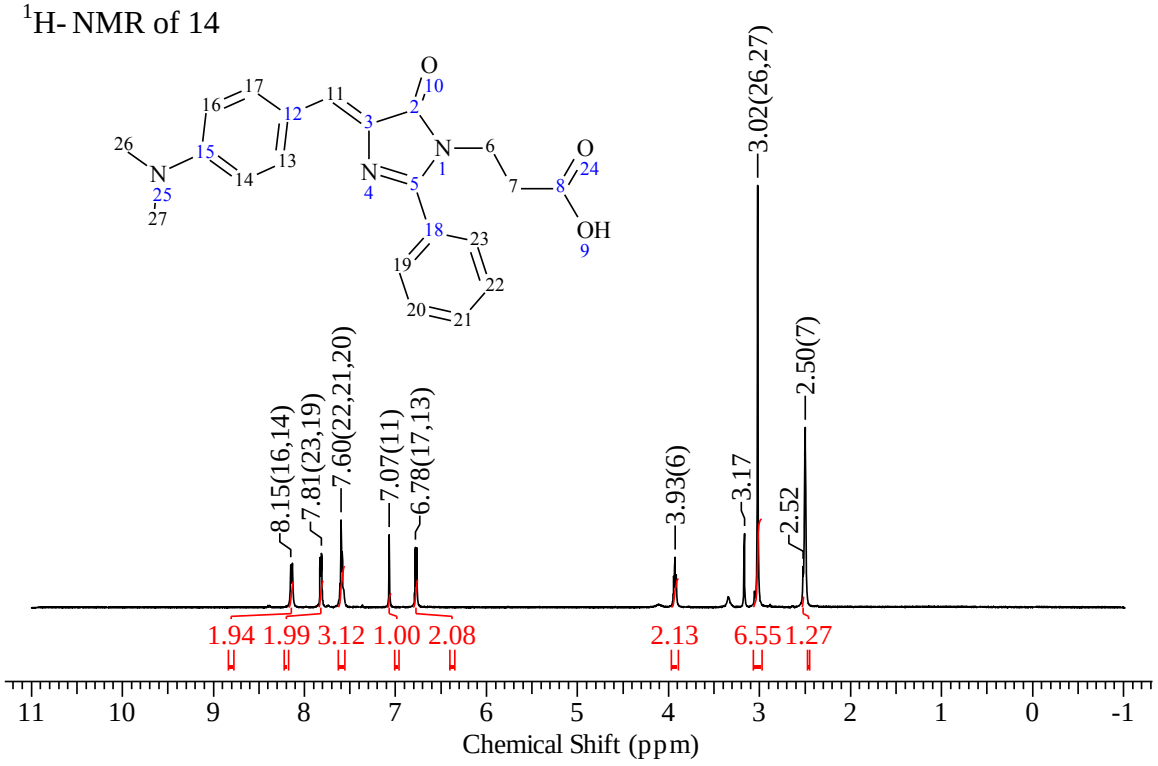
8.15(16,14)
7.81(23,19)
7.60(22,21,20)
7.07(11)
6.78(17,13)
3.93(6)
3.17
3.02(26,27)
2.52
2.50(7)
1.94 1.99 3.12 1.00 2.08
2.13
6.55 1.27
11 10 9 8 7 6 5 4 3 2 1 0 -1
Chemical Shift (ppm)

^{1}H- NMR of 15

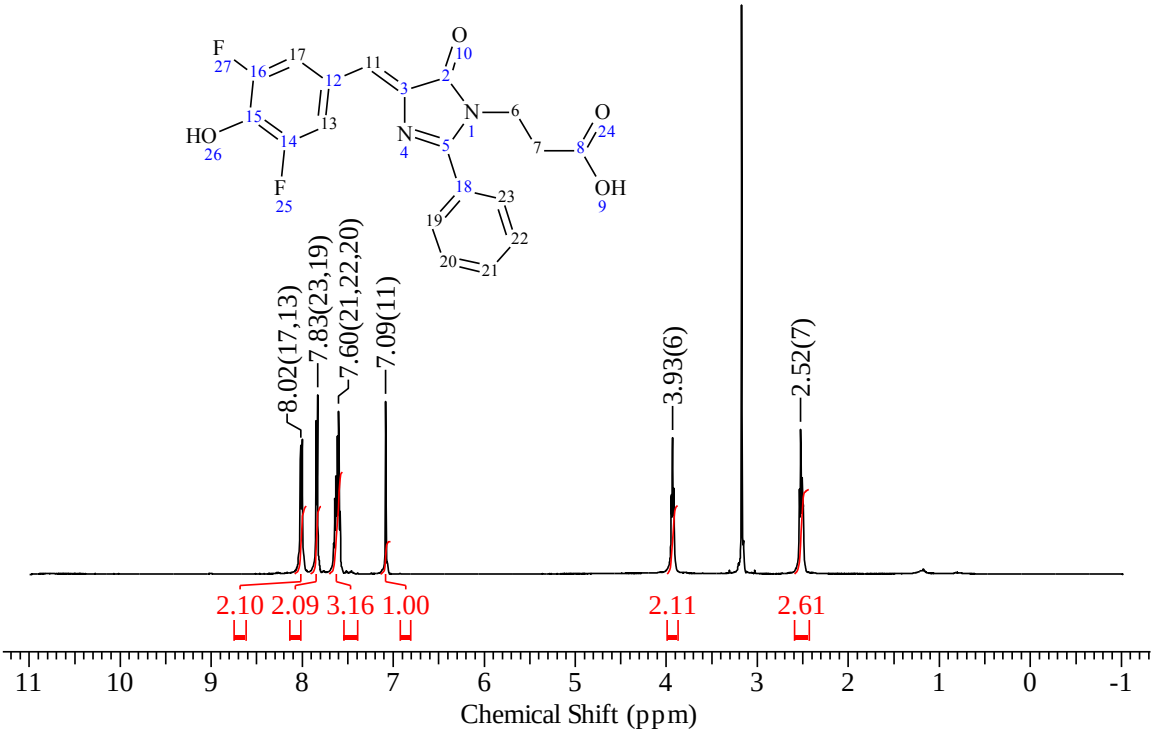

^{13}C-NMR of 15

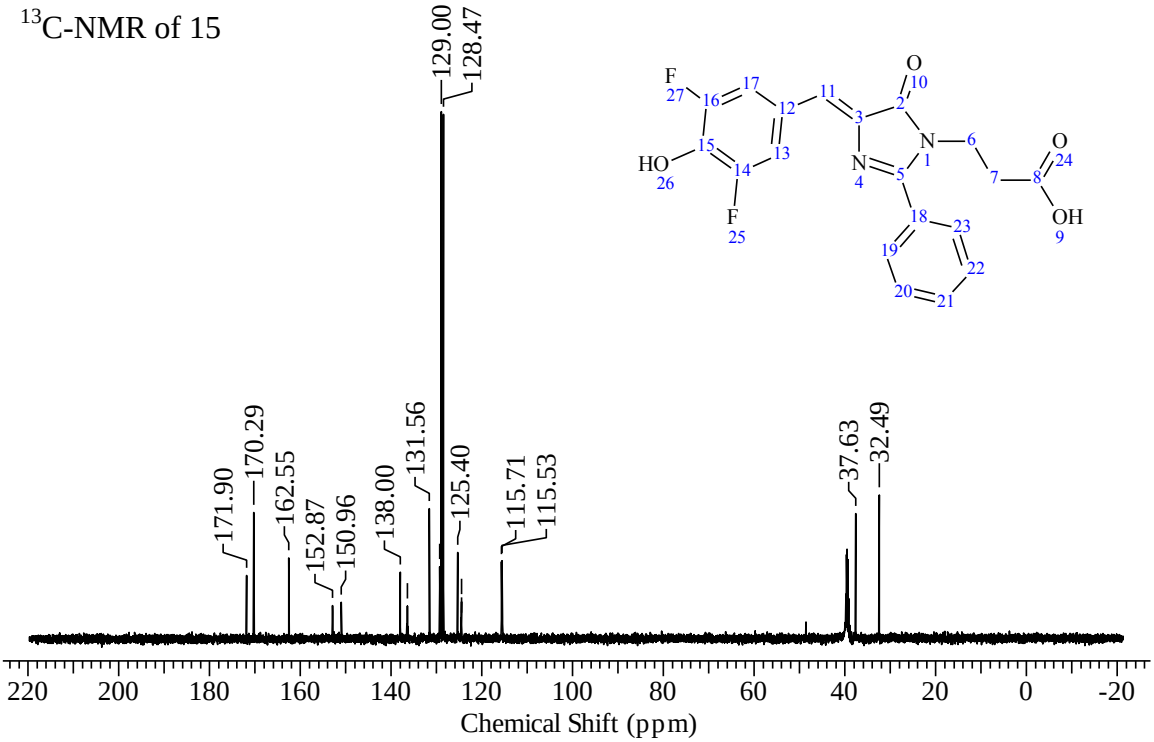

^{1}H- NMR of 23

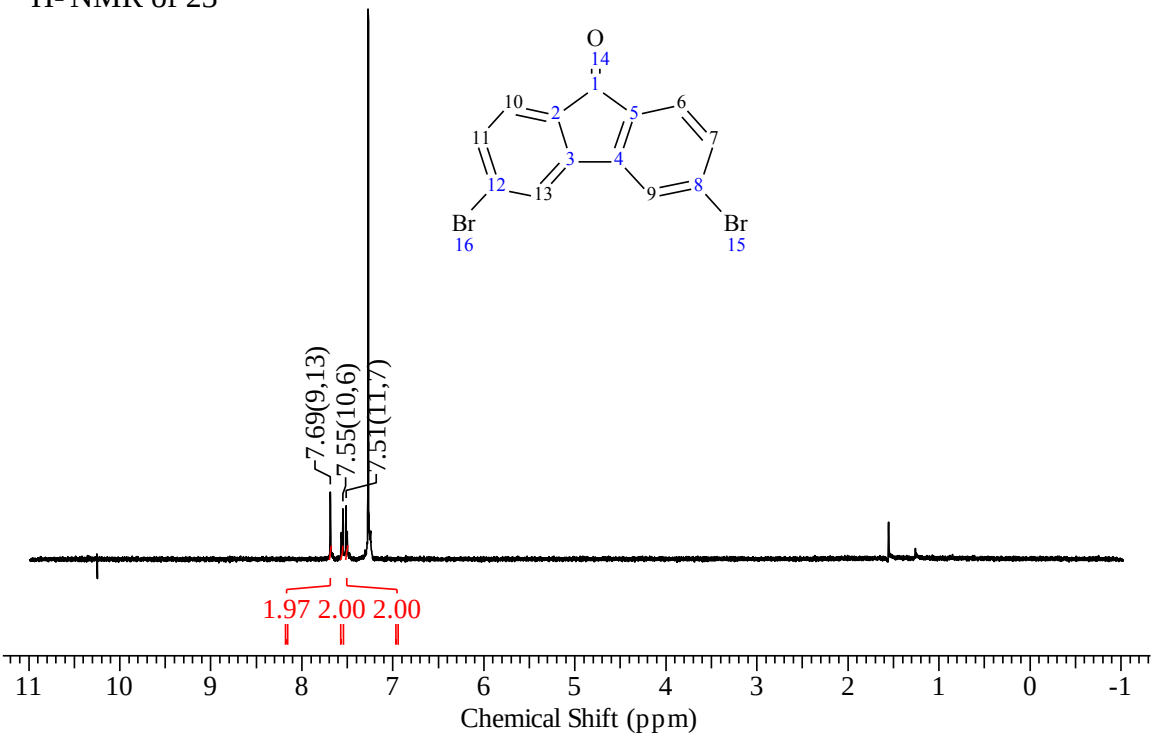

^{1}H- NMR of 24

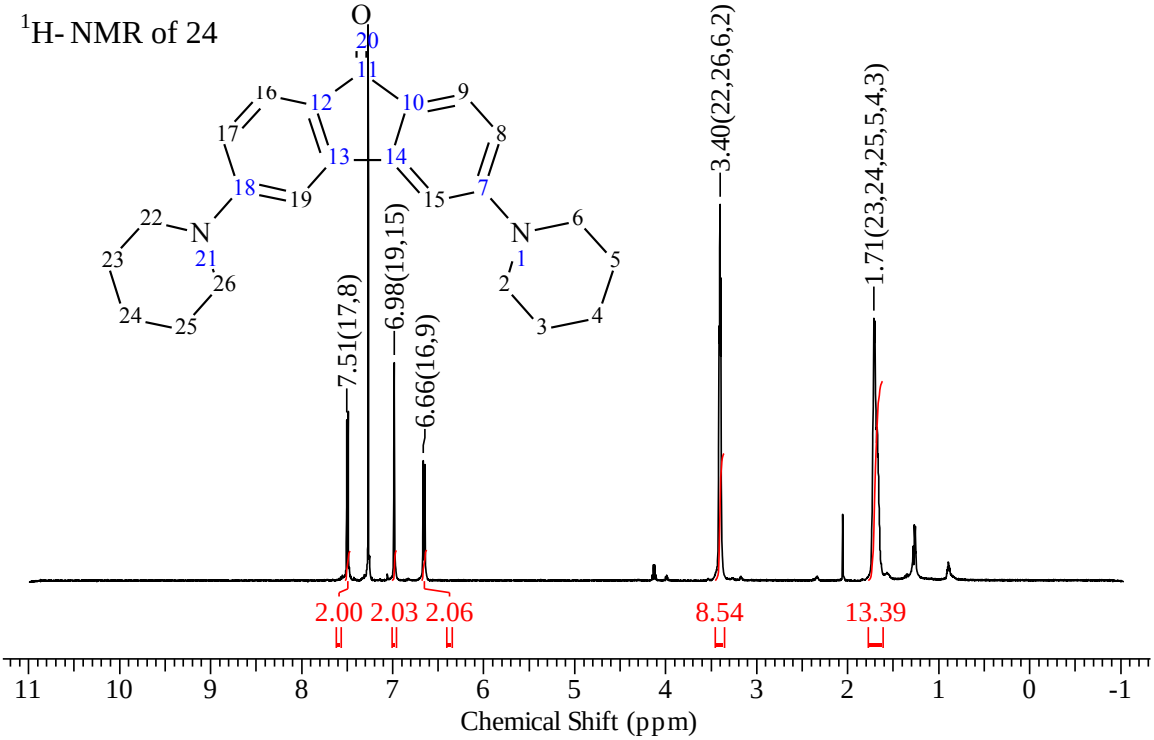

^{1}H- NMR of 25

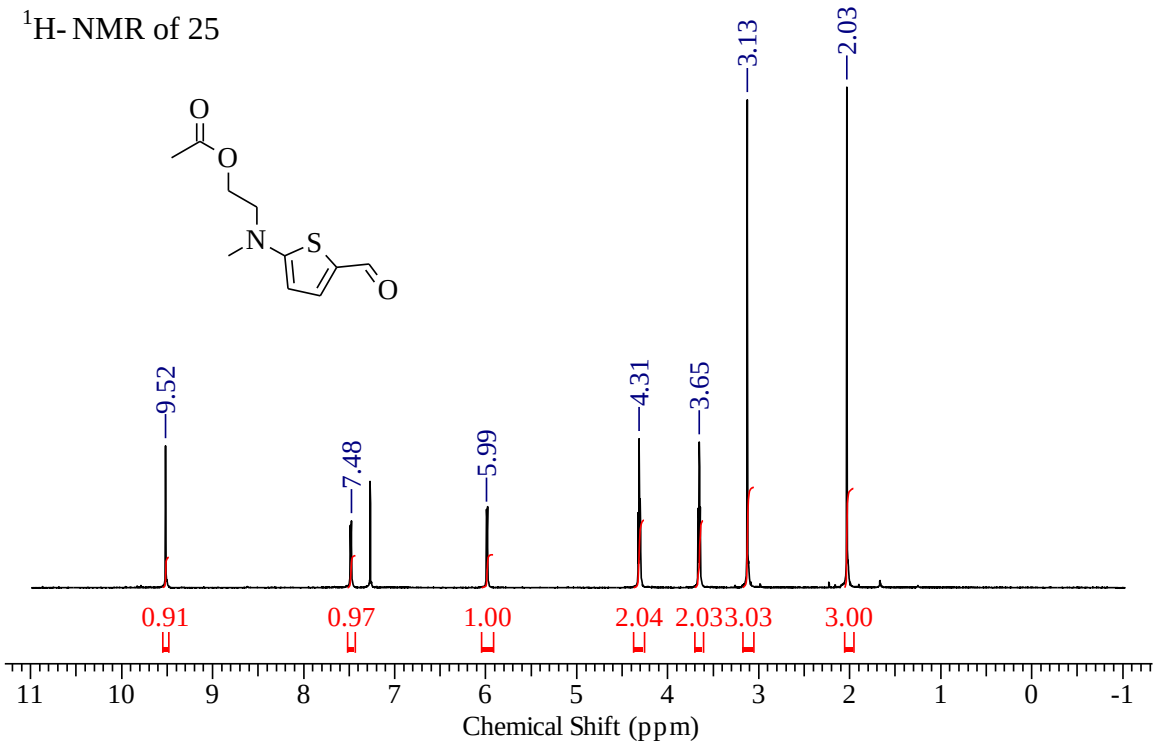

^{1}H- NMR of 26

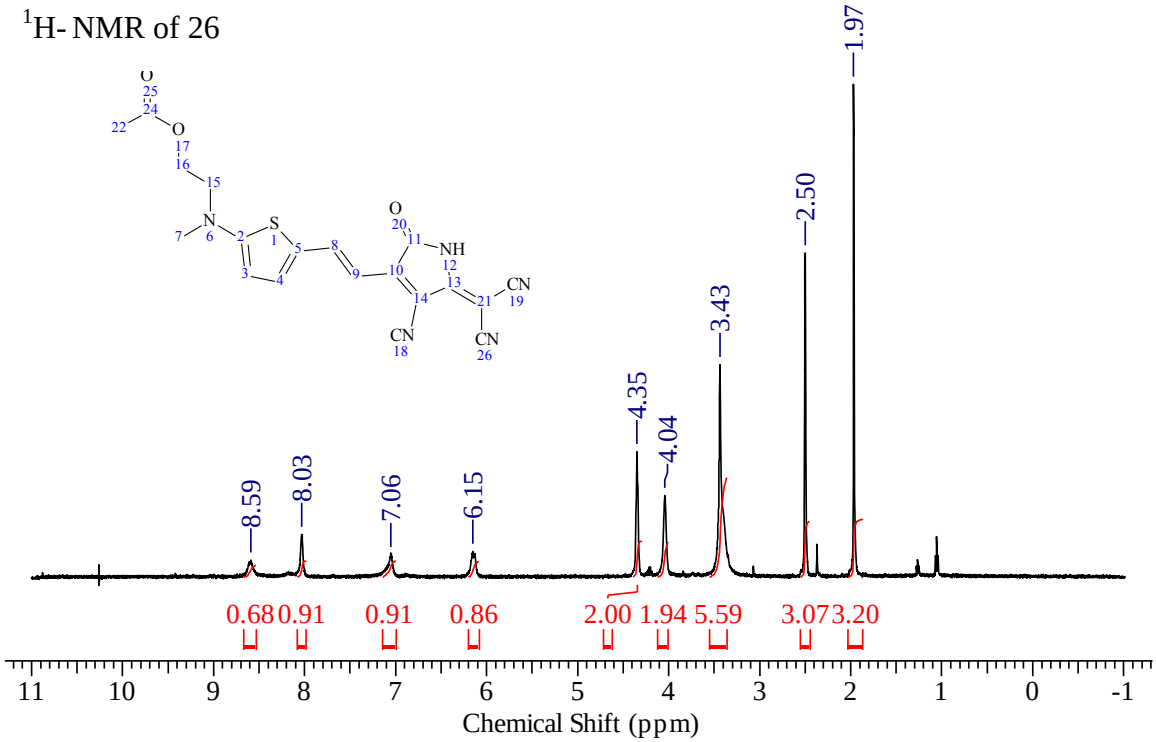

^{1}H- NMR of 27

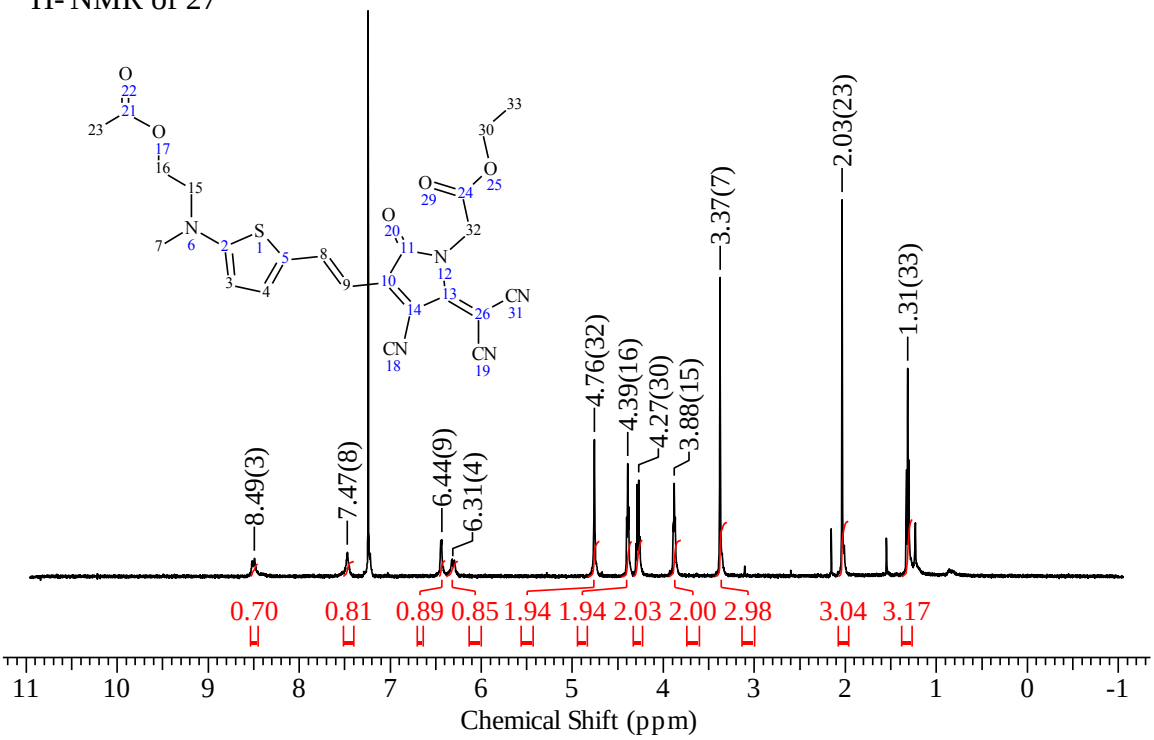
8.49(3)
7.47(8)
6.44(9)
6.31(4)
4.76(32)
4.39(16)
4.27(30)
3.88(15)
3.37(7)
2.03(23)
1.31(33)
0.70
0.81
0.89
0.85
1.94
1.94
2.03
2.00
2.98
3.04
3.17
11
10
9
8
7
6
5
4
3
2
1
0
-1
Chemical Shift (ppm)

REFERENCES CITED

(1) Chalfie, M. T., Yuan; Euskirchen, G; Ward, W. W.; Prasher, D. C. Green Fluorescent Protein as a Marker for Gene Expression. *Science* **1994**, *263*, 802-805.

(2) Paige, J. S.; Wu, K. Y.; Jaffrey, S. R. RNA mimics of green fluorescent protein. *Science* **2011**, *333*, 642-646.

(3) Martynov, A. A. P. V. I. GFP Family: Structural Insights into Spectral Tuning. *Chemistry and Biology* **2008**, *15*, 755-764.

(4) Clark, T. B.; Orr, M. E.; Flynn, D. C.; Goodson, T. Synthesis and Optical Properties of Two-Photon Absorbing GFP-type Probes. *The Journal of Physical Chemistry C* **2011**, *115*, 7331-7338.

(5) Baffour-Awuah, N. Y. A.; Zimmer, M. Hula-twisting in green fluorescent protein. *Chemical Physics* **2004**, *303*, 7-11.

(6) Wu, L.; Burgess, K. Syntheses of Highly Fluorescent GFP-Chromophore Analogues. *Journal of the American Chemical Society* **2007**, *130*, 4089-4096.

(7) Shui, B.; Ozer, A.; Zipfel, W.; Sahu, N.; Singh, A.; Lis, J. T.; Shi, H.; Kotlikoff, M. I. RNA aptamers that functionally interact with green fluorescent protein and its derivatives. *Nucleic acids research* **2012**, *40*, e39.

(8) Drobizhev, M.; Makarov, N. S.; Tillo, S. E.; Hughes, T. E.; Rebane, A. Two-photon absorption properties of fluorescent proteins. *Nature methods* **2011**, *8*, 393-399.

(9) Ikejiri, M.; Tsuchino, M.; Chihara, Y.; Yamaguchi, T.; Imanishi, T.; Satoshi, O.; Miyashita, K. Design and Concise Synthesis of a Novel Type of Green Fluorescent Protein Chromophore Analogue. *Organic Letters* **2012**, *14*, 4406-4409.

(10) Katritzky, A. R.; Yoshioka-Tarver, M.; El-Gendy, B. E.-D. M.; Hall, C. D. Synthesis and photochemistry of pH-sensitive GFP chromophore analogs. *Tetrahedron Letters* **2011**, *52*, 2224-2227.

(11) Baranov, M. S.; Solntsev, K. M.; Baleeva, N. S.; Mishin, A. S.; Lukyanov, S. A.; Lukyanov, K. A.; Yampolsky, I. V. Red-Shifted Fluorescent Aminated Derivatives of a Conformationally Locked GFP Chromophore. *Chemistry – A European Journal* **2014**, *20*, 13234-13241.

(12) Baldridge, A.; Solntsev, K. M.; Song, C.; Tanioka, T.; Kowalik, J.; Hardcastle, K.; Tolbert, L. M. Inhibition of twisting of a green fluorescent protein-like chromophore by metal complexation. *Chemical communications* **2010**, *46*, 5686-5688.

(13) Hsu, Y.-H.; Chen, Y.-A.; Tseng, H.-W.; Zhang, Z.; Shen, J.-Y.; Chuang, W.-T.; Lin, T.-C.; Lee, C.-S.; Hung, W.-Y.; Hong, B.-C.; Liu, S.-H.; Chou, P.-T. Locked ortho- and para-Core Chromophores of Green Fluorescent Protein; Dramatic Emission Enhancement via Structural Constraint. *Journal of the American Chemical Society* **2014**, *136*, 11805-11812.

(14) Baranov, M. S.; Lukyanov, K. A.; Borissova, A. O.; Shamir, J.; Kosenkov, D.; Slipchenko, L. V.; Tolbert, L. M.; Yampolsky, I. V.; Solntsev, K. M. Conformationally Locked Chromophores as Models of Excited-State Proton Transfer in Fluorescent Proteins. *Journal of the American Chemical Society* **2012**, *134*, 6025-6032.

(15) Sutharsan, J.; Lichlyter, D.; Wright, N. E.; Dakanali, M.; Haidekker, M. A.; Theodorakis, E. A. Molecular rotors: Synthesis and evaluation as viscosity sensors. *Tetrahedron* **2010**, *66*, 2582-2588.

(16) Shank, N. I.; Pham, H. H.; Waggoner, A. S.; Armitage, B. A. Twisted cyanines: a non-planar fluorogenic dye with superior photostability and its use in a protein-based fluoromodule. *Journal of the American Chemical Society* **2013**, *135*, 242-251.

(17) Goh, W. L.; Lee, M. Y.; Joseph, T. L.; Quah, S. T.; Brown, C. J.; Verma, C.; Brenner, S.; Ghadessy, F. J.; Teo, Y. N. Molecular Rotors As Conditionally Fluorescent Labels for Rapid Detection of Biomolecular Interactions. *Journal of the American Chemical Society* **2014**, *136*, 6159-6162.

(18) Haidekker, M. A.; Brady, T. P.; Lichlyter, D.; Theodorakis, E. A. A Ratiometric Fluorescent Viscosity Sensor. *Journal of the American Chemical Society* **2006**, *128*, 398-399.

(19) Dolgosheina, E. V.; Jeng, S. C. Y.; Panchapakesan, S. S. S.; Cojocaru, R.; Chen, P. S. K.; Wilson, P. D.; Hawkins, N.; Wiggins, P. A.; Unrau, P. J. RNA Mango Aptamer-Fluorophore: A Bright, High-Affinity Complex for RNA Labeling and Tracking. *ACS Chemical Biology* **2014**, *9*, 2412-2420.

(20) Willets, K. A.; Nishimura, S. Y.; Schuck, P. J.; Twieg, R. J.; Moerner, W. E. Nonlinear Optical Chromophores as Nanoscale Emitters for Single-Molecule Spectroscopy. *Accounts of Chemical Research* **2005**, *38*, 549-556.

(21) Rumble, C.; Rich, K.; He, G.; Maroncelli, M. CCVJ Is Not a Simple Rotor Probe. *The Journal of Physical Chemistry A* **2012**, *116*, 10786-10792.

(22) Atkins, P. P., J.; Friedman, R: *Quanta, Matter, and Change: A molecular Approach to Physical Chemistry*; W.H. Freeman and Co: New York, 2010.

(23) Nielsen, M.; Andersen, L.; Rocha-Rinza, T. Absorption tuning of the green fluorescent protein chromophore: synthesis and studies of model compounds. *Monatsh Chem* **2011**, *142*, 709-715.

(24) Tolbert, L. M.; Baldridge, A.; Kowalik, J.; Solntsev, K. M. Collapse and Recovery of Green Fluorescent Protein Chromophore Emission through Topological Effects. *Accounts of Chemical Research* **2012**, *45*, 171-181.

(25) Paige, J. S.; Nguyen-Duc, T.; Song, W.; Jaffrey, S. R. Fluorescence Imaging of Cellular Metabolites with RNA. *Science* **2012**, *335*, 1194.

(26) Nakayama, S.; Luo, Y.; Zhou, J.; Dayie, T. K.; Sintim, H. O. Nanomolar fluorescent detection of c-di-GMP using a modular aptamer strategy. *Chemical communications* **2012**, *48*, 9059-9061.

(27) Kellenberger, C. A.; Wilson, S. C.; Sales-Lee, J.; Hammond, M. C. RNA-based fluorescent biosensors for live cell imaging of second messengers cyclic di-GMP and cyclic AMP-GMP. *Journal of the American Chemical Society* **2013**, *135*, 4906-4909.

(28) Ramanujan, V. K. Metabolic imaging in multiple time scales. *Methods* **2014**, *66*, 222-229.

(29) Huang, H.; Suslov, N. B.; Li, N. S.; Shelke, S. A.; Evans, M. E.; Koldobskaya, Y.; Rice, P. A.; Piccirilli, J. A. A G-quadruplex-containing RNA activates fluorescence in a GFP-like fluorophore. *Nature chemical biology* **2014**.

(30) Wang, P.; Querard, J.; Maurin, S.; Nath, S. S.; Le Saux, T.; Gautier, A.; Jullien, L. Photochemical properties of Spinach and its use in selective imaging. *Chemical Science* **2013**, *4*, 2865.

(31) Song, W.; Strack, R. L.; Svensen, N.; Jaffrey, S. R. Plug-and-play fluorophores extend the spectral properties of Spinach. *Journal of the American Chemical Society* **2014**, *136*, 1198-1201.

(32) Filonov, G. S.; Moon, J. D.; Svensen, N.; Jaffrey, S. R. Broccoli: Rapid Selection of an RNA Mimic of Green Fluorescent Protein by Fluorescence-Based Selection and Directed Evolution. *Journal of the American Chemical Society* **2014**, *136*, 16299-16308.

(33) Da Costa, J. B.; Andreiev, A. I.; Dieckmann, T. Thermodynamics and kinetics of adaptive binding in the malachite green RNA aptamer. *Biochemistry* **2013**, *52*, 6575-6583.

(34) Wang, T.; Ray, J. Aptamer-based molecular imaging. *Protein & cell* **2012**, *3*, 739-754.

(35) Lee, J.; Lee, K. H.; Jeon, J.; Dragulescu-Andrasi, A.; Xiao, F.; Rao, J. Combining SELEX Screening and Rational Design to Develop Light-Up Fluorophore−RNA Aptamer Pairs for RNA Tagging. *ACS Chemical Biology* **2010**, *5*, 1065-1074.

(36) Duan, N.; Wu, S.; Chen, X.; Huang, Y.; Xia, Y.; Ma, X.; Wang, Z. Selection and Characterization of Aptamers against Salmonella typhimurium Using Whole-Bacterium Systemic Evolution of Ligands by Exponential Enrichment (SELEX). *Journal of agricultural and food chemistry* **2013**, *61*, 3229-3234.

(37) Willets, K. A.; Ostroverkhova, O.; He, M.; Twieg, R. J.; Moerner, W. E. Novel Fluorophores for Single-Molecule Imaging. *Journal of the American Chemical Society* **2003**, *125*, 1174-1175.

(38) Jang, S.-H.; Luo, J.; Tucker, N. M.; Leclercq, A.; Zojer, E.; Haller, M. A.; Kim, T.-D.; Kang, J.-W.; Firestone, K.; Bale, D.; Lao, D.; Benedict, J. B.; Cohen, D.; Kaminsky, W.; Kahr, B.; Brédas, J.-L.; Reid, P.; Dalton, L. R.; Jen, A. K. Y. Pyrroline Chromophores for Electro-Optics. *Chemistry of Materials* **2006**, *18*, 2982-2988.

(39) Davies, J. A.; Elangovan, A.; Sullivan, P. A.; Olbricht, B. C.; Bale, D. H.; Ewy, T. R.; Isborn, C. M.; Eichinger, B. E.; Robinson, B. H.; Reid, P. J.; Li, X.; Dalton, L. R. Rational Enhancement of Second-Order Nonlinerarity: Bis-(4-methoxyphenyl)*hetero*-aryl-amino Donor-based Chromophore: Design, Synthesis, and Electrooptic Activity. *Journal of the American Chemical Society* **2008**, *130*, 10565.

(40) Ma, X.; Liang, R.; Yang, F.; Zhao, Z.; Zhang, A.; Song, N.; Zhou, Q.; Zhang, J. Synthesis and properties of novel second-order NLO chromophores containing pyrrole as an auxiliary electron donor. *Journal of Materials Chemistry* **2008**, *18*, 1756.

(41) Dufresne, S.; Bourgeaux, M.; Skene, W. G. Tunable spectroscopic and electrochemical properties of conjugated push-push, push-pull and pull-pull thiopheno azomethines. *Journal of Materials Chemistry* **2007**, *17*, 1166-1177.

(42) Lerestif, J. M.; Perrocheau, J.; Tonnard, F.; Bazureau, J. P.; Hamelin, J. 1,3-Dipolar cycloaddition of imidate ylides on imino-alcohols: Synthesis of new imidazolones using solvent free conditions. *Tetrahedron* **1995**, *51*, 6757-6774.

(43) Baldridge, A.; Kowalik, J.; Tolbert, L. M. Efficient Synthesis of New 4-Arylideneimidazolin-5-ones Related to the GFP Chromophore by 2+3 Cyclocondensation of Arylideneimines with Imidate Ylides. *Synthesis* **2010**, *2010*, 2424-2436.

(44) Argentini, M.; Dos Santos, D. F.; Weinreich, R.; Hansen, H.-J. Synthesis of an o-Carboranyl Derivative of 4-[5-(4-Methyl-1-piperazinyl)-2,5‘-bi-1H-benzimidazol-2‘-yl]phenol. *Inorganic Chemistry* **1998**, *37*, 6018-6022.

(45) Takeuchi, H.; Hagiwara, S.; Eguchi, S. A new efficient synthesis of imidazolinones and quinazolinone by intramolecular aza-Wittig reaction. *Tetrahedron* **1989**, *45*, 6375-6386.

(46) Gros, L.; Lorente, S. O.; Jimenez; Yardley, V.; Rattray, L.; Wharton, H.; Little, S.; Croft, S. L.; Ruiz-Perez, L. M.; Gonzalez-Pacanowska, D.; Gilbert, I. H. Evaluation of Azasterols as Anti-Parasitics. *Journal of Medicinal Chemistry* **2006**, *49*, 6094-6103.

(47) Prim, D.; Kirsch, G.; Nicoud, J.-F. Efficient Synthesis of N,N-Disubstituted 5-Aminothiophene-2-carboxaldehydes by Nucleophilic Aromatic Substitution in Water. *Synlett* **1998**, *1998*, 383-384.

(48) Karak, S.; Homnick, P. J.; Renna, L. A.; Venkataraman, D.; Mague, J. T.; Lahti, P. M. Solution-Processed Photovoltaics with a 3,6-Bis(diarylamino)fluoren-9-ylidene Malononitrile. *ACS Applied Materials & Interfaces* **2014**, *6*, 16476-16480.

(49) Estrada, L. A.; Neckers, D. C. Synthesis and Photophysics of Ambipolar Fluoren-9-ylidene Malononitrile Derivatives†. *The Journal of organic chemistry* **2009**, *74*, 8484-8487.

(50) Nakatsuji, S.; rsquo; ichi; Yahiro, T.; Nakashima, K.; Akiyama, S.; Nakazumi, H. Synthesis and Absorption Spectral Properties of New Merocyanine Dyes Derived from 1,1 Diaryl-2-propyn-1-ols. *Bulletin of the Chemical Society of Japan* **1991**, *64*, 1641-1647.

(51) Filonov, G. S.; Moon, J. D.; Svensen, N.; Jaffrey, S. R. Broccoli: Rapid Selection of an RNA Mimic of Green Fluorescent Protein by Fluorescence-Based Selection and Directed Evolution. *Journal of the American Chemical Society* **2014**.

(52) Howell, L. A.; Gulam, R.; Mueller, A.; O’Connell, M. A.; Searcey, M. Design and synthesis of threading intercalators to target DNA. *Bioorganic & Medicinal Chemistry Letters* **2010**, *20*, 6956-6959.

(53) Lawrence, N. J.; Hepworth, L. A.; Rennison, D.; McGown, A. T.; Hadfield, J. A. Synthesis and anticancer activity of fluorinated analogues of combretastatin A-4. *Journal of Fluorine Chemistry* **2003**, *123*, 101-108.

(54) Mittelbach, M. An improved and facile synthesis of 2-amino-1,1,3-tricyanopropene. *Monatshefte für Chemie / Chemical Monthly* **1985**, *116*, 689-691.